ILLINOIS TOLLWAY RESEARCH PROGRAM

APPLICATIONS FOR FOAMED GLASS LIGHTWEIGHT AGGREGATE

FINAL REPORT

By

Haifang Wen, PhD, PE, Professor
Shafkat Bin Jafar, Graduate Student
Mohammadreza Barzegar, PhD, Former Graduate Student
Dept. of Civil & Environmental Engineering
Washington State University

Michael P. McGuire, PhD, PE, Associate Professor
Lafayette College
and
Tuncer Edil, PhD, PE, Professor Emeritus
University of Wisconsin at Madison

Submitted to:

Illinois State Toll Highway Authority

May 25, 2025

DISCLAIMER

The contents of this report reflect the views of the authors who are responsible for the facts and the accuracy of the data presented herein. The contents do not necessarily reflect the official views or policies of Washington State University or the Illinois State Toll Highway Authority. This report does not constitute a standard, specification, or regulation.

ACKNOWLEDGEMENTS

This study was funded by the Illinois State Toll Highway Authority (Illinois Tollway). The authors greatly appreciate the sponsorship of the Authority and especially the input and support from Mr. Dan Gancarz and Ms. Cynthia Williams of Illinois Tollway, Mr. Ross Bentsen of Interra, Mr. Jay Behnke of S.T.A.T.E Testing, LLC, Ms. Theresa Loux of AeroAggregates, LLC, and the rest of the project panel members (Mr. Ahmad Hamad of WSP, Ms. Jess Hansen of the Illinois Association of Aggregate Producers, Mr. Stephen Jones of the Illinois DOT, Mr. Nicholas Laga of WSP, Mr. Scott Paloian of the Chicago Department of Transportation, and Ms. Heather Shoup of the Illinois DOT). We would also like to thank the agencies that responded to our survey, especially Ms. Beverly Miller (Pennsylvania DOT) for her input. Thanks also go to WSDOT Eastern Region, specifically Mr. Riley Bender and Mr. David Olsen, for conducting WSDOT TM-15 tests on FGA and nuclear density gauge tests.

TECHNICAL REPORT DOCUMENTATION PAGE

1. Report No.	2. Government Accession No	3. Recipient's Catalog No
4. Title and Subtitle Application for Foamed Glass Lightweight Aggregate		5. Report Date May 2025 6. Performing Organization Code
7. Authors Haifang Wen, Shafkat Bin Jafar, Mohammadreza Barzegar, Michael P. McGuire, and Tuncer Edil		8. Performing Organization Report No.
9. Performing Organization Name and Address Department of Civil and Environmental Engineering Washington State University Spokane Street, Pullman, WA 99164		Work Unit No. (TRAIS) Contract or Grant No. RR-23-9290
12. Sponsoring Agency Name and Address Illinois State Toll Highway Authority 2700 Ogden Ave Downers Grove, IL 60515		13. Type of Report and Period Covered 8/2023-5/2025 14. Sponsoring Agency Code

15. Supplementary Notes

16. Abstract

Foamed glass aggregate (FGA) is a processed recycled aggregate made from waste glass. The process involves grinding the glass into powder and melting it at a high temperature (e.g., 1600°F) with a foaming reagent (e.g., 2% by weight). In addition to its low compacted unit weight, FGA possesses several unique engineering properties, such as a high friction angle, good thermal insulation, and high permeability. With these properties, the utilization of FGA could be a sustainable practice that contributes to the reduction of fill settlement over soft-ground, environmental preservation, and lower greenhouse gas emissions. However, as with any emerging or unconventional material, a comprehensive engineering study of FGA is essential before its widespread application to prevent unsatisfactory performance in specific use cases. To that end, the research team conducted extensive literature reviews and surveys. The team then procured two types of FGA samples (wet and dry foaming) and two conventional soils, sand and embankment clay (used as references) for laboratory experiments. These experiments included testing for basic FGA characteristics, gradations, volumetric and electrochemical properties, aerodynamic properties, axial compression compaction, one-dimensional consolidation tests, dynamic triaxial tests, and direct shear tests. A pilot construction was also carried out. Additionally, economic and environmental analyses were performed, and the results were compared with those for lightweight cellular concrete (LCC). Based on the tests and analyses, a draft construction specification was developed, and a design guide for the use of FGA was also provided.

17. Key Words Foamed glass aggregate, settlement, triaxial, pH, resistivity, compaction, acceptance	18. Distribution Statement

19. Security Classif. (of this report)	19. Security Classif. (of this page)	20. No. of Pages 98	21. Price

Table of Contents

LIST OF FIGURES

LIST OF TABLES

CHAPTER 1: INTRODUCTION

1.1 Background

Recycled and lightweight fill materials are increasingly used in construction due to their ability to address challenging site conditions, accelerate project timelines, and reduce reliance on natural resources, while contributing to sustainability goals. One such material gaining recognition is foamed glass aggregate (FGA), produced from recycled glass. The manufacturing process involves grinding the glass into powder, melting it at high temperatures (approximately 1600°F) with a foaming agent (e.g., 2% by weight), and cooling it to form lightweight, angular particles (Betti et al., 2014).

FGA is notable for its low dry unit weight (8–15 pounds per cubic foot, which is much lower than that of conventional materials exceeding 100 pcf) and high friction angle (Arulrajah, 2015; Loux, 2019). It is typically free draining, with minimal fines and particle sizes ranging between 0.5 and 2.5 inches. Closed-cell FGA is more commonly utilized in construction for its structural advantages (Loux, 2019). The material has been employed in various states, such as Arizona, Pennsylvania, and Virginia, for applications such as highway embankments, retaining wall backfill, and bridge abutments (Betti et al., 2014). Its lightweight nature minimizes settlement risks and reduces the need for extensive soil excavation, as demonstrated in projects like the Nassau Expressway realignment, where FGA effectively mitigated flooding and settlement concerns (Loux and Filshill, 2021a).

Despite its advantages, FGA presents several characteristics that require further investigation. Excessive compaction during placement can crush the material, generating fines and reducing its volume (McGuire et al., 2021). Achieving optimal compaction without excessively crushing the material requires careful control of construction methods and equipment. Additionally, the behavior of FGA under dynamic traffic warrants further investigation. Its low density raises concerns regarding buoyancy during flooding and susceptibility to wind erosion. As an emerging and unconventional material, a comprehensive engineering study of FGA is essential before its widespread application to prevent unsatisfactory performance in specific use cases.

1.2 Objectives

The objective of the proposed project is to conduct a systematic study on the performance of FGA, explicitly tailored to the conditions and requirements of its intended applications by Illinois Tollway, such as highway embankments, retaining wall backfill, and bridge abutments.

1.3 Organization of Report

This report consists of five chapters. Chapter 1 introduces the background and objectives of the research. Chapter 2 presents the findings of a literature review of related topics and the current practices of highway agencies based on survey results. Chapter 3 describes the study materials and the laboratory tests conducted to determine the performance of FGA in embankments. Chapter 4 presents the test and analysis results. Chapter 5 provides conclusions, recommendations for further study, and a draft special provision for the construction of FGA. Appendix A provides a design guide for the use and application of FGA.

CHAPTER 2: LITERATURE REVIEW AND SURVEY RESULTS

To understand the state-of-the-art and state-of-the-practice regarding the use of foamed glass for geotechnical applications, the research team reviewed the relevant literature and synthesized the results herein. In addition, the team surveyed highway agencies to gather information on their current practices.

2.1 Literature Review

2.1.1 Introduction

Glass stands out as an exceptionally recyclable material, offering the potential for continuous reuse or recycling (Robert et al., 2021). Current estimates reveal that globally, only 21% of the total annual glass production, approximately 27 million tons, is recycled (Recovery, 2018). The substantial volume of accumulated waste glass worldwide presents a significant opportunity for the recycling market. This situation highlights the importance of further research and development to explore new applications for recycled glass (Mustafa et al., 2023a).

Lightweight fill materials are gaining attention as construction materials in civil engineering applications. Among their advantages, such as thermal insulation, the primary aim of using lightweight fill materials is to reduce the overall weight of fills, thereby addressing concerns related to excessive settlements and vertical or lateral bearing failures (Horpibulsuk et al., 2014; Arulrajah et al., 2015a). Foamed glass aggregate (FGA), a processed recycled glass product, is utilized as a lightweight fill material in construction projects situated over soft ground or in proximity to load-sensitive infrastructure. This application has been in practice for over 25 years since its initial production in Europe (McGuire et al., 2021).

Several case studies from different states in the U.S. have demonstrated its broad applications. FGA has been used (AERO Aggregates, 2019):

- Over soft soils in embankments or as structural backfill by the Departments of Transportation (DOTs) in Maine, Minnesota, New Hampshire, New Jersey, New York, Pennsylvania, and Virginia, as well as the Federal Highway Administration.
- Over-sensitive utilities (e.g., sewer lines, water mains, or culverts) by DOTs in the District of Columbia, Michigan, New Jersey, Pennsylvania, and Rhode Island.

- Slope stability (e.g., instability issues or sloping 1:1 to eliminate the need for a retaining wall) by DOTs of Minnesota and Pennsylvania, as well as the Federal Highway Administration.
- Reduction of lateral pressure to adjacent structures (e.g., bridge abutments or retaining walls) by the DOTs of New Jersey and Pennsylvania.
- Ease of construction (e.g., during rain and snow, in flooded areas, or tidal zones) by the DOTs of New Hampshire and Pennsylvania.

Even though FGA has been used in Europe and Japan for decades, there is a need for a systematic study of FGA for geotechnical applications in the U.S. This literature review focuses on the engineering properties of FGA as an embankment or structural backfill material. It is noted that when compared to conventional soils, relatively limited information of FGA has been published.

2.1.2 Foamed Glass Aggregate (FGA) Production

Foamed glass is produced industrially using a process that involves cleaning and crushing glass particles, known as cullet. These particles are ground to a fine powder (typically finer than 0.0039 in.), as shown in Figure 1, and combined with a foaming agent in liquid (wet foaming process), e.g., glycerin, or powder form (dry foaming process), e.g., silicon carbide. The resulting powder is evenly spread onto a conveyor belt, which passes through a furnace where it is heated to temperatures ranging from 1,454 to 1,832°F for melting (Guo et al., 2010; Steurer, 2012; Auvinen et al., 2013; Arulrajah et al., 2015a).

The intense heat and activation of the foaming agent cause the glass volume to expand several times. Notably, over 90% of foamed glass consists of air bubbles. Upon cooling, the foamed glass fractures into pieces due to inherent thermal stress as it transitions from high temperature to ambient temperature, resulting in a distribution of particle sizes known as foamed glass aggregate, as shown in Figure 2 (Auvinen et al., 2013; Arulrajah et al., 2015a).

FIGURE 1. Glass waste cullets (Betti et al., 2014).

FIGURE 2. Foamed glass aggregate manufactured (Loux et al., 2019).

Numerous studies have explored the impact of various production parameters on the characteristics of FGA. These parameters can be broadly categorized into three groups: the type of glass utilized (Méar et al., 2006; Østergaard et al., 2019), the type of foaming agent employed (König et al., 2019; Østergaard et al., 2019), and the production temperature applied (Bernardo & Albertini, 2006; Méar et al., 2007; Mucsi et al., 2013; König et al., 2020). For example, researchers have investigated the impact of production temperature on FGA's porosity, particle density, crushing strength, and other properties. Bernardo et al. (2006) found that the heating rate correlates directly with relative density, which is the ratio between the measured density of the foams and the density of the employed glass.

While the predominant method for producing FGA in practical applications involves the use of a dry foaming agent, there are instances where a wet foaming agent is employed (AERO Aggregates - TN220, 2022). FGA particles can be either open-cell or closed-cell. The degree of pore interconnection within FGA determines its structural classification as closed-cell or open-cell (König et al., 2020). Closed-cell FGA, which has relatively few interconnected pore spaces, comprises the majority of FGA currently used in civil engineering applications (AERO Aggregates - TN220, 2022). Both closed- and open-cell FGA have high hydraulic permeability and are considered free-draining materials.

2.1.3. Gradation of FGA

While the gradation of FGA may differ among production facilities, it consistently falls under the classification of coarse granular material (Auvinen et al., 2013; McGuire et al., 2021; Mustafa & Szendefy, 2023a), as illustrated in Figure 3. The nominal particle size of FGA can range from 0.5 to 2.5 inches (Lenart & Kaynia, 2019; Loux et al., 2019; Mustafa et al., 2022). The reported average coefficients of uniformity (Cu) and curvature (Cc) are 1.6 and 1.13, respectively (Lenart & Kaynia, 2019; Mustafa & Szendefy, 2023a).

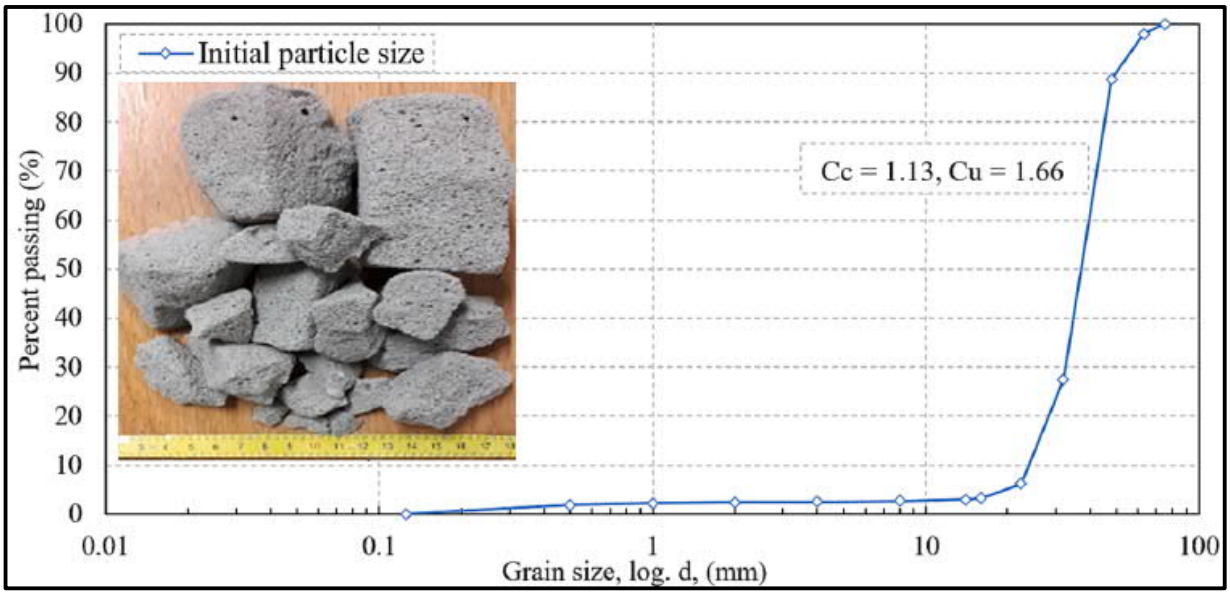

FIGURE 3. Grain size distribution of FGA in Hungary (Mustafa & Szendefy, 2023).

2.1.4. Density, Moisture content, and Particle Breakdown of FGA

The density of FGA is heavily influenced by its production procedures. Mustafa et al. (2022) noted a bulk unit weight of 10 lb/ft³ for FGA from a Hungarian producer, while Lenart et al. (2019)

reported a loose unit weight of 15 lb/ft³ for Norwegian FGA. McGuire et al. (2021) reported a loose unit weight ranging from 12 to 15 lb/ft³ for FGA in the U.S.

Auvinen et al. (2013) provided additional density measurements, including dry bulk density, dry compacted density, and long-term density in a road structure, compiled in Table 1.

TABLE 1. Properties of Foamed Glass (Auvinen et al., 2013) **(Note: 1 kg/m^3 = 0.0624 lb/ft^3 and 1 mm = 0.039 in.).**

Properties	Variations recorded in technical literature	Measurement values
Granular size	10-50/10-60 mm	10-60 mm
Dry bulk density	180~230 kg/m^3	210 kg/m^3 ± 15%
Dry compacted density	225~290 kg/m^3	220~280 kg/m^3
Long-term in a road structure density	270~530 kg/m^3	350 kg/m^3
Long-term underwater density	-	600 kg/m^3
Water absorption short-term (4 weeks)	30~60 weight-%	60 weight-%
Water absorption long-term (1 year)	40~116 weight-%	100 weight-%

Regarding compacted unit weight, Betti et al. (2014) utilized a gyratory compactor to compact FGA, resulting in a density range of 25 to 29 lb/ft³. McGuire et al. (2021) reported that the compacted field unit weight of FGA ranged from 13 to 19 lb/ft³, depending on the levels of compaction efforts and compaction methods. Various compacted unit weight of FGA at different volume reduction (or compression ratios: uncompacted height over compacted height) are detailed in Table 2 (AERO Aggregate – TN 303, 2018). Moist compacted unit weight was achieved by adding 6% moisture content by volume.

TABLE 2. Compacted and Uncompacted Unit Weight of FGA in the Field (AERO Aggregate – TN 303, 2018).

Compression ratio	Dry unit weight (pcf)	Moist unit weight (pcf)
1.0 (uncompacted)	15.00	18.74
1.1	16.50	20.62
1.2	18.00	22.49
1.25	18.75	23.43
1.3	19.50	24.37

Typically, conventional aggregates experience a maximum fines content increase of 1% after compaction (Ramamurthy et al., 1974). However, FGA particles, owing to their high porosity, are more prone to breakdown during compaction, depending on the compaction methods and efforts. This issue is crucial, as changes in gradation can significantly impact the behavior of the constructed layer under diverse loading and environmental conditions. Researchers have, therefore, investigated the particle size distribution of FGA before and after various compaction methods. Mustafa et al. (2023c) examined the grain size distribution of FGA under different static compression compaction levels. As illustrated in Figure 4, when the volume reductions increase from 10%, 20%, and 30% to 40% based on static compaction, the gradations become finer (Mustafa et al., 2023c). To demonstrate the impact of different compaction methods, an early study by Swan et al. (2016) compacted FGA using Standard and Modified Proctor methods. Figure 5 indicates that higher compaction (solid red line) results in significantly more particle breakdown than standard energy (blue lines). FGA, after compaction using either standard or modified Proctor protocols, exhibits a distribution curve akin to well-graded material rather than poorly graded material (Swan et al., 2016).

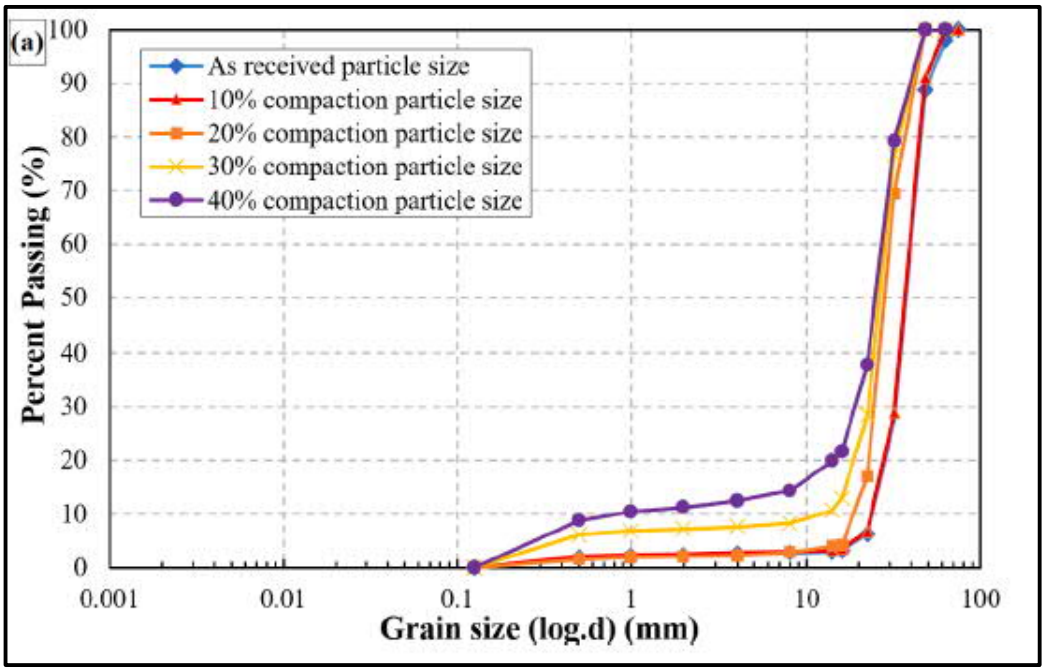

FIGURE 4. Gradation of FGA before and after compaction (Mustafa et al., 2023c).

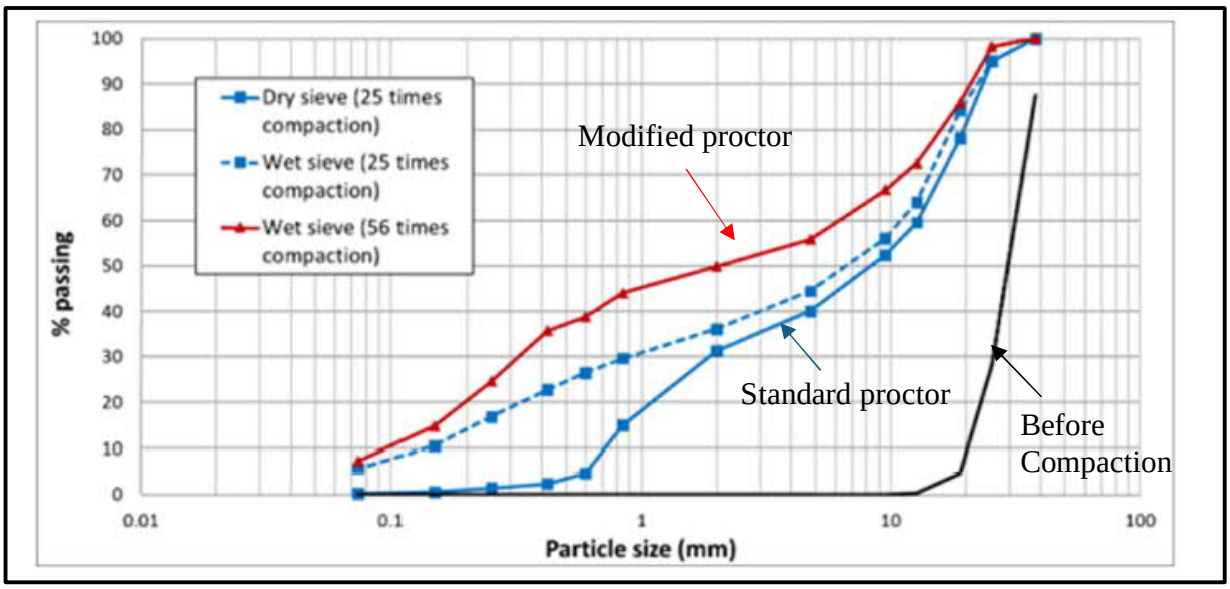

FIGURE 5. Comparison of standard and modified proctor test effects on the particle size distribution of FGA (Swan et al., 2016). **[Arrows and Annotations Added]**

2.1.5. Mechanical Properties

Researchers have investigated the mechanical properties of FGA, including the California bearing ratio (CBR), resilient modulus (M_r), friction angle (Φ'), cohesion (c'), and long-term creep.

2.1.5.1. Friction Angle (Φ') and Cohesion (c')

Illinois DOT's specification for the effective internal friction angle of mechanically stabilized earth (MSE) wall select fill is a minimum of 34°, based on AASHTO T236 (direct shear test method) (IDOT, 2022). Arulrajah et al. (2015b) noted that, based on a linear strength envelope, the internal friction angle and pseudo-cohesion of FGA in direct shear tests were approximately 54.2° and 3.29 psi, respectively, with normal stresses ranging from 1.45 psi to 5.8 psi. Swan et al. (2016) tested FGA's friction angle using direct shear tests, comparing as-received gradation with modified gradation after compaction, and observed a decrease in the friction angle with an increase in the range of normal stresses applied (see Table 3). This phenomenon can be attributed to the breakdown of FGA during shearing at high normal stress levels (Swan et al., 2016).

TABLE 3. Friction Angle and Pseudo-Cohesion of FGA under Various Normal Stress Ranges (Swan et al., 2016) **(note: 1 kPa = 0.145 psi).**

Tested material	Range of normal stress (kPa)	Peak friction angle (°)	Peak cohesion (kPa)
As-received LWA-FG	14.4 to 57.5	56	2.1
As-received LWA-FG	35.9 to 144	29	45.8
As-received LWA-FG	144 to 426	27	46.0
Modified LWA-FG	144 to 426	31	51.5

Loux and Filshill (2021b) reported that the friction angle of FGA samples ranged from 41 to 55 degrees. In a comparative study assessing FGA against traditional embankment or backfill material, Nicks et al. (2024) examined two FGAs (FGA 1—wet foaming and FGA 2—dry foaming) and compared them to AASHTO No. 8 open-graded aggregate (diabase). Both FGAs and No. 8 aggregate underwent testing in dry and saturated conditions to simulate field scenarios under various environments. As detailed in Table 4, the conventional aggregate exhibited the highest friction angle from direct shear tests; however, the FGAs, which were compacted to an 11% volume reduction, also displayed high friction angle values (Nicks et al., 2024). The residual friction angle of FGA was markedly higher than that of No. 8 aggregate.

TABLE 4. Comparison of Friction Angle of FGAs and AASHTO No. 8 (Nicks et al., 2024).

		FGA-1			FGA-2			No. 8		
Test condition	Duration	$\varphi_{s,2\,\%}{}^{\circ}$	$\varphi_{s,p\,\%}{}^{\circ}$	$\varphi_{r\,\%}{}^{\circ}$	$\varphi_{s,2\,\%}{}^{\circ}$	$\varphi_{s,p\,\%}{}^{\circ}$	$\varphi_{r\,\%}{}^{\circ}$	$\varphi_{s,2\,\%}{}^{\circ}$	$\varphi_{s,p\,\%}{}^{\circ}$	$\varphi_{r\,\%}{}^{\circ}$
Dry	LD	37.7	56.4	54.8	42.8	60.9	56.7	56.2	61.1	48.4
	SD	38.5	58.5	58.0	45.7	60.2	58.0	57.7	61.4	46.3
Saturated	LD	28.6	55.4	54.7	48.8	59.4	59.2	57.2	64.4	49.9
	SD	37.0	56.3	56.2	45.8	60.5	56.6	54.1	61.6	48.7

Note: LD = Long duration (28-day); SD = Short duration (about 10 minute); $\varphi_{s,2\,\%}$= Secant friction angle at 2% lateral strain; $\varphi_{s,p\,\%}$= Peak secant friction angle; $\varphi_{r\,\%}$= Residual friction angle.

2.1.5.2. California Bearing Ratio (CBR), and Modulus (M_r)

The California Bearing Ratio (CBR), which represents the ratio of a material's penetration resistance to that of standard crushed stone, serves as an indicator of strength and bearing capacity under loading (Thakur & Han, 2015). Arulrajah et al. (2015b) reported CBR values for FGA samples ranging from 9% to 12%. However, the CBR is significantly influenced by the compaction level of the samples. Betti et al. (2014) demonstrated the impact of compaction efforts on the CBR of two FGA samples (FGA 1—wet foaming and FGA 2—dry foaming) in Figures 6 and 7, respectively. Table 5 outlines the expected CBR values for conventional embankment soils (Christopher et al., 2006) for comparison purposes. FGA has a CBR similar to sandy materials rather than fine-grained soils (Christopher et al., 2006).

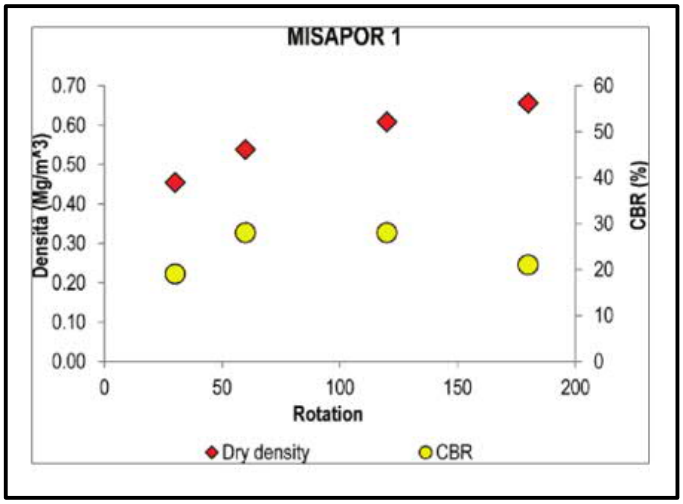

FIGURE 6. CBR vs degree of compaction (number of rotations of gyratory compactor) for FGA1 (Betti et al., 2014).

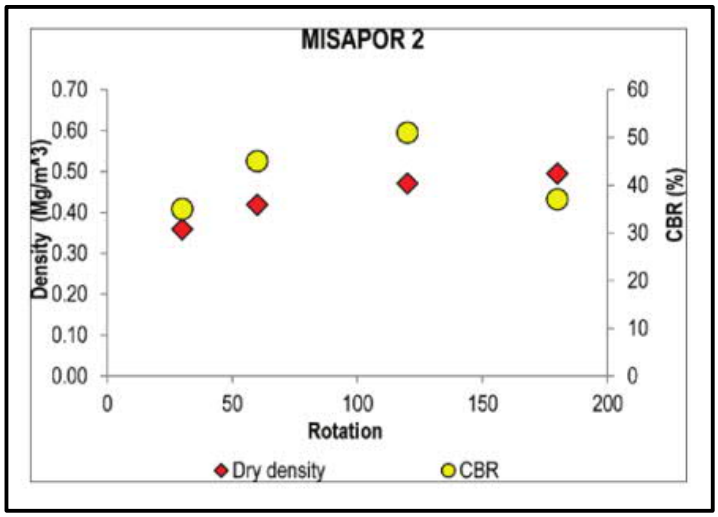

FIGURE 7. CBR vs degree of compaction (number of rotations of gyratory compactor) for FGA2 (Betti et al., 2014).

TABLE 5. California Bearing Ratios (CBRs) of Embankment Soils (Christopher et al., 2006).

USCS soil classification	Field CBR
Silty Sand (SM)	20-40
Clayey Sand (SC)	10-20
Low plastic silt (ML)	5-15
Low plastic clay (CL)	5-15
High plastic silt (MH)	4-8
High plastic Clay (CH)	3-5

However, the utilization of CBR test outcomes for assessing conventional fill materials was found to be limited, as it inadequately reflects field performance due to large strain (Camargo et al., 2013). To better simulate the actual performance of FGA, researchers recommended measuring various moduli, such as resilient modulus, shear modulus, and stiffness modulus.

The resilient modulus, a measure of a sample's stiffness under repeated loads in triaxial tests, can more accurately simulate traffic load conditions in the field (Barzegar et al., 2023). Auvinen et al. (2013) reported that the resilient modulus of FGA ranges between 10 ksi and 21 ksi. In a study by Mustafa et al. (2023a), the findings of Auvinen et al. (2013) were corroborated. For comparison, conventional crushed aggregates have resilient moduli ranging from 16.0 to 25.6 ksi

(Guthrie & Jackson, 2015), while fine-grained soils can have a resilient modulus of approximately 10 ksi (Lee et al., 2002).

The shear modulus is the ratio between shear stress and shear strain. Lenart et al. (2019) employed a cyclic triaxial setup to confine FGA samples using confining pressure and measure the shear modulus (Lenart & Kaynia, 2019). The shear modulus of FGA ranges from 4.2 ksi to 23.7 ksi (29 MPa to 163 MPa), depending on the shear strain level. When compared to conventional soils, as shown in Table 6 (Sawangsuriya, 2012), the shear moduli of FGA are close to those of conventional sandy materials.

TABLE 6. Typical Ranges of Shear Modulus for Different Types of Soils (Sawangsuriya, 2012) (1MPa = 0.145 ksi).

Soil type	Shear modulus (MPa)
Dense sands & gravels	69-345
Silty sand	27.6-138
Medium stiff clay	6.9-34.5
Soft clays	2.75-13.75

The elastic modulus, also known as stiffness modulus, is a parameter used to examine the behavior of materials within the elastic region of deformations. Betti et al. (2014) used a lightweight deflectometer (LWD) to obtain the stiffness modulus in the field. Based on Equation 1, the elastic modulus (E) varies in the range of 7 ksi to 10 ksi, depending on the applied stress (Betti et al., 2014).

$$E = \frac{f(1v^2)\sigma_0 a}{d_0} \quad (1)$$

where:

f = plate rigidity factor;

a = load plate radius;

σ_0 = maximum value of the applied stress;

d_0 = maximum value of the measured deflection.

Based on a large-scale uniaxial compression test in a test box, Steurer (2012) studied the stiffness modulus of FGA under different compaction levels and applied stresses. Figure 8 illustrates the effects of static compaction and pressure levels on the stiffness modulus. As expected, when the compaction level increases, the stiffness modulus also increases. Additionally, the stiffness modulus increases as normal stress increases (likely due to further consolidation) but then decreases as normal stress increases further.

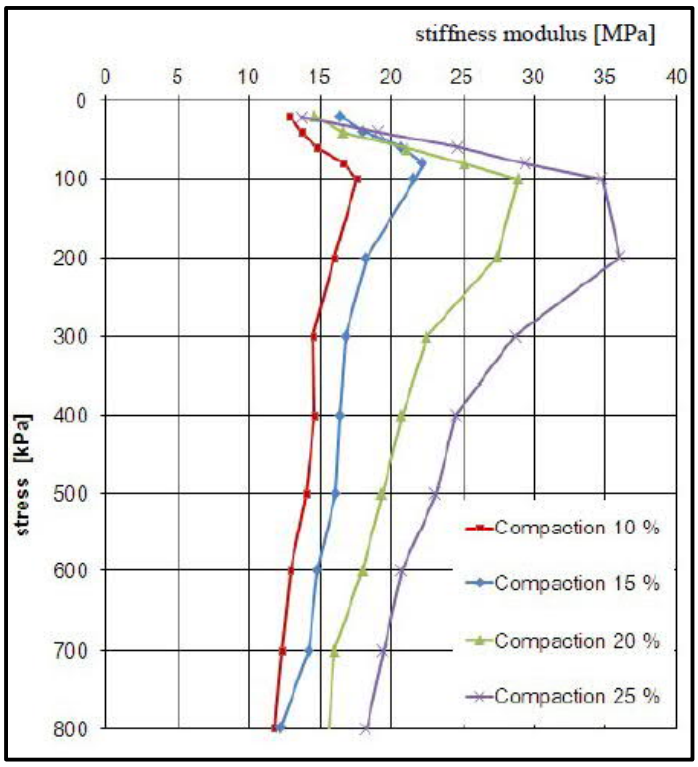

FIGURE 8. Stiffness modulus of FGA statically compacted to different levels under various applied stresses (Steurer, 2012).

2.1.5.3. Climatic Effects and Hydraulic Properties

Temperature, moisture, and freeze-thaw cycles are the three primary climatic factors influencing the engineering characteristics of fill materials. The thermal conductivity of foamed glass can vary widely, ranging from 16.4 $mWm^{-1}K^{-1}$ up to 215 $mWm^{-1}K^{-1}$ (Skogstad et al., 2005; Méar et al., 2007; König et al., 2019; Mustafa et al., 2023b). For comparison, the average thermal conductivity of many soil minerals is 2.9×10^{3} $mWm^{-1}K^{-1}$ and while for soil organic matter, it is 0.25×10^{3} $mWm^{-1}K^{-1}$ (Hanson et al., 1999). Researchers have extensively investigated the parameters influencing the thermal conductivity of foamed glass (Skogstad et al., 2005; Østergaard et al., 2019; König et al., 2019; Mustafa et al., 2023b). For instance, Østergaard et al. (2019) studied

the impact of foaming agent-generated gas composition on FGA properties. Additionally, humidity conditions, temperatures, and compaction ratios were also studied as influential parameters on FGA's thermal properties (Mustafa et al., 2023b).

Due to its extremely low thermal conductivity, Scarinci et al. (2005) proposed FGA as a material resistant to freeze-thaw cycles. In a study by Skogstad et al. (2005), the freeze-thaw resistivity of FGA was tested by immersing the material in water for 28 days and subjecting the FGA particles to 300 freeze-thaw cycles. Each cycle involved one hour of exposure to cold air (-4°F) followed by one hour in room-temperature water (68°F). The FGA exhibited no deterioration, and the freeze-thaw cycles had no impact on the compressive strength of FGA.

Another test for measuring the resistance of aggregates to freeze-thaw cycles is the soundness test. AASHTO requires the magnesium sulfate soundness of aggregate used in MSE wall backfill to be no more than 30%, whereas FGA has a soundness value ranging from 4.1% to 14% (Loux and Filshill, 2021b). Illinois DOT's specification for Na_2SO_4 soundness is a maximum of 15% (IDOT, 2022). The hydraulic conductivity, or permeability, of compacted FGA is high ($k > 1$ cm/s), which constitutes a free-draining material (Loux et al., 2019). For comparison, the average saturated hydraulic conductivities for seven gravels and nine sandy soils were 0.324 cm/s and 0.014 cm/s, respectively (Oh et al., 2022).

2.1.5.4. Creep and Permanent Deformation

2.1.5.4.1. Introduction to Soil Settlement

Soil settlement occurs in three distinct stages: (1) immediate or elastic settlement, (2) primary consolidation, and (3) secondary compression or creep (Bergaya et al., 2013). Elastic settlement occurs during or immediately after construction (Kong, 2016). Primary consolidation settlement results from the dissipation of excess pore pressure and the subsequent volume change in the soil (Zou et al., 2016). Secondary compression, also known as one-dimensional creep, involves ongoing volume changes due to micro shear strain and has the potential for long-term continuation. Creep can originate from deviatoric or shear stress and involves the accumulation of time-dependent macro shear strain under sustained shear stress, regulated by the viscosity of the soil structure (Mitchell & Soga, 2005). As depicted in Figure 9, creep settlement becomes prominent when soil is subjected to high or prolonged stresses.

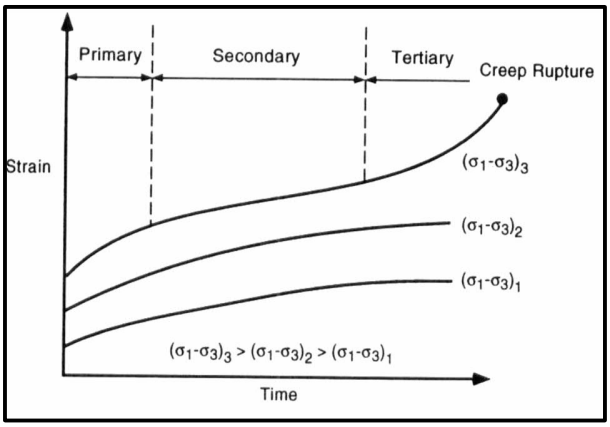

FIGURE 9. Creep modes under constant deviatoric stress (Mitchell & Soga, 2005).

2.1.5.4.2. Creep Characteristics of FGA

Steurer et al. (2012) studied the creep characteristics of FGA samples with diverse grain properties under varying confining pressures. The creep behavior of FGA over time is notably influenced by factors such as confining pressure, compaction level, and grain porosity. In Figure 10, FGA's creep strain increment between stress intervals (not accumulated creep) increased as applied stresses increased, reached a peak, and then decreased. This phenomenon might occur because FGA undergoes further compaction during the initial stress steps, making it stiffer. As expected, higher compaction levels result in lower creep strain increments.

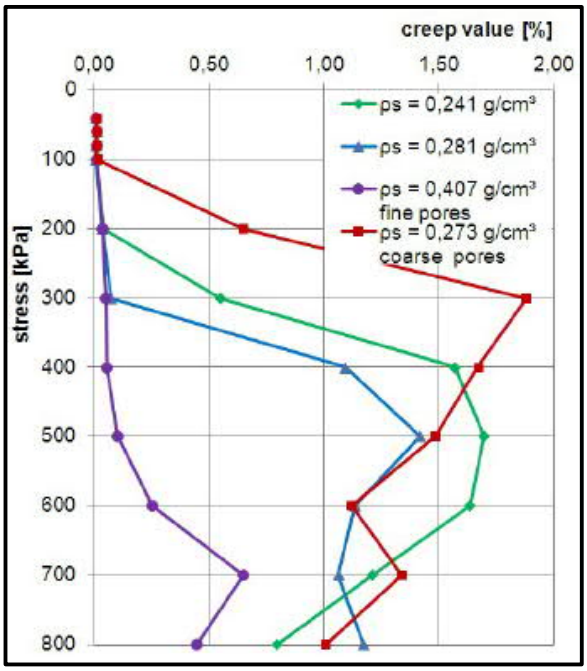

FIGURE 10. Incremental creep strain of FGA with various densities under long-term confined compression test (Steurer, 2012).

Swan et al. (2016) examined the impact of loading duration on the static compression behavior of FGA. The long-term creep performance of FGA was assessed over 7 days at a pressure of 3.48 psi. The creep test indicated that after 100 hours (6,000 minutes) of loading, the creep strain remained stable at the beginning, followed by an accelerated rate of 6.56×10^{-8} per minute (see Figure 11) (Swan et al., 2016).

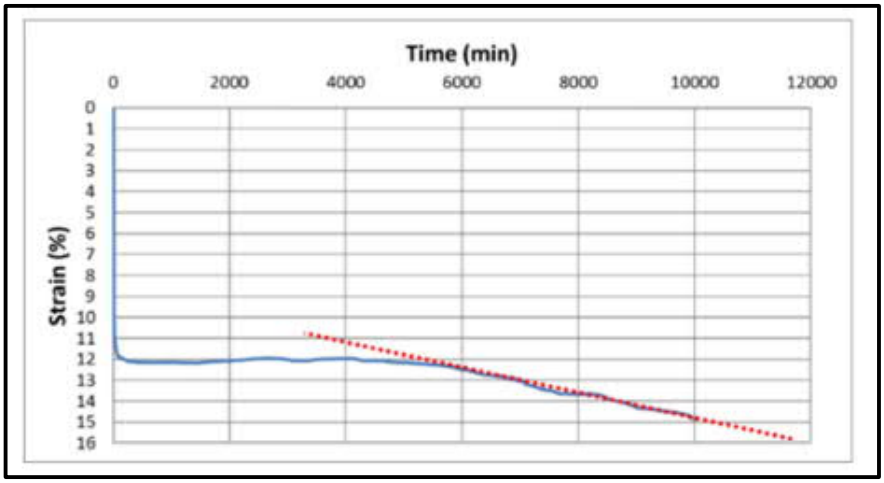

FIGURE 11. Vertical strain vs time for 7 days under 3.5 psi (24 kPa) (Swan et al., 2016).

According to research by Mustafa et al. (2023c) and Nicks et al. (2024), the creep of FGA stabilizes after the initial settlement. However, this finding might vary depending on the specific type of FGA and the compaction method under consideration. The study by Mustafa et al. (2023c) indicated that as volume reduction increases (i.e., 40% volume reduction), Figure 12 shows that FGA can sustain a higher static load without tertiary creep, as defined in Figure 9. In the study by Nicks et al. (2024), two types of FGA exhibited significantly different behaviors. Figure 13 illustrates the long-term performance of two FGA types and a conventional aggregate. In contrast to the similar behavior between FGA-2 (dry foaming) and AASHTO No. 8 (diabase), FGA-1 (wet foaming) exhibited significantly greater creep and took longer to reach settlement stability.

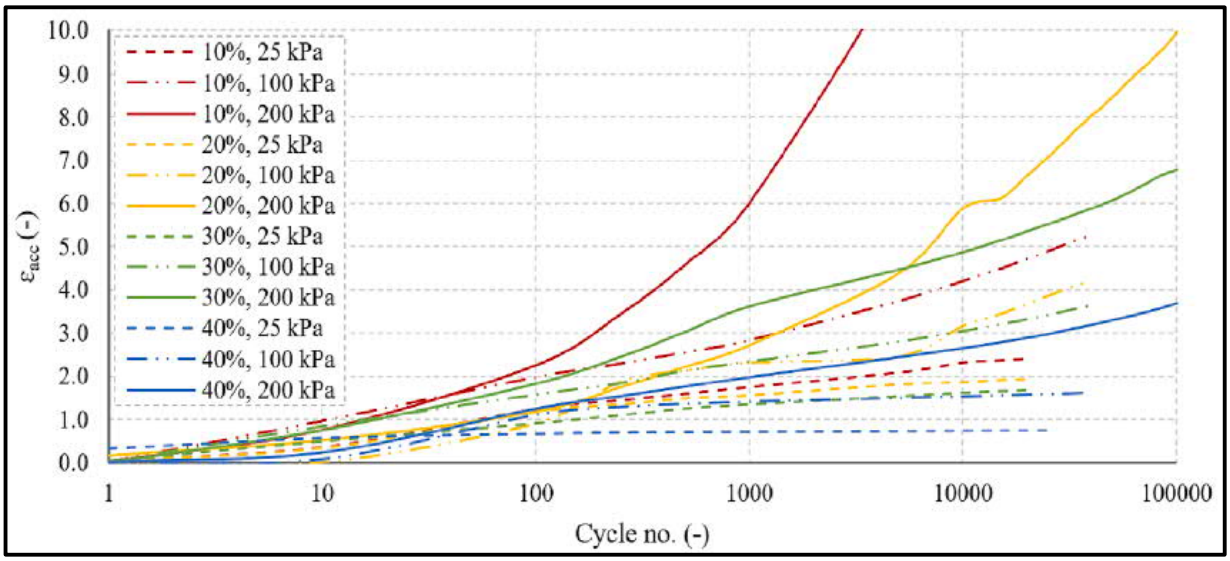

FIGURE 12. Accumulated strain for various compaction ratios and deviatoric stresses for FGA in cyclic loading tests (Mustafa et al., 2023c).

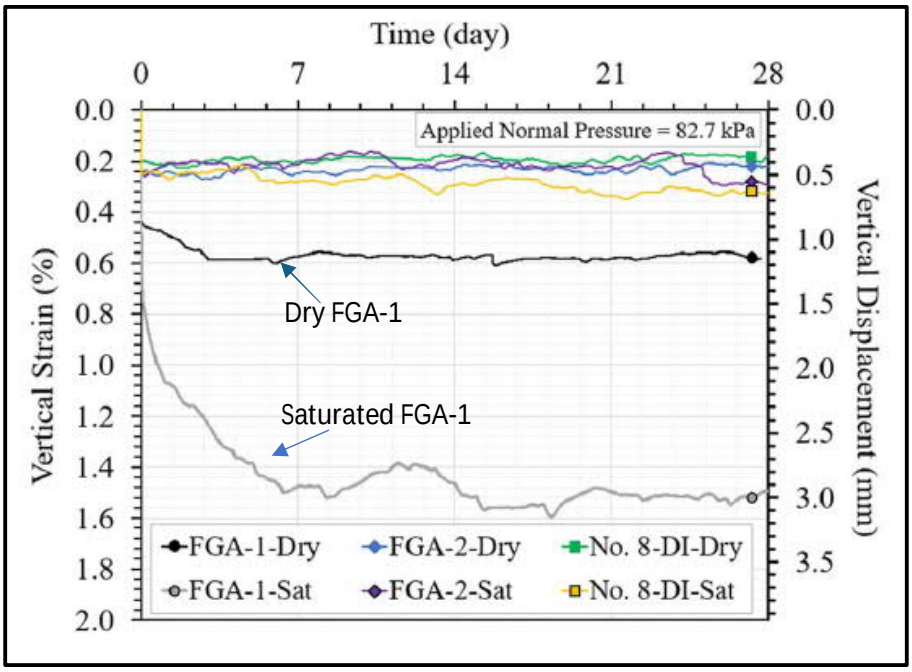

FIGURE 13. Change in vertical strain of FGA-1, FGA-2 and conventional aggregates in a period of 28 days under 82.7 kPa of pressure (Nicks et al., 2024). **(Arrows and Annotations added)**

2.1.5.5. Other Properties of FGA

An issue associated with the utilization of FGA in MSE walls incorporating steel and geosynthetic reinforcements is the potential susceptibility of steel to corrosion or geosynthetics to degradation. AASHTO and Illinois DOT mandate that the geomaterials used in MSE walls must exhibit a pH within the range of 5.0–10.0 for steel reinforcement and 4.5–9 for geosynthetic reinforcement (AASHTO, 2017; IDOT, 2022). Loux and Filshill (2021b) reported a pH range for FGA of 9.2–9.4, based on modified AASHTO test methods. However, research conducted by Arulrajah et al. (2015a) yielded a pH value for FGA of 10.48, following Australian Standard 1289.4.3.1.

In addition to pH considerations, AASHTO and Illinois DOT require geomaterials to meet specific criteria concerning electrical resistivity, chloride content, and sulfate content. A summary of the reported value for FGA is provided in Table 7. Note that the test methods used to determine the reported values were different from the methods specified by Illinois DOT.

TABLE 7. Summary of Electrochemical Requirements for MSE Wall (Loux and Filshill, 2021b)**.**

Parameters	FGA Reported Values
pH	9.2-9.4
Resistivity	• >3,366,000 Ω.m (As received) • 52,020 Ω.m (Initial – 100% Saturated) • 18,666 Ω.m (24-hr Soak – 100% Saturated) • 13,158 Ω.m (48-hr Soak – 100% Saturated)
Chlorides	<10-19 ppm
Sulfates	<10-11 ppm

2.1.6. Placement and Compaction in the Field

In contrast to conventional sources of embankment or structural fill, the placement of FGA in the field requires careful consideration. This emphasis on FGA placement stems from its vulnerability to breakdown during the compaction process. Frydenlund et al. (2007) provided recommendations for FGA compaction based on their study of several cases in Norwegian public roads. One of their suggestions was to place FGA layers at a thickness of 19.7 in (0.5 m) and compact them with 3–4 passes using a 30-ton crawler excavator (Frydenlund & Aabøe, 2007). Loux and Filshill (2021b) reported that suitable equipment for compacting FGA should exert a pressure of 4.35–7.25 psi and complete compaction in four passes, discouraging the use of static or vibratory rollers unless higher compaction levels are necessary (Loux and Filshill, 2021b). McGuire et al. (2021) conducted a comprehensive study to assess the performance of various compaction equipment in different scenarios. Table 8 outlines the equipment, and the thicknesses of FGA lifts used in their study. A LiDAR scanner was employed to determine the volume of FGA before compaction, during different passes, and post-compaction, as shown in Figure 14 (McGuire et al., 2021).

TABLE 8. The Number and the Thicknesses of the Lifts and the Passes Scanned (McGuire et al., 2021).

Test	Compactor	Lift	Thickness, ft (mm)	Passes scanned
A-1	John Deere dozer	1	2 (610)	1,2,4
A-2	John Deere dozer	1 2	2 (610)	1,2,4 1,2,4,8,16
B-1	Doosan excavator	1 2 3	2 (610)	1,2,4 1,2,4 1,2,4,8,16
C-1	Komatsu excavator	1 2 3	2 (610)	1,2,4 1,2,4 1,2,4,8,16
C-2	Komatsu excavator	1 2	1 (305) 3 (915)	1,2,4,8,16 1,2,4,8,16
D-1	Wacker plate	1 2 3	1 (305) 1 (305) 2 (610)	1,2,4 1,2,4 1,2,4,8,16
D-2	Wacker plate	1 2	1 (305)	1,2,4 1,2,4,8
E-1	Bomag roller	1	2 (610)	1,2,4,8

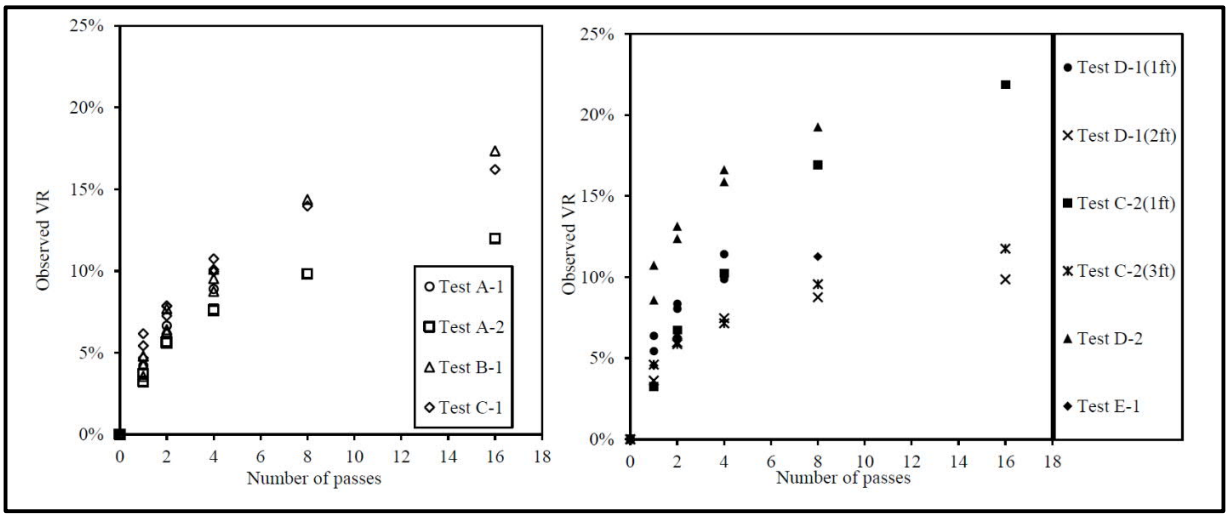

FIGURE 14. Volume reduction vs. number of passes of various equipment (McGuire et al., 2021).

McGuire et al. (2021) determined that, after leveling a loose lift of FGA with a rake, four passes of tracked equipment on a two-foot lift or four passes of a vibratory compactor on a one-foot lift would, on average, reduce the fill volume by 9.15% and 13.25%, respectively. Qamhia et al. (2023) corroborated the findings of McGuire et al. (2021) and recommended the use of a dozer or tracked excavator capable of applying a pressure of 600 to 1000 psf. They suggested limiting the lift thickness to a maximum of 24 inches and applying compaction in two to four passes (Qamhia et al., 2023).

2.2 Survey of State Highway Agencies

To understand state agencies' practices regarding the use of FGA, the research team distributed a questionnaire to highway agency members affiliated with the AASHTO Committee on Materials and Pavements. Responses from 15 state Departments of Transportation (DOTs) were recorded, which is as expected for such a niche material in the U.S. Based on these responses, the research team contacted several state DOTs for interviews. Engineers from three DOTs (NY, PA, and VT) agreed to further discussions via virtual meetings. The following section summarizes the survey responses, special provisions provided by the agencies, and interview results. Given the commonality of initial letters among several DOTs, state abbreviations are used for clarity.

2.2.1 Use of FGA as Fill by State Agencies

According to the responses, nine DOTs (AR, CT, FL, HI, ME, NY, PA, TX, and VT) allow using FGA for geotechnical applications through their special provisions, while the other six states do not. Note that it is possible that some agencies that have used FGA did not respond to this survey.

2.2.2 Applications of FGA

FGA has been used or is going to be used by agencies for highway embankment (AR, CT, HI, ME, NY, PA, and VT), MSE wall select fill (FL, PA, and VT), bridge abutment backfill (ME, NY, PA), other retaining wall backfills (NY and PA), and trench backfill (NY). In terms of site conditions that warrant the use of FGA, FGA has been placed over soft soils (CT, HI, ME, NY, PA, and VT); over sensitive underground structures (AR and PA); and when expedited construction is needed (CT, ME, and PA). PA DOT does not permit the use of FGA for bedding and does not recommend the use of FGA for trench backfill.

2.2.3 Appealing Characteristics of FGA

Survey responses highlight several appealing features of FGA, starting from the most preferred characteristic:

- Lightweight nature
- High friction angle
- Recycled material composition
- High permeability
- High insulating properties

In addition, easy placement was also considered another benefit of FGA by DOTs (AR, FL, and IN). Ease of construction was not ranked because only three agencies selected it. Table 9 shows a summary of the rankings provided by the agencies.

TABLE 9. Summary of Ranking of FGA Characteristics (Note: The lower number indicates more appealing characteristics).

States	Lightweight	High Friction	Recycled Materials	High Permeability	High Thermal Insulation	Ease of Construction
AR	1	2	3	5	4	x
CT	1		3	2		
FL	1	3	2	4	5	x
HI	x		x			
IN			2		3	1
ME	1	2	4	3	5	
NY	1	3	2			
PA	1	2	4	3	5	
VT	1	3	2	4	5	
Average	**1**	**2.5**	**2.75**	**3.5**	**4.5**	

Note: "x" indicates that agencies marked it without providing rankings.

2.2.4 Consideration of Moisture Content of the FGA for the Geotechnical Design

One of the critical properties for settlement and other geotechnical analyses is the unit weight of FGA. Seven states assume FGA to be at its natural moisture condition, but the DOTs of AR and CT consider FGA to be at its saturated surface dry (SSD) state for design purposes. PA

DOT uses a constant unit weight of 23.5 pcf for design, which accounts for natural moisture and compaction.

2.2.5 Specifications on Engineering Properties of FGA

Most agencies specify unit weight, gradation, and friction angle for FGA. Currently, NY DOT only specifies a loose, moist unit weight of no more than 20 pcf for FGA in embankments. FL DOT specifies a maximum loose moist bulk unit weight of 22 pcf, minimum compressive strengths, and a minimum apparent peak friction angle of 53˚ for normal stresses between 500 and 1,200 psf. For embankment and MSE wall backfill, the DOTs of PA and VT also limit the dry unit weight and in-place compacted dry unit weight to 15 pcf and 20 pcf maximum, respectively. PA DOT specifies a maximum 1,200 psf bearing pressure on FGA in embankments before creep considerations are addressed through settlement analysis, and pullout testing is required to confirm strap pullout for MSE wall internal stability. Table 10 provides a summary of engineering properties specified by agencies.

2.2.6 Consideration of Buoyancy for FGA

Due to the lightweight nature of FGA, it is buoyant in water, which can affect the design. The DOTs of AR and PA control the water surface below the design elevation of FGA. The DOTs of CT, IN, ME, NY, PA, and VT require the minimum use of ballast material, typically natural soil placed on top of FGA.

2.2.7 Compaction in the Field

The compaction of FGA in the field may vary depending on the location and the type of structure near the construction site. In general, notes on compaction in the field can be summarized in the following sections:

(a) Open space

All states mandate that the maximum lift thickness of the FGA layer be two feet. Only a tracked excavator or dozer capable of applying a ground pressure of 625–1025 psf is allowed. Compaction may be achieved in four passes, covering 100% of the cross-sectional area.

(b) Confined space or near sensitive structures

For both confined spaces and areas near sensitive structures, all states except VT DOT limit the compaction layer height to one foot. VT DOT has specified two feet for confined spaces and one foot for areas near sensitive structures.

Compaction shall be performed using a plate compactor weighing 110–220 lbs or a small vibrating plate with a maximum weight of 250 lbs.

TABLE 10. Summary of Engineering Properties of FGA Specified by Agencies.

Locations	Density	Compressive strength	Gradation	Friction angle	pH	Others
Embankment	IN, ME, NY, PA	PA	IN, ME	ME, PA,		IN: Degradation during compaction and environmental fire resistance; PA: Maximum 1250 psf weight before creep is to be addressed.
MSE wall select fill	FL, IN, PA (Minimum unit weight)	FL, PA	FL, IN	FL, IN, PA	FL	IN: Degradation during compaction, permeability, and environmental fire resistance; PA: Pullout testing.
Other retaining wall	IN, PA	PA	IN	IN, PA		IN: Degradation during compaction, permeability, and environmental fire resistance.
Bridge abutment backfill	ME, PA	PA	IN, ME	IN, ME, PA		IN: Degradation during compaction, permeability, and environmental fire resistance.
Pipe bedding	IN		IN			IN: Degradation during compaction and environmental fire resistance; PA: Not permitted.
Trench backfill	IN		IN			IN: Degradation during compaction and environmental fire resistance; PA: Not recommended.

(c) Degree of compaction control

DOTs of AR, FL, ME, and PA rely on the number of passes made on each lift. In addition, DOTs of AR and ME require the presence of a DOT representative to verify the quality of compaction. VT DOT is considering the use of LiDAR to measure the percentage of compaction of the original lift thickness. NY DOT is currently experimenting with the use of a lightweight deflectometer (LWD). Although VA DOT did not respond to this survey, its special provision on FGA requires a 20% volume reduction for compaction. However, VA DOT does not specify the method for measuring volume reduction.

2.2.8 FGA Breakdown During the Compaction

DOTs of AR, FL, and PA reported FGA breakdown during construction. To mitigate potential particle breakdown, FL DOT does not allow construction vehicles to traverse FGA unless it is specifically for compaction. PA and NY DOT engineers observed that FGA can be dusty during placement.

2.2.9 Covering the Constructed FGA Layer

The lightweight nature of FGA may make it susceptible to erosion due to high wind speeds or precipitation. AR and NY DOTs are concerned that if left uncovered, buoyancy could be a concern for FGA. FL DOT does not require FGA to be covered. DOTs of AR, CT, ME, NY, PA, and VT cover FGA after construction, and geotextile is used between the capping layer and FGA to prevent the migration of fines into or out of FGA. ME DOT uses geotextile and riprap to cover FGA and prevent lateral movement. CT DOT's special provision specifies that conventional soil available on-site be used. PA DOT requires a minimum of 6 inches of capping materials, which may include conventional embankment materials, conventional subbase materials, topsoil, or rock.

In summary, FGA has attracted significant attention due to its unique characteristics. It has been applied in Europe and Japan for more than 20 years. However, its long-term field performance in the U.S. has yet to be fully documented, especially in comparison with conventional soils. FGA has been employed by U.S. agencies for geotechnical applications, mostly within the past six years. Therefore, laboratory experiments would provide valuable insights into the expected performance of FGA under Illinois Tollway's traffic and climatic conditions before its widespread use.

CHAPTER 3: MATERIALS AND TESTING

To study the performance of FGA in embankments, the research team conducted laboratory tests on two sources of FGA, one from the dry-foaming process (FGA1) and the other from the wet-foaming process (FGA2), and compared the results to conventional embankment soils and conventional mechanically stabilized earth (MSE) wall select fill material, used in Illinois Tollway projects. As no performance issue has been reported when these conventional embankment soils and MSE wall select fill materials were used, these conventional materials are considered the benchmark for comparative purposes.

3.1 Characterization of FGA and Benchmark Materials

3.1.1 Sampling

The project team procured FGA from two distinct sources. The first source, designated as FGA1, was produced using a dry foaming process. The second source, designated as FGA2, was manufactured using a wet foaming method. Figure 15 shows the as-received FGA1 and FGA2.

In addition to FGA materials, the research team utilized an embankment soil, designated as EMB1, sourced from a previous Illinois Tollway project (Wen et al., 2022). EMB1 is a conventional glacial till embankment soil commonly used in Illinois Tollway projects. Furthermore, sand—a standard mechanically stabilized earth (MSE) wall select fill material frequently employed in Tollway projects—was supplied by the Illinois Tollway's supporting consultant. Figure 16 illustrates the EMB1 soil and sand used in this study.

(a) (b)

FIGURE 15. As-received FGA: (a) FGA1, (b) FGA2

(a) (b)

FIGURE 16. As-received soils: (a) EMB1, (b) Sand

3.1.2 Gradations and Soil Characteristics

Upon the arrival of FGAs, three samples from each source were collected and tested to determine the as-received gradations of FGA1 and FGA2, respectively, in accordance with AASHTO T11 and T27. Sand gradation was established following the same guidelines as FGAs. EMB1 gradation was determined in accordance with AASHTO T27 and T88. Figure 17 compares the gradation of as-received gradation of FGA1, FGA2, sand, and EMB1. It showed that FGA1 is slightly finer than FGA2. Both FGAs demonstrate steep gradation curves, reflecting their open-graded nature with minimal fine content in smaller sieve ranges. EMB1 was characterized based on AASHTO T89 and T90 and classified as AASHTO A-6. Table 11 presents the plastic limit, liquid limit, and plasticity index values of EMB1 (Wen et al. 2022).

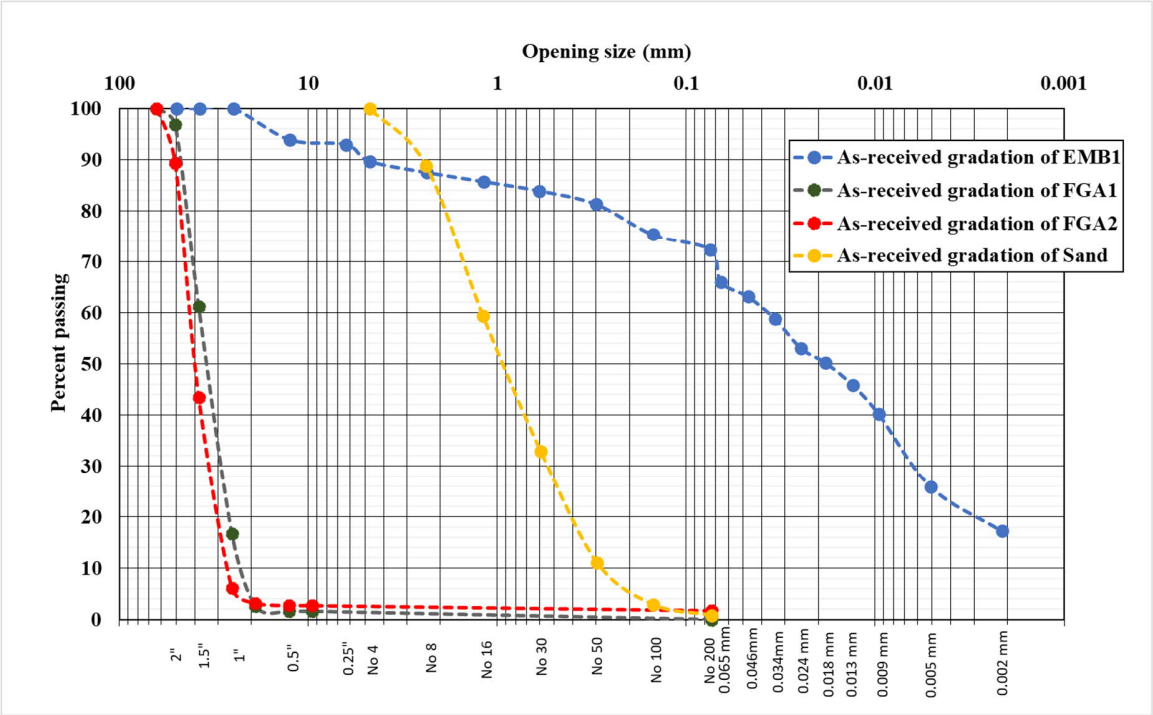

FIGURE 17. As-received gradations of materials in this study

TABLE 11. Characteristics of EMB1

	EMB1
Plastic Limit (%)	23
Liquid Limit (%)	36
Plasticity Index	13

3.1.3 Moisture-Density Relationship

Standard Proctor compaction tests were conducted on sand and EMB1 to determine their Optimum Moisture Content (OMC) and Maximum Dry Density (MDD), in accordance with AASHTO T 99 Method C, as specified by the Illinois DOT's Standard Specifications. Figure 18 illustrates the relationship between water content and dry density for these two materials.

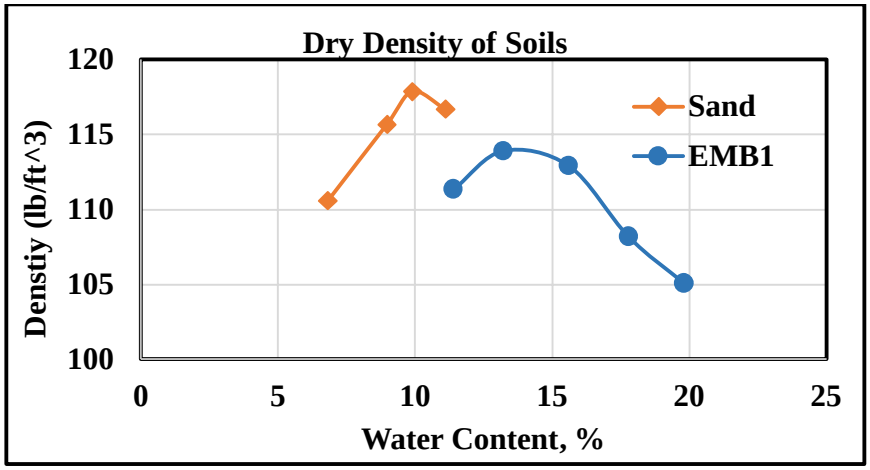

FIGURE 18. Dry density of sand and EMB1

3.1.4 Volumetric Properties of FGA

The dry loose unit weight of FGA1 and FGA2 was determined in dry conditions following ASTM C29. FGA1 showed higher dry unit weight (12.6 pcf) than FGA2 (10 pcf). The bulk specific gravity (G_{sb}) of FGA1 and FGA2 in oven-dry conditions was determined to be 0.35 and 0.31, respectively, in accordance with AASHTO T 85.

To determine the short-term and long-term water absorption of FGA1 and FGA2, both materials were submerged in water at room temperature for 4 days in accordance with ASTM C127, and for 4 weeks according to EN 12087. As shown in Figure 19, FGA1 exhibited absorption values of 8.5% after 4 days and 23.8% after 4 weeks. In comparison, FGA2 exhibited absorption values of 5.4% after 4 days and 16.2% after 4 weeks. The difference between short-term and long-term absorption indicated that both FGAs had a high absorption capacity but absorbed water slowly.

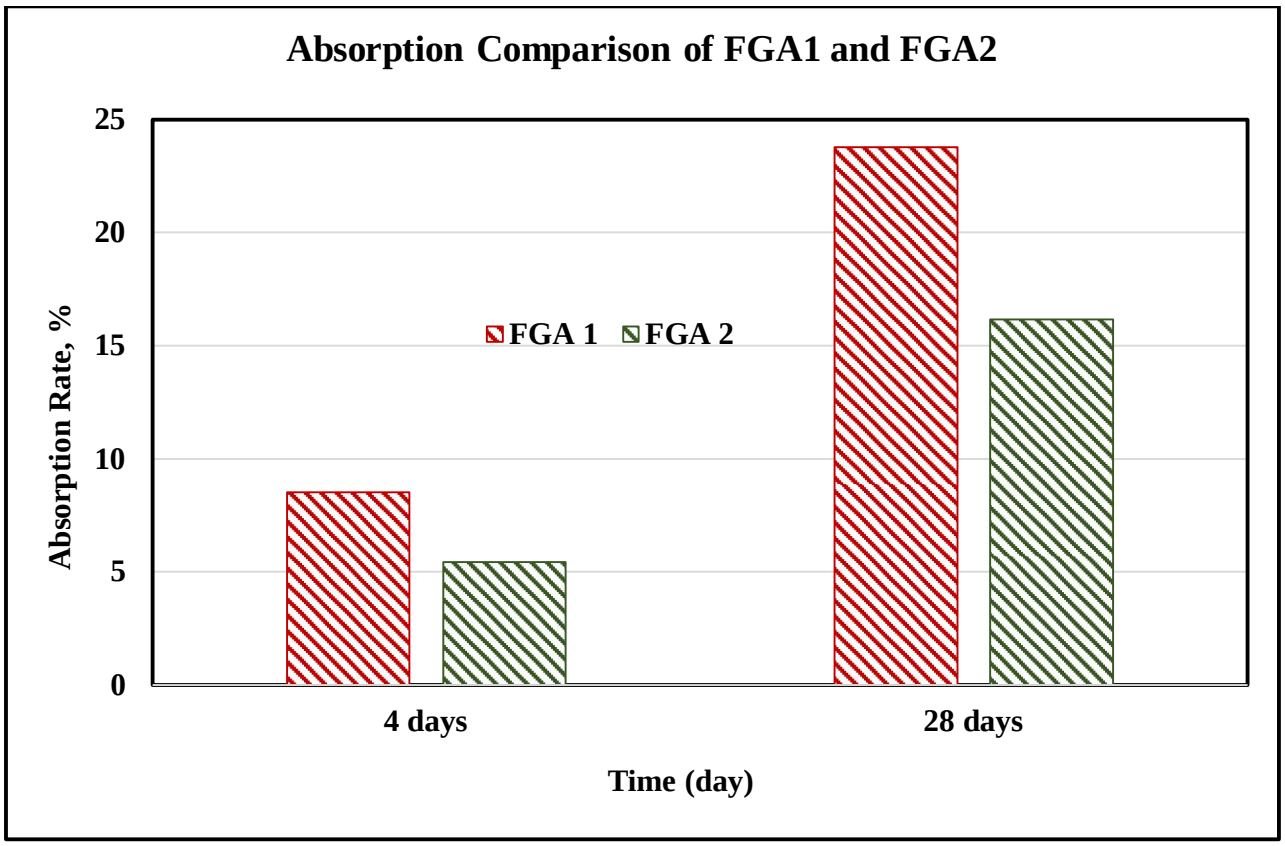

FIGURE 19. Water Absorption Rates of FGA1 and FGA2

3.1.5 Electrochemical Properties of FGA

Electrochemical characteristics of FGA are important properties for MSE backfill in terms of long-term durability of soil reinforcement and were studied in this project. Flood Testing Laboratory Inc. in Chicago, IL, was retained by this project team to measure the electrochemical properties of FGA1 and FGA2 following Illinois Modified AASHTO test methods. To be precise, they were tested for resistivity (Illinois Modified AASHTO T288), chloride level (AASHTO T291), sulfate soundness (Illinois Modified AASHTO T290), organic content (AASHTO T267) and pH (AASHTO T 289). FGA1 and FGA2 particles were crushed to pass the #10 sieve (2 mm) particles, and the ratio of the particles to water by mass was 1:1 for pH testing for AASHTO T288 and T289.

3.1.6 Axial Compression Compaction of FGA

To assess the compressibility of FGA1 and FGA2, confined compressive strength tests were performed on three samples of dry FGA in accordance with EN 1097-11:2013, a standard test for lightweight fill materials in Europe. The process begins with sampling, where granular

material meeting the required gradation is selected. The sample is prepared by filling a cylindrical mold with the aggregate in a loose condition. As shown in Figure 20, a closed-loop servo-hydraulic test machine, called a GCTS system, was used to apply axial compressive pressure through a piston covering the top surface of the material at a uniform rate of 13.5 lbs per second, to achieve 10%, 20%, and 30% height reductions in a 10-in diameter by 10-in-tall mold.

FIGURE 20. Axial compression compaction by closed-loop servo-hydraulic test machine

The confined axial compressive strengths at a given height reduction were calculated by Equation 2 as follows.

$$\sigma_c = \frac{F}{A} \tag{2}$$

where:

F = Applied force

A = Cross-sectional area of the mold

3.2. Aerodynamic Test of FGA

To assess the wind erodibility of FGA when it is daylighted after placement in the field, FGA1 was subjected to an aerodynamic test. The test was conducted using a custom-built device previously developed at WSU. As illustrated in Figure 21, the apparatus consists of a sealed wooden box with an opening on one side. Inside the box, FGA samples were placed for testing. A

blower is installed to generate controlled airflow directed at the FGA, simulating wind conditions. A digital anemometer is used to measure wind speed near the aggregates to determine the threshold wind speed that initiated erosion. The wooden box included a transparent section to allow observation and monitoring during testing.

FIGURE 21. Aerodynamic test setup

3.3. Laboratory Compaction Methods

Based on the literature review, different methods of laboratory compaction to mimic field compaction were experimented with to determine an appropriate laboratory sample preparation method. These methods included Standard Proctor (AASHTO T 99), Modified Proctor (AASHTO T 180), gyratory compaction (AASHTO T 312), compression compaction (EN 1097-11), vibratory hammer (ASTM D7382), vibratory table compaction (ASTM D4253), and Washington DOT's (WSDOT) Test Method 15 (Laboratory Theoretical Maximum Dry Density of Granular Soil and Soil/Aggregate) which includes vertical compression pressure and horizontal tapping.

As illustrated in Figures 22 and 23, the Modified and Standard Proctor tests involved compacting the FGA sample in a 6-in-diameter mold, using either a rubber plate or a steel plate placed on top to avoid excessive crushing of FGA particles by the hammer. For each test, the sample height was measured after every 10 blows to monitor volume reduction trends. The final change in volume was calculated after the total number of blows, and the sample's dry density was determined by dividing the sample's mass by its final volume.

(a) (b)

FIGURE 22. Modified Proctor (a) during compaction (b) after compaction

(a) (b)

FIGURE 23. Standard Proctor (a) before compaction (b) after compaction

In the gyratory compaction test, the sample was compacted with and without a rubber disc placed on top of FGA, respectively, and measurements of height were recorded after each gyration

to determine the density. During the compaction, the sample was subjected to 10 gyrations. Figure 24 depicts the device and FGA1 after the gyratory compaction.

(a) (b)

FIGURE 24. Gyratory compaction (a) before compaction (b) after compaction

The WSDOT TM-15 compaction method, which is designed for the determination of the moisture and density relationship of granular materials, involves using a 10-inch diameter mold and applying horizontal tapping simultaneously, as shown in Figure 25. Compaction was achieved by gradually applying a 2,000-pound force within two minutes per lift. However, this method and its customized device are specific to the northwest states and not readily available for widespread use.

(a) (b)

FIGURE 25. WSDOT compaction (a) before test (b) after test

Vibratory table compaction (Figure 26) was also performed in accordance with ASTM D4253. However, for large particles such as FGA, a large diameter (e.g., 10-in) mold was used. A surcharge load of 157 lbs was required, which is cumbersome to handle, making this method unsuitable for routine use.

FIGURE 26. Vibratory table compaction

Vibrating hammer compaction was also conducted in accordance with ASTM D7382. A steel plate was placed on top of the FGA. Compaction was performed in a single layer until a 10% increase in density (or 10% height reduction) was achieved with a vibrating hammer, as illustrated in Figure 27. However, it is hard to precisely control the height reduction with a vibrating hammer.

FIGURE 27. Vibrating hammer compaction

3.4 One-Dimensional (1-D) Consolidation Tests

3.4.1 Introduction

1-D consolidation tests were conducted in accordance with AASHTO T 216. In this test protocol, each load increment is maintained until the change in deformation becomes relatively negligible (typically within 24 hours). During the consolidation process, the specimen height is measured at different time increments. The collected data were used to compare the effective stress and void ratio or vertical strain. Two distinct test setups were utilized to perform one-dimensional consolidation tests, both designed to simulate similar conditions. Short-term deformation under static load, was assessed using a closed-loop servo-hydraulic test machine, the GCTS system. The duration of each test was 24 hours. Linear variable differential transducers (LVDTs) were mounted on top of the mold to measure deformation accurately, as shown in Figure 28. For assessing long-term tests, a custom-built setup developed at WSU for the previous Illinois Tollway project was modified accordingly and then employed (Wen et al., 2022). This setup, illustrated in Figure 29, employed pneumatic pressure to apply controlled loads onto a steel plate positioned on top of the sample. The applied pressure was calibrated using a digital load cell, while deformation was measured with digital dial gauges.

Sand and EMB1 samples were prepared in 6-in diameter molds, while FGA1 and FGA2 samples were prepared in 10-in diameter molds to maintain the appropriate ratio between the maximum particle size and the mold diameter. FGA particles were screened through a 2-in sieve for this test. All samples were subjected to an initial seating load of 1 psi prior to testing to ensure proper contact between the steel plate and the sample.

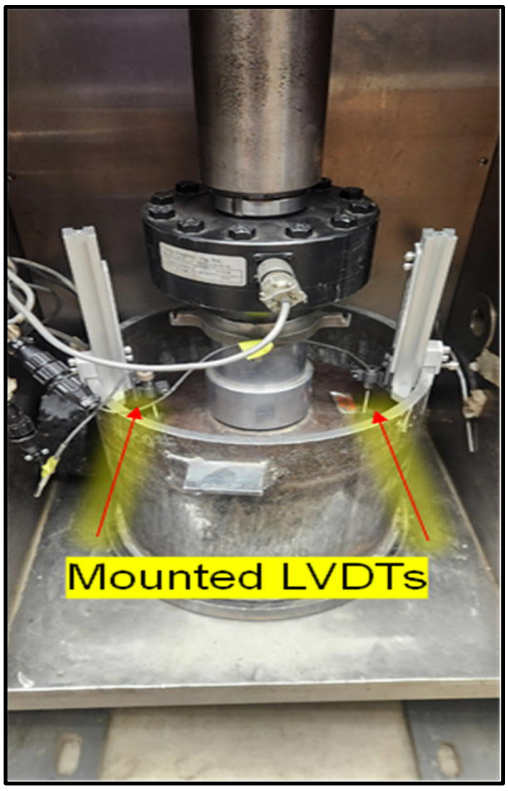

FIGURE 28. One-dimensional consolidation test with hydraulic GCST system

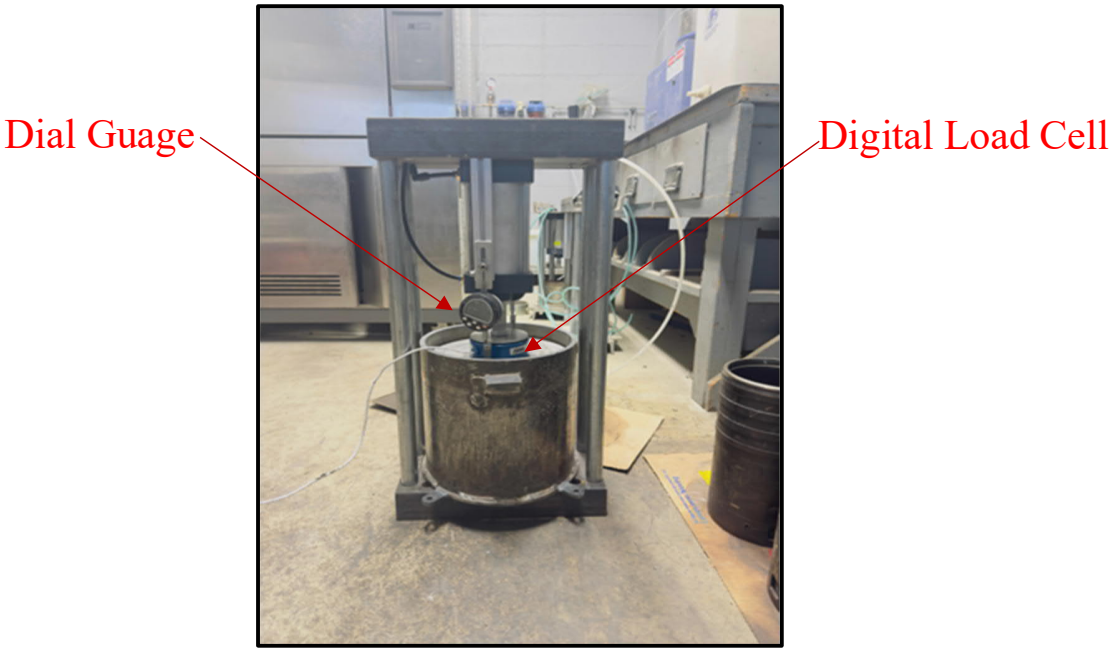

FIGURE 29. One dimensional consolidation test with pneumatic pressure frame

3.4.2 Test Procedure

3.4.2.1. Same Stress Level for 24 hours

FGAs were compressed up to 10, 20, and 30% height reduction under static (very slow) compaction. Based on the results for FGA1 later, it was found that a 10% height reduction was sufficient for sample preparation. Therefore, FGA2 was compacted to 10% height reduction only. Sand and EMB1 were compacted to 95% of their maximum dry density (based on standard proctor in accordance with IDOT specifications) at optimum moisture content, respectively. Compacted samples were then subjected to 1-D consolidation under a vertical stress level of 4 psi for 24 hours. This pressure level represents the overburden pressure at the bottom of a 22-ft FGA embankment beneath a 3-ft pavement structure. This 25-ft pavement and embankment profile was selected based on the previous Illinois Tollway study (Wen et al. 2022).

3.4.2.2. Same Stress Level for 30 Days

Although not part of the original work plan, 30-day 1-D consolidation tests were included to determine the long-term compression of FGAs in accordance with AASHTO T216 using the pneumatic pressure frame. Of special interest is whether the FGA particles continue to crush under a static load for an extended duration, which may lead to excessive settlement. Static compaction to 10% height reduction or 10% increase in density was applied to the FGA samples. Due to time constraints, the applied pressure was 4 and 12.9 psi for FGA1, and 4 psi for FGA2. The 12.9 psi stress level is the maximum pneumatic pressure available in the laboratory to evaluate the behavior of FGA1 under a large load level (e.g., under the footing of a structure).

3.4.2.3. Multiple Load Incremental Level

To determine the magnitude and rate of consolidation of EMB1 and sand and the rate of compression of FGAs, 1-D consolidation with incremental loading was conducted in accordance with AASHTO T216. Five stress levels- 1.8 psi, 3.6 psi, 7.2 psi, 14.4 psi, and 29 psi- were applied for 24 hours at each pressure level. The data were recorded at 0.1, 0.25, 0.5, 1, 2, 4, 8, 15, 30, 60, 120, 240, 480, and 1440 minutes. Both FGA1 and FGA2 were statically compacted to achieve a 10% height reduction. Sand and EMB1 were compacted to 95% of their maximum dry density at their respective optimum moisture contents.

3.5 Direct Shear Test

To measure the resistance of the FGA samples to shear, direct shear tests were performed in accordance with AASHTO T236. To implement this, a direct shear device (6-in-diameter) was

used for this study, as shown in Figure 30. Normal pressure was applied through a pneumatic air cylinder. The shear force was imposed through the hydraulic GCTS system, which recorded the shear force and displacement over time during the test. Particles were screened through a 1.5-inch sieve and were statically compacted until a 10% height reduction was achieved. The shear tests were conducted under dry conditions. The confining stress levels were controlled at 1.33, 3.11, 4.44, 8.85, and 13.27 psi (9.2, 21.5, 30.6, 61, and 91.5 kPa), respectively. The shear displacement was set at 0.04 in./min. Because no apparent peak shear load occurred, the shear pressure at 10% shear strain was used as the shear strength.

FIGURE 30. Direct shear test setup

In one of the previous studies, the manufactured direct shear device and data collection procedure were verified using a clean, dry, loose sand (Wen et al., 2022). Dry sand should have minimal to no cohesion; only friction between particles provides resistance to shear pressure. Based on the data collected, the cohesion and friction angle were determined to be 0 psi and 45º, respectively, as shown in Figure 31, which confirms the theory of zero cohesion for dry sand. Therefore, the fabricated shear device was found to be effective.

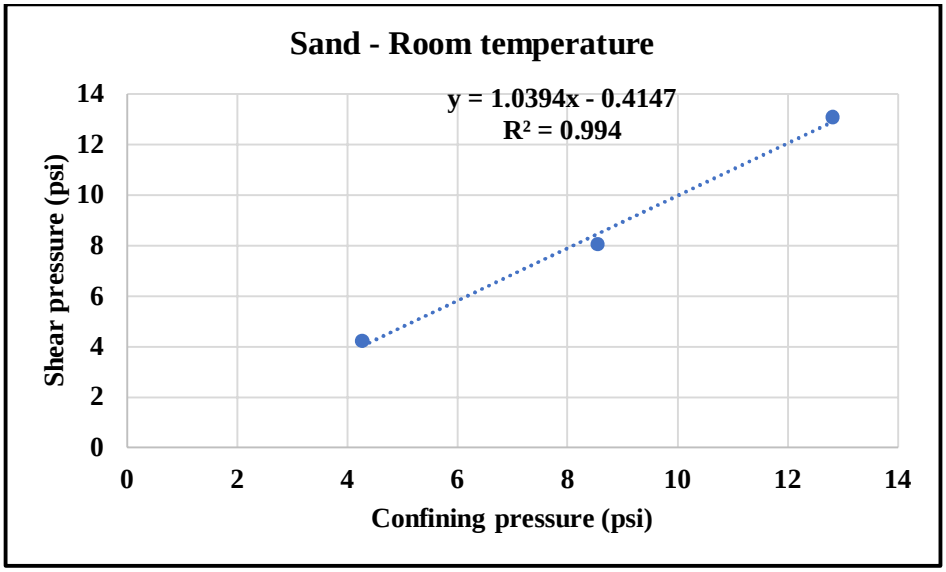

FIGURE 31. Direct shear test result for sand (Wen et al. 2022)

3.6 Dynamic Triaxial Test

Dynamic triaxial tests were conducted to simulate the impact of traffic loading on the EMB1 and FGA samples in an embankment. EMB1 samples were compacted in a split mold with a diameter of 6 in. in six layers, each with a height of 2 inches, to reach a target height of 12 inches, in accordance with AASHTO T 307-99 (2017), as illustrated in Figure 32(a). The mass of each layer was determined using the corrected OMC and 95% MDD. A triaxial chamber was used to provide an air-tight environment so that the target confining pressure could be reached during the test. The water valves for drainage were kept open during the tests. FGA samples were statically compacted in one layer to achieve a 10% height reduction. Also, instead of applying air confinement in an enclosed cell, vacuum suction pressure was used, for the ease of testing, as shown in Figure 32(b). Two linear variable differential transducers (LVDTs) were used to measure the axial deformation over 6-in. spacing. Frame LVDT readings were used to determine the resilient modulus of FGA.

(a) (b)

FIGURE 32. Dynamic triaxial test setup for (a) EMB1 and (b) FGA

The same stress levels for triaxial tests were applied based on the previous Illinois Tollway study, which utilized a finite element program analysis of typical pavement structures for the Illinois Tollway using EverFE (Wen et al., 2022). The confining pressure at the bottom of the base layer was 4.35 psi, the seating and the cyclic load were 2.9 psi. Figures 33 and 34 show the traffic loading pattern and applied stress used for the analysis, respectively. Axial loading was applied using haversine-shaped loading, a 0.1-second load pulse followed by a 0.9-second rest period, as shown in Figure 35.

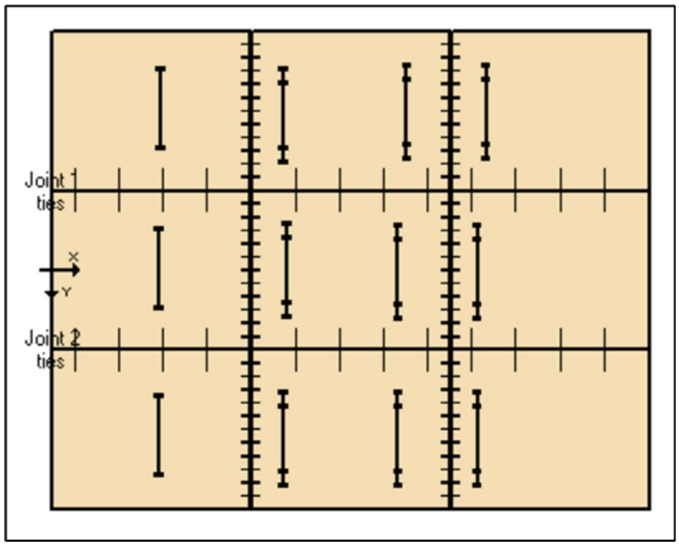

FIGURE 33. EverFE design vehicles: wheel loading pattern

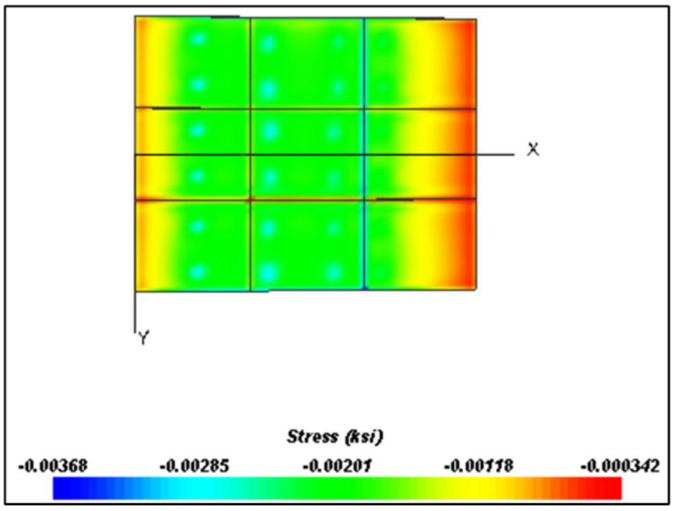

FIGURE 34. Stress levels based on EverFE analysis

3.7 Test Embankment Construction

To study the field compaction of FGA, a field experiment was conducted. A 10'×12'×2' test site was prepared with loosely raked FGA1, which was laterally confined with concrete barriers. The FGA1 was subjected to six passes of a tracked backhoe, which exerted a ground track pressure of 900 psf. This pressure falls within the recommended ground pressure between 625 and 1,025 psf. After each pass, density was measured with a nuclear density gauge (Figure 36(a)) and the surface elevation was measured in tracked areas with a laser level (Figure 36(b)).

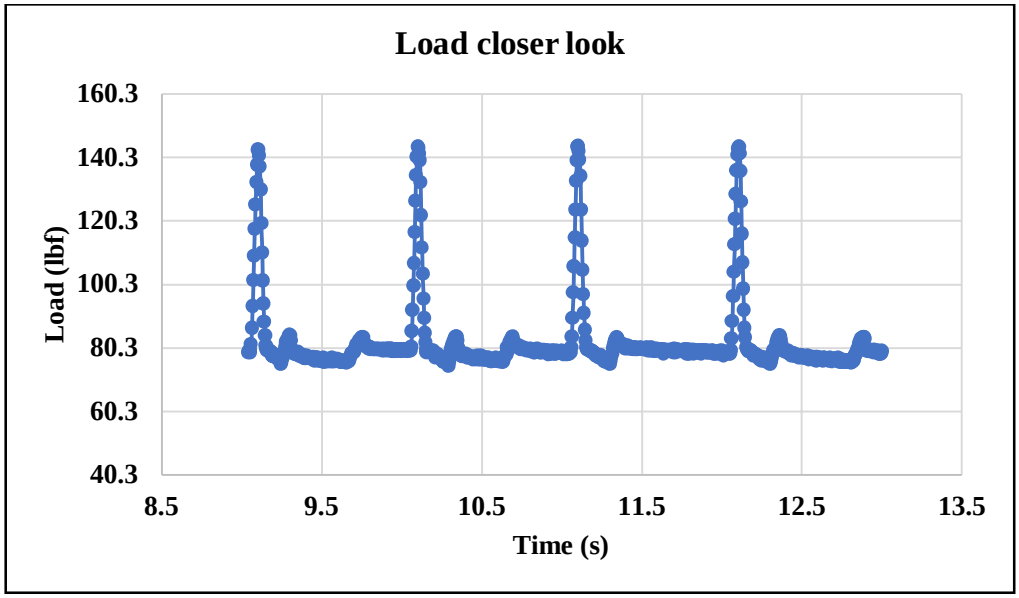

FIGURE 35. Load pattern for triaxial tests

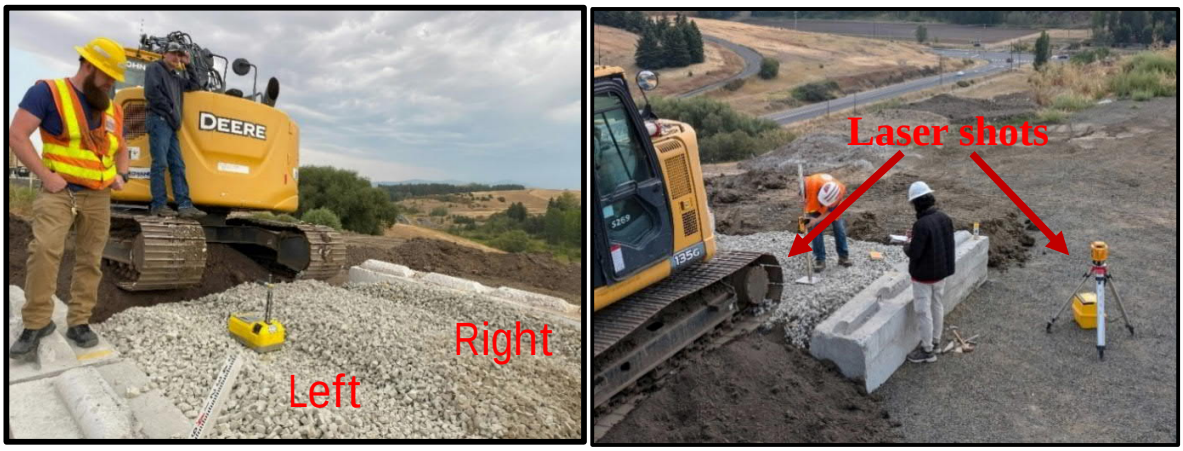

(a) (b)

FIGURE 36. (a) Density measurement and (b) elevation shot

3.8 Summary of Tests

Table 12 presents a summary of the testing program covering all of the tests conducted in this study, including:

- Characterization of tested materials
- Volumetric properties of FGAs
- Proctor test
- Aerodynamic test
- Laboratory compaction
- Direct Shear
- Dynamic Triaxial
- Pilot construction

- One dimensional consolidation for various stress levels, compaction methods and duration

TABLE 12. Summary of Testing Schedule

Tests			EMB1	Sand	FGA1		FGA2	
					<2 in.	<1.5 in.	<2 in.	<1.5 in.
Gradation			x	x	-	-	-	-
Atterberg Limit			x	-				
Proctor (Standard)			x	x				
Electrochemical Properties			-	-	x	-	x	-
Axial Compression Compaction					x	-	x	-
Aerodynamic					x	-	x	-
Volumetric Properties	Initial Bulk Density		-	-	x	-	x	-
	Specific Gravity		-	-	x	-	x	-
	Absorption		-	-	x	-	x	-
Laboratory Compaction	Modified and Standard Proctor		-	-	x	-	x	-
	Gyratory Compaction		-	-	x	-	x	-
	WSDOT Compaction		-	-	x	-	x	-
	Vibratory Table Compaction		-	-	x	-	x	-
	Vibratory Hammer Compaction		x	x	x	x	x	x
1-D	30 days/1 stress	4 psi	-	-	x	-	x	-
		12.9 psi	-	-	x	-	-	-
	5 days/5 stresses	1.8-29 psi	x	x	x	-	x	-
	1 day/1 stress	4 psi	x	x	x	-	x	-
		12.9 psi	-	-	x	-	x	-
Direct Shear	Large		-	-	-	x	-	x
Dynamic Triaxial	Large		x	-	-	x	-	x
Pilot Construction					-	-	-	-

Note: 'X' tested; '-' not tested; shaded cells: not applicable.

CHAPTER 4: ANALYSIS AND RESULTS

After the laboratory tests were completed, the research team analyzed the results to determine the performance of the FGA samples and to compare the FGA's performance to that of the EMB1 and sand as reference materials.

4.1 Electrochemical Properties of FGA

To determine the viability of FGA as MSE wall select fill, the electrochemical properties of FGA1 and FGA2 were tested by Flood Testing Laboratory, Inc., in accordance with Illinois Modified AASHTO methods. Table 13 summarizes the results for FGA1 and FGA2, showing that the organic, sulfate, and chloride contents complied with IDOT specifications. However, the pH values of both FGA1 and FGA2 were 12.4, exceeding the IDOT upper limit of 10.0 for steel reinforcement. Additionally, the resistivity of FGA1 and FGA2 was 387 ohm-cm and 160 ohm-cm, respectively—significantly below the IDOT minimum requirement of 3,000 ohm-cm. Illinois-modified AASHTO T288 and T290 specify that particles be crushed to pass the #10 sieve, and a that a 1:1 particle-to-water ratio by mass is used for pH testing. Due to the lightweight nature of FGA, the particle-to-water ratio by volume for FGA is significantly larger than that for conventional soils and aggregates.

TABLE 13. Electrochemical Properties of FGA1 and FGA2 by Flood Testing Laboratory, Inc.

Chemical and Physical Analysis			
Procedures	**FGA1**	**FGA2**	**IDOT Specifications**
Organic Content (AASHTO T 267)	0.80%	0.80%	<1.0%
pH (AASHTO T 290)	12.4	12.4	5.0 – 10.0 (steel strap)
Sulfates (AASHTO T290)	28 ppm	24 ppm	<200 ppm
Chlorides (AASHTO T 291)	1.5 ppm	3.7 ppm	<100 ppm
Minimum Resistivity (AASHTO T 288)	387 ohm-cm	160 ohm-cm	>3000 ohm-cm

There is no widely accepted national specification for lightweight aggregates as MSE wall select fill. The South Carolina DOT has special provisions for pH and resistivity of lightweight fill materials. Soil Consultants, Inc., South Carolina, was engaged to perform pH and resistivity tests on FGA1. Sample preparation followed SC-T-143 with as-received gradation (without crushing to

pass the #10 sieves), while pH and resistivity tests adhered to ASTM D1293 Method B and ASTM D1125 Method A, respectively, using a 1:1 particle-to-water ratio by mass for pH testing. Table 14 presents the measured values, which show that FGA1's pH values were lower than results from Illinois-modified methods but still exceeded IDOT's upper limit of 10, and its resistivity remained below the required minimum of 3,000 ohm-cm.

TABLE 14. pH and Resistivity of FGA1 by Soil Consultants, Inc – South Carolina

Test	Test Methods	Sample ID	Test Results			
pH	SC-T-143, D1293, Method B	Sample #1	10.58	10.72	10.73	10.74
		Sample #2	10.64	10.85	10.78	10.80
Resistivity Ohm-cm	SC-T-143, D1125, Method A	Sample #1	2794	2794	2794	2790
		Sample #2	2785	2788	2795	2794

4.2 Axial Compression of FGA

Following EN 1097-11:2013 test method (European Committee for Standardization, 2013), axial compression tests were conducted on dry FGA1 and FGA2, as well as saturated FGA1 with a GCTS system to assess their compressibility. In accordance with EN 1097-11:2013, “confined strengths,” defined as confined stiffness at 10 and 20% deformation (or height reduction), need to be greater than 7,000 and 15,000 lb/ft^2, respectively. Figure 37 indicates that there is no significant difference between dry and saturated conditions in terms of compaction efforts. Figure 38 shows that FGA1 and FGA2 exhibited a confined strength of about 5,000 lb/ft^2 at 10% deformation, less than the 7,000 lb/ft^2 required confined strength. However, at 20% deformation, dry FGA1 and FGA2’s confined strengths were around 14,200 lb/ft^2. FGA1 and FGA2 had similar confined strengths at different deformation levels. The confined strength of saturated FGA1 at 20% deformation was around 12,000 lb/ft^2.

Additionally, sieve analyses were conducted on the compacted samples in accordance with AASHTO T27 and compared to the as-received gradation. As shown in Figure 39, greater particle breakdown was observed with increased compression effort, particularly when the compression level increased from 10% to 20% and from 20% to 30% deformation, compared to the change from 0% to 10%.

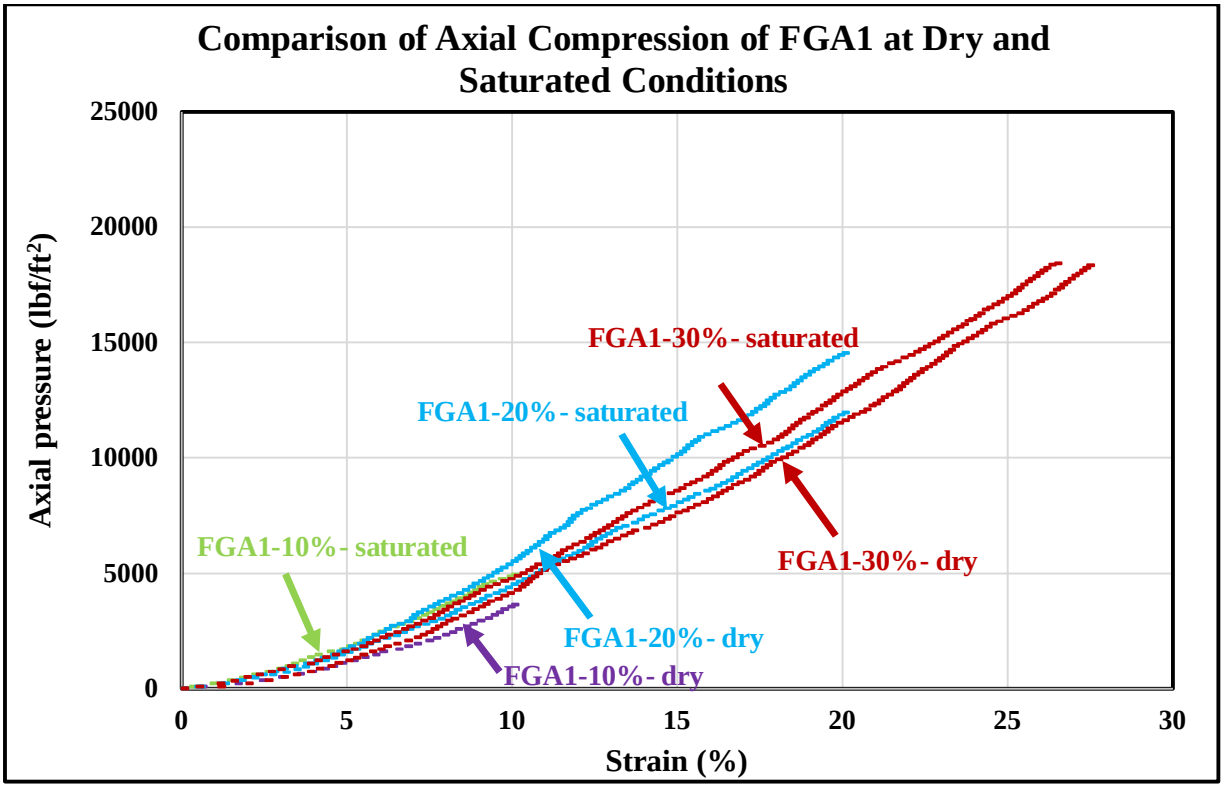

FIGURE 37. Comparison of axial compression of FGA1 at dry and saturated conditions

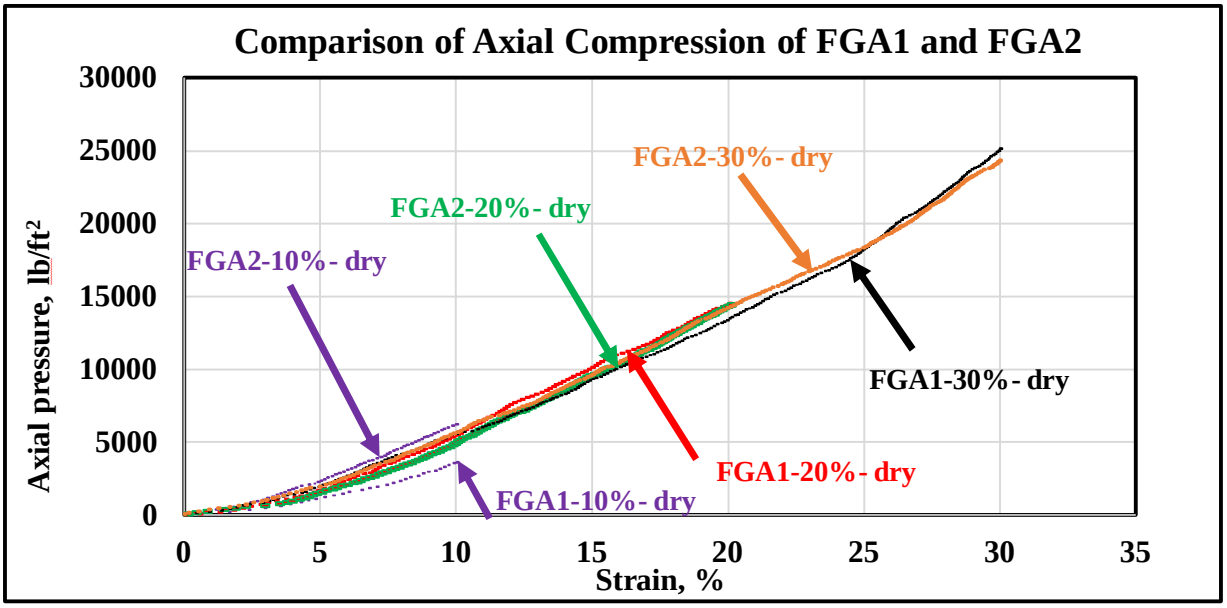

FIGURE 38. Comparison of axial compression of FGA1 and FGA2

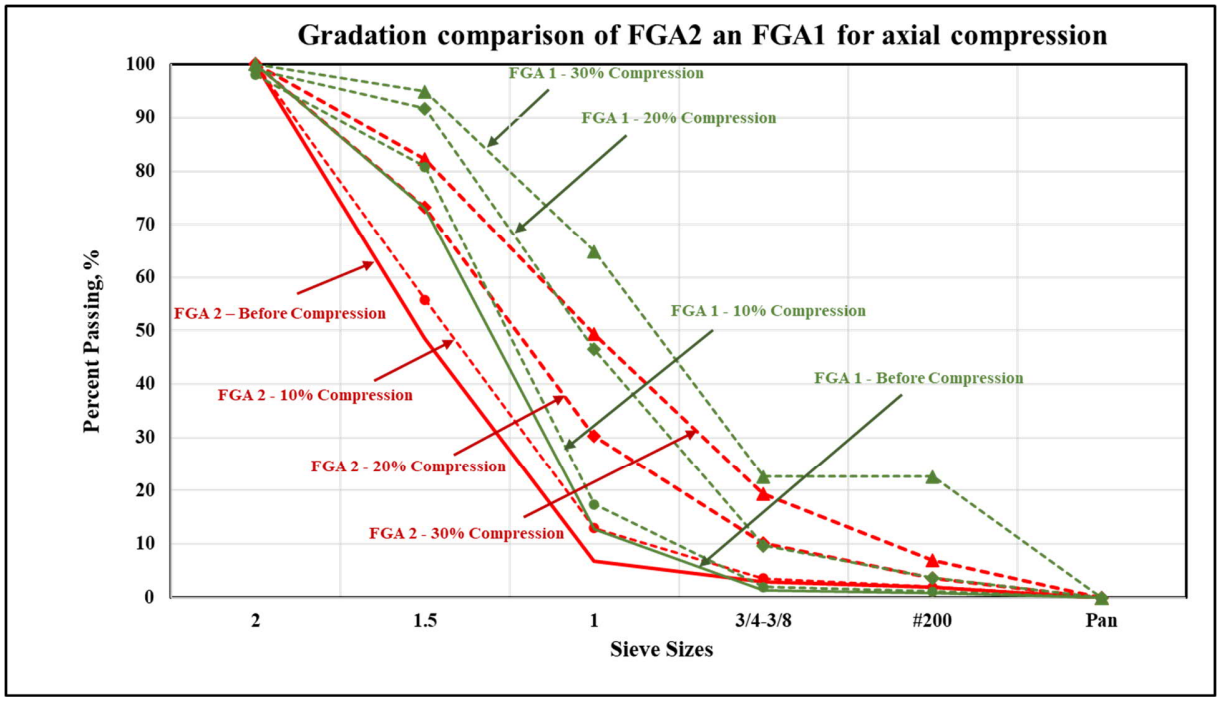

FIGURE 39. Gradation comparison of FGA1 and FGA2 for axial compression

4.3 Aerodynamic Test of FGA1

The susceptibility of FGA1 to wind erosion arises from its low density. An aerodynamic test, shown in Figure 40, was conducted to evaluate its wind erodibility and determine the threshold wind speed that initiates particle erosion with a custom-built device at WSU.

It was found that wind erosion occurred at a wind speed of 60 mph. The record wind speed in Chicago is 87 mph (Skilling, 2014), which indicates that FGA needs to be covered with conventional materials. It is noted that wind speed is typically measured 10 meters (or 33 ft) above the ground. However, in some cases, the embankment can also be significantly higher (e.g., 25 ft, as used in this study) than the ground. Therefore, the worst-case scenario was used in this recommendation.

FIGURE 40. Aerodynamic test on FGA1

4.4 Laboratory Sample Preparation Methods

Based on the literature review, different methods of laboratory compaction were experimented with to determine an appropriate laboratory compaction method for proper sample preparation. Figure 41 presents the compacted unit weights achieved with various methods, while Figure 42 shows the unit weight growth with increasing compactive efforts, with the maximum number of blows or gyrations being 100%. The Modified Proctor with a steel plate on top of FGA1 and the gyratory compactor with a steel plate generated the highest unit weight, followed by the modified Proctor with a rubber plate and the gyratory compactor with a rubber plate. The Standard Proctor with a steel plate at 56 blows and WSDOT TM15 produced unit weights close to gyratory compaction with 0-5 gyrations and a rubber plate. The vibratory table compaction for 10 minutes had the lowest unit weight. The compaction methods for conventional materials presented several limitations. The Proctor test (Standard and Modified) faced challenges due to the 6-in mold being too small to accommodate FGA, which has a nominal maximum aggregate size of 2.5 inches. Additionally, in a Modified Proctor test, the rammer impact caused significant particle breakage, regardless of whether a steel plate or rubber pad was used on top. Gyratory compaction exerted very high pressure (600 kPa or 87 psi), resulting in the most significant changes in gradation due to particle breakdown. The WSDOT TM-15 test, which utilizes a 10-in mold and horizontal tapping, showed promise but is currently not readily available or widely accessible for use. Gradations of FGA1 samples were determined before and after compaction, as shown in Figure 43. Compaction methods that resulted in higher density crushed the FGA particles to finer gradations.

To address these challenges, the vibratory table and axial/static compression compaction methods were also explored. Figure 43 depicts that the vibratory table compaction for 10 minutes and axial compression at 10% deformation demonstrated a key advantage in preserving particle integrity, as they avoided excess particle breakage observed in other methods. Despite the promising results of the vibratory table method, its high cost, large surcharge, and limited availability make it less practical for routine laboratory use. Static compaction, therefore, was primarily used in the sample preparation in this study.

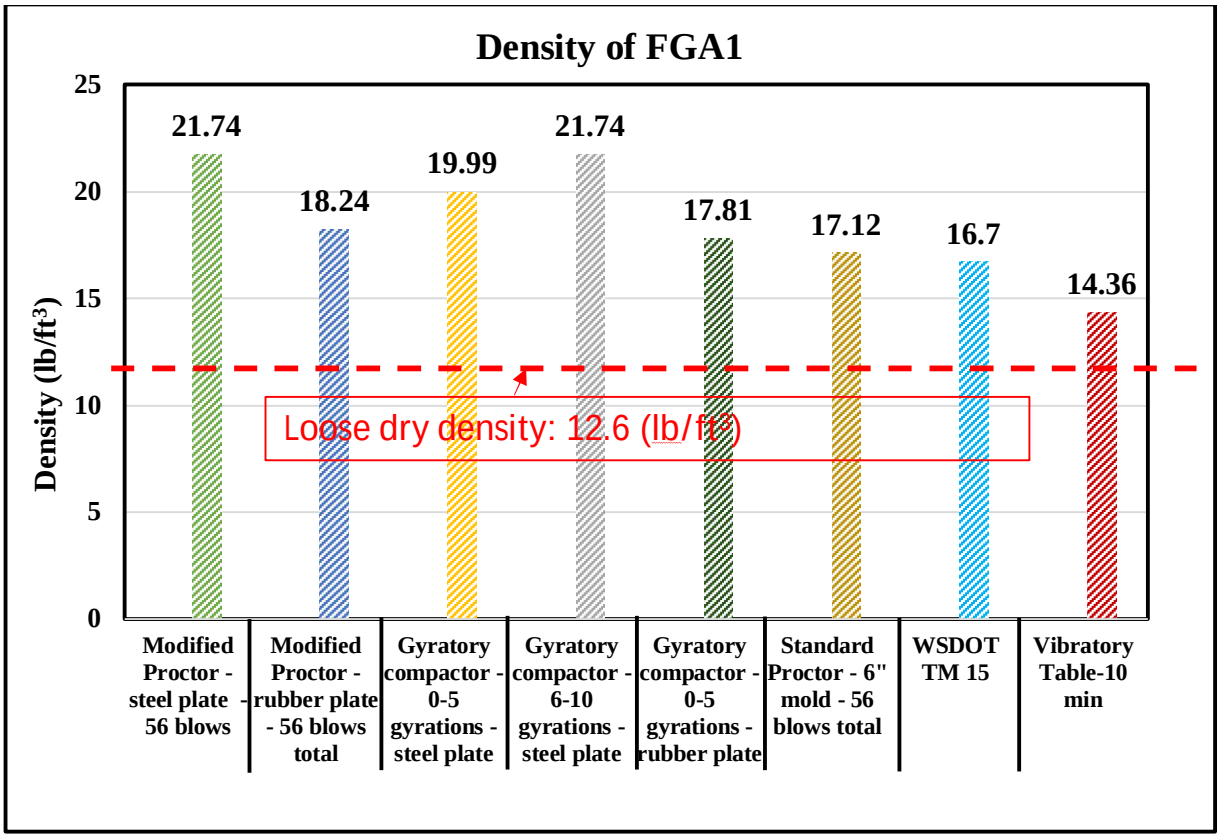

FIGURE 41. Comparison of FGA1 density at different compaction method

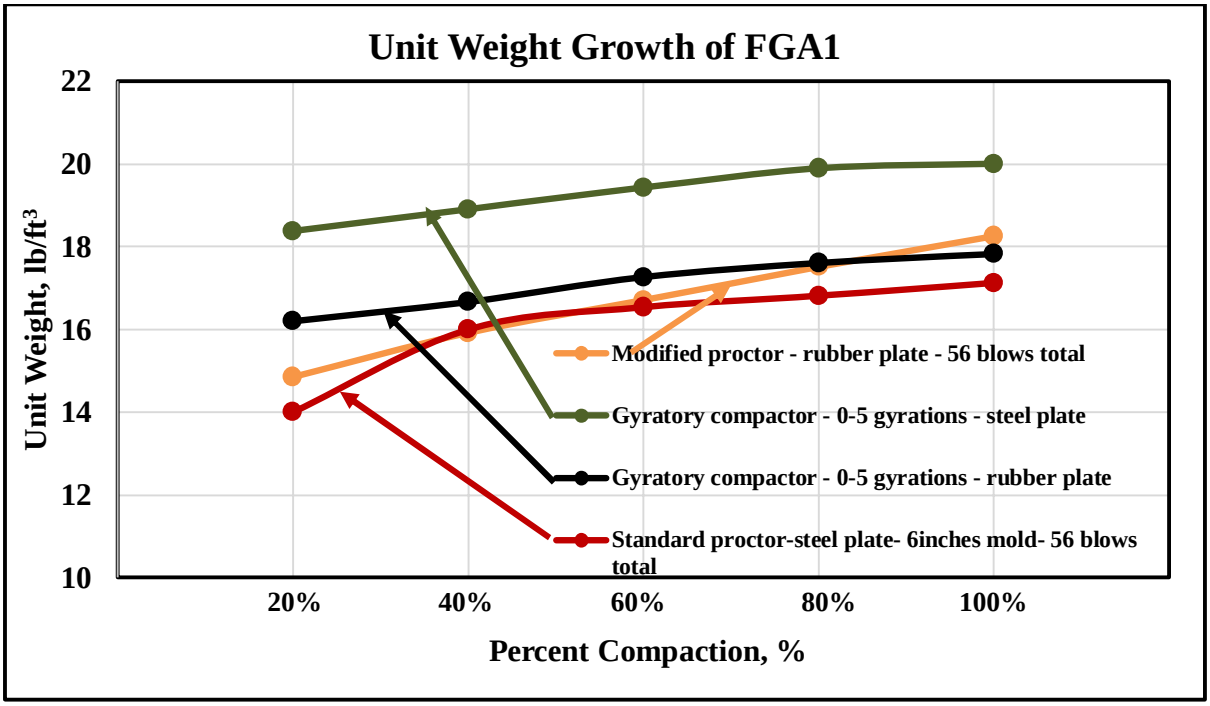

FIGURE 42. Unit weight growth of FGA1 under various compaction methods (maximum number of blows or gyrations being 100%**)**

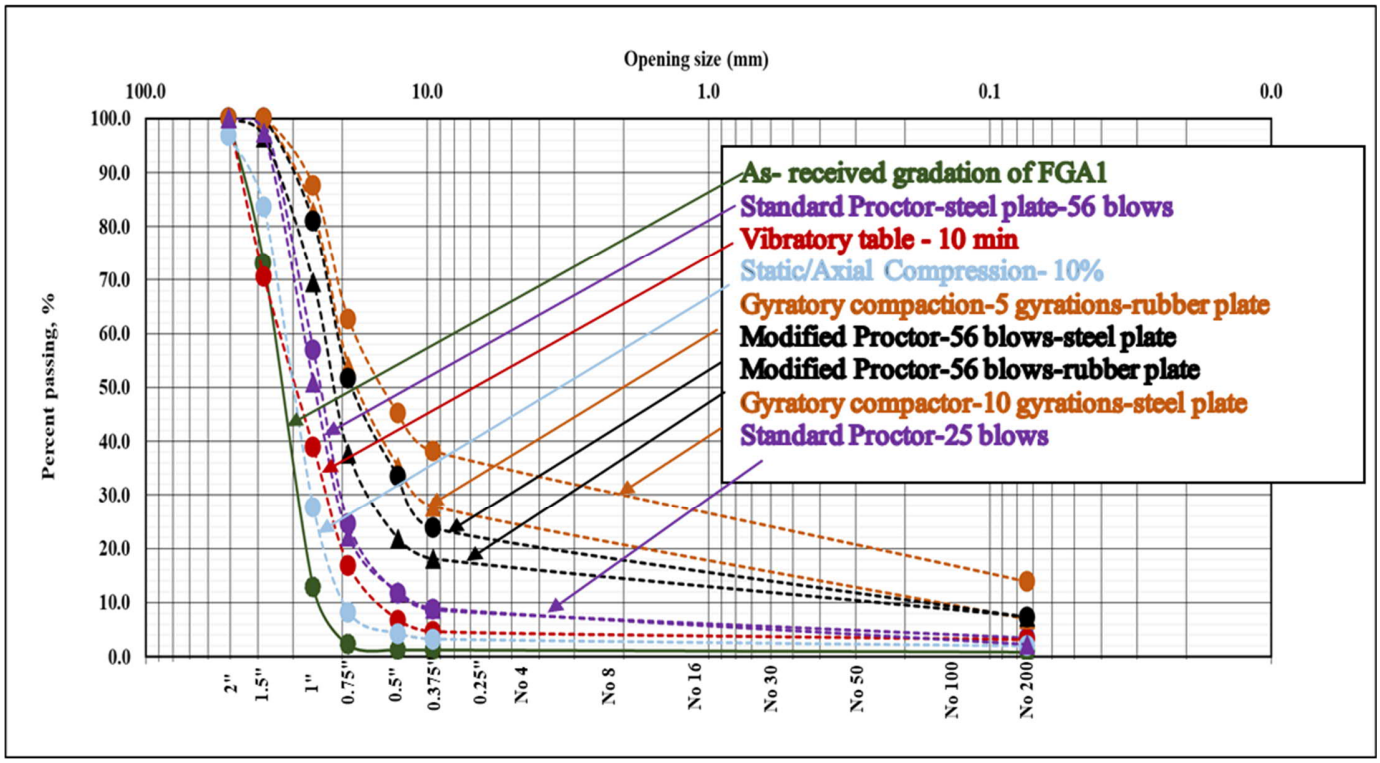

FIGURE 43. Gradation of FGA1 before and after compression

4.5 1-D Consolidation Test

4.5.1 1-D Consolidation for 24 Hours

To evaluate the creep behavior of FGA1, the material (< 2 inches) was first compacted with static compaction to 10, 20, and 30% height reduction and then subjected to a 1-D consolidation test under a static load of 4 psi for 24 hours. The results were compared with those of embankment clay (EMB1) and sand. EMB1 and sand were compacted to 95% MDD at OMC.

As shown in Figure 44, for statically compacted FGA1, when compaction efforts increased from 10% to 20% and 30% volume reduction, the consolidation of FGA1 slightly increased, likely due to particle crushing. Overall, 10% static compaction of FGA1 led to consolidation that was lower than that of sand and EMB1 under the same stress level. Figure 44 also indicates that 10% vibratory table compaction for 10 minutes exhibited consolidation comparable to 10% static compaction and lower consolidation than that of sand or EMB1. For the preparation of samples for other tests in this study, a 10% height reduction based on static compaction was used. This aligns with the compaction efforts for sample preparation of 11% height reduction used by Nicks et al. (2024), which was based on the field compaction study by McGuire et al. (2021).

Only two replicates of FGA2 were compacted to 10% height reduction. Subsequently, they were tested under a pressure of 4 psi. FGA2 also demonstrated creep that was significantly lower than clay (EMB1), comparable to sand, but slightly higher than FGA1, as shown in Figure 44.

FGA1 and FGA2 were also tested for a stress level of 12.9 psi with a pneumatic pressure frame for 24 hours. Figure 45 demonstrates the results. Higher compression values are observed, but still very low, 0.1% for FGA1 and 0.21% for FGA2 at the end of 24 hours. Note that the observed vertical stepwise increase in deformation in FGAs and EMB1 during consolidation may be attributed to the crushing of FGA particles and the breakdown of lumps (smaller than ¾ inch) formed during EMB 1 sample preparation.

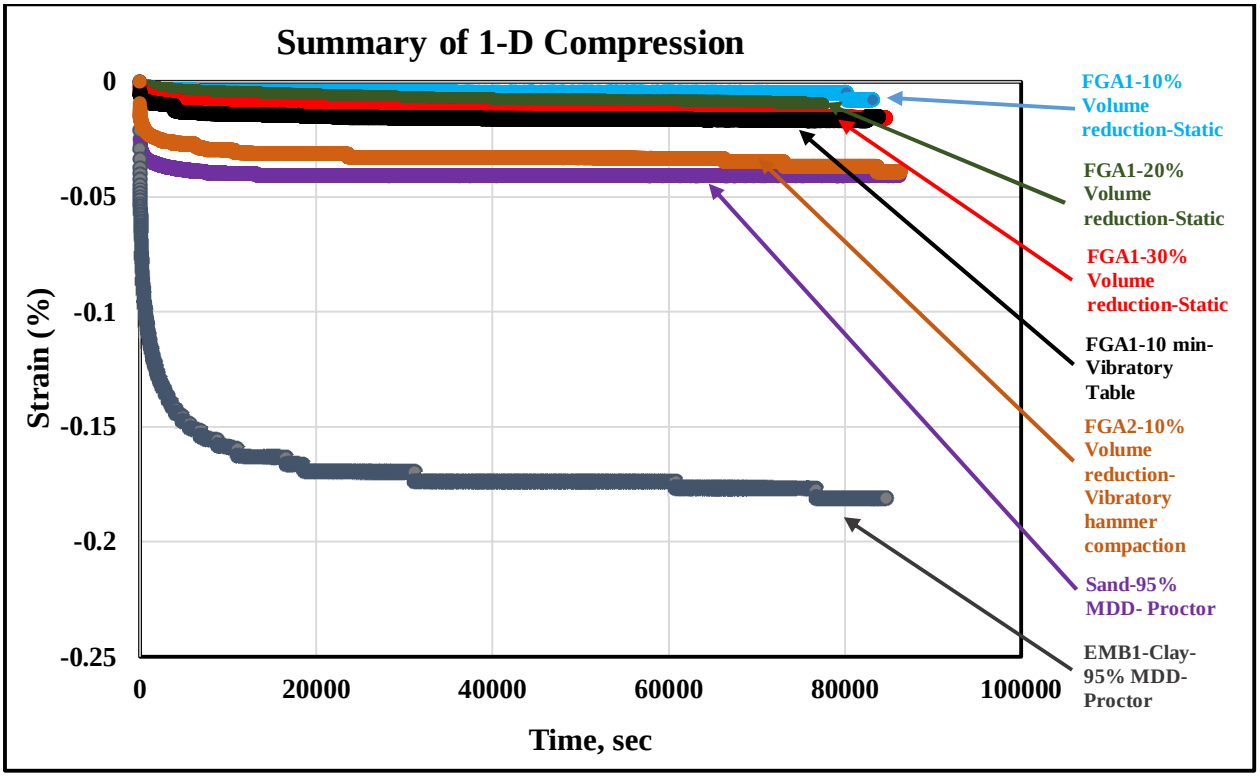

FIGURE 44. Summary of 1-day 1-D consolidation test at stress level of 4 psi

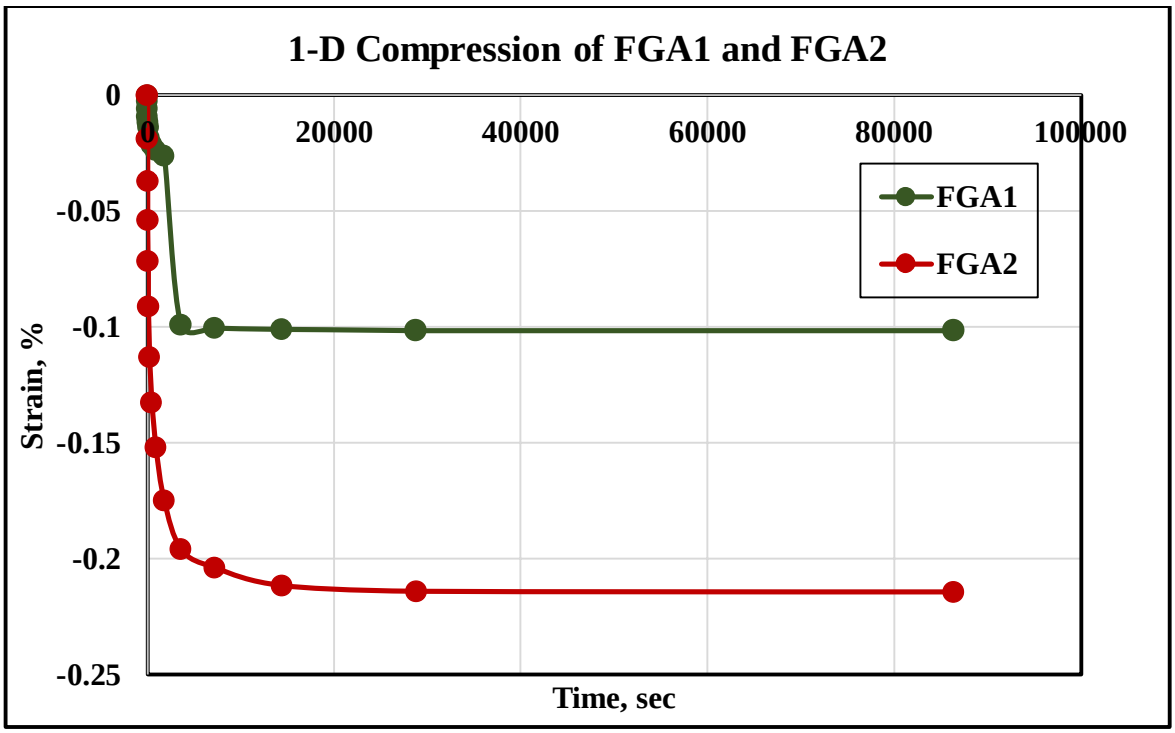

FIGURE 45. Comparison of 1-day 1-D compression of FGA1 and FGA2 at 12.9 psi

4.5.2 Same Stress Level for 30 days

To evaluate the long-term deformation of FGA under static loads, 30-day 1-D consolidation tests were performed. Figures 46 and 47 illustrate the 30-day consolidation behavior of FGA1 and FGA2 under 4 psi, and FGA1 at 12.9 psi, respectively. The consolidation results for FGA1 and FGA2 at 4 psi were highly comparable. However, it is noted that after the first week, FGA1 experienced a minimal stepwise increase in consolidation, likely due to the crushing of FGA1 particles. This was not observed in FGA2. This is more evident in Figures 48 and 49 when a semi-logarithmic time scale is used. The semi-logarithmic relationship with respect to time was used to regenerate the graph for estimating 50 years of secondary settlement (creep), as illustrated in Figures 48 and 49. This approach facilitated the determination of the secondary consolidation curve, enabling the prediction of consolidation over a 50-year period. In Figures 48 and 49, the red-circled zone was selected for extrapolating settlement trends beyond one day (172,800 seconds in the figures). Subsequently, as shown in Figures 50 and 51, prediction lines were drawn to estimate deformation over 50 years for FGA1 and FGA2 at 4 psi and FGA1 at 12.9 psi, respectively. The predicted minimal secondary settlement was 0.01% for FGA1 at 4 psi and 0% for FGA2 at 4 psi, whereas 0.06% for FGA1 at 12.9 psi. Note that these are secondary settlements, assuming primary settlement occurred during the construction, and thus, the intercepts in linear regressions in Figures 50 and 51 represent primary settlements.

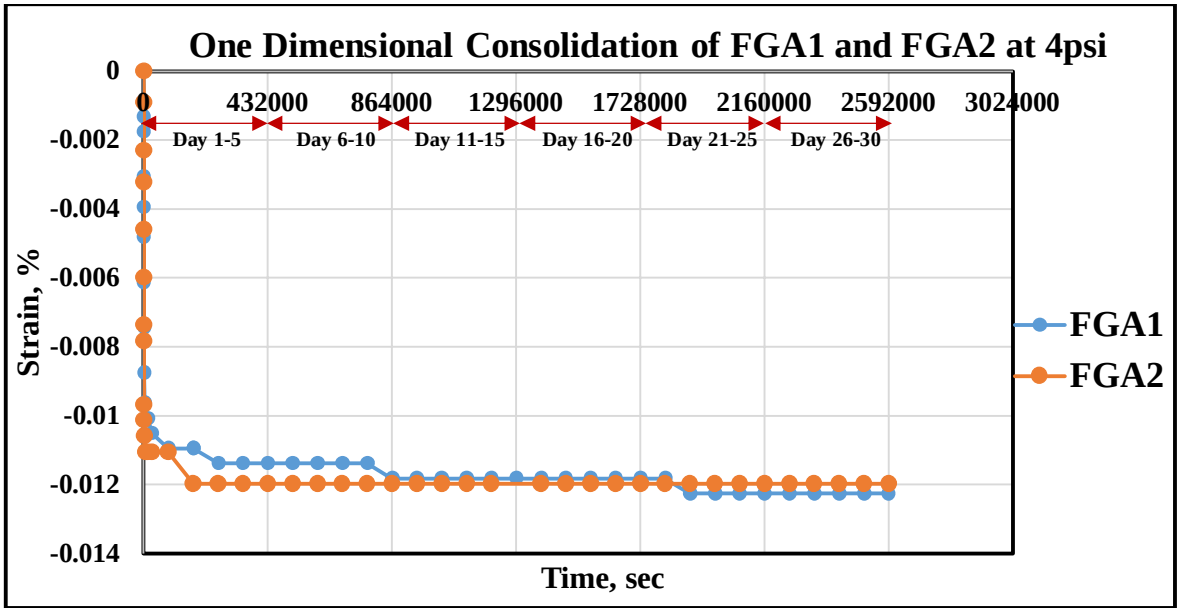

FIGURE 46. 30 days one-dimensional consolidation on FGA1 and FGA2 under static load of 4 psi

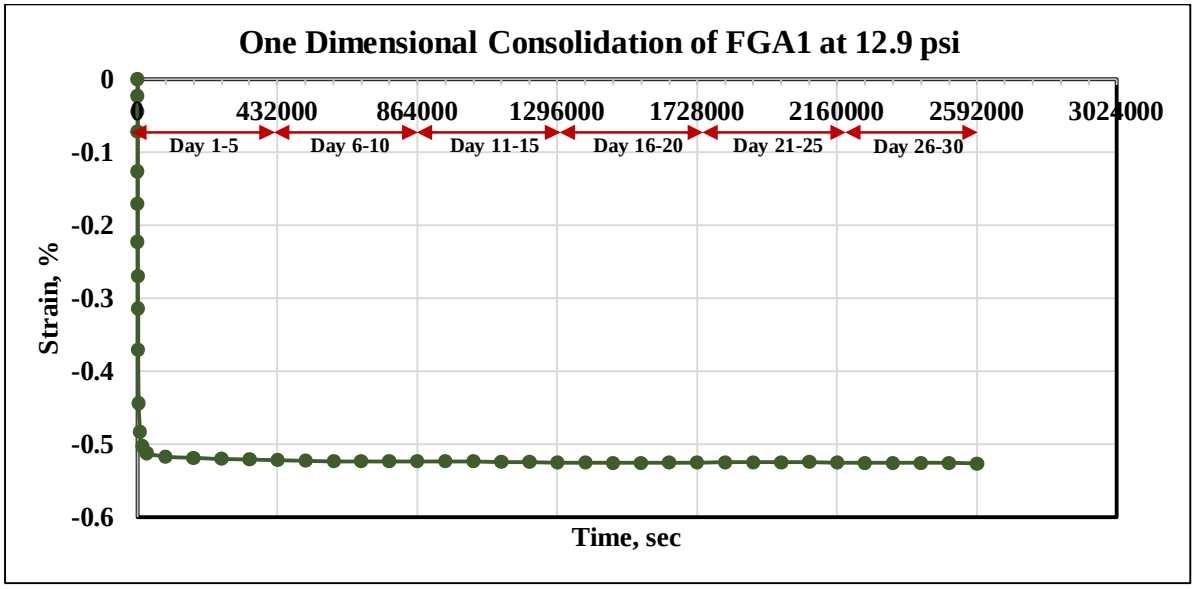

FIGURE 47. 30 days one-dimensional consolidation on FGA1 under a static load of 12.9 psi

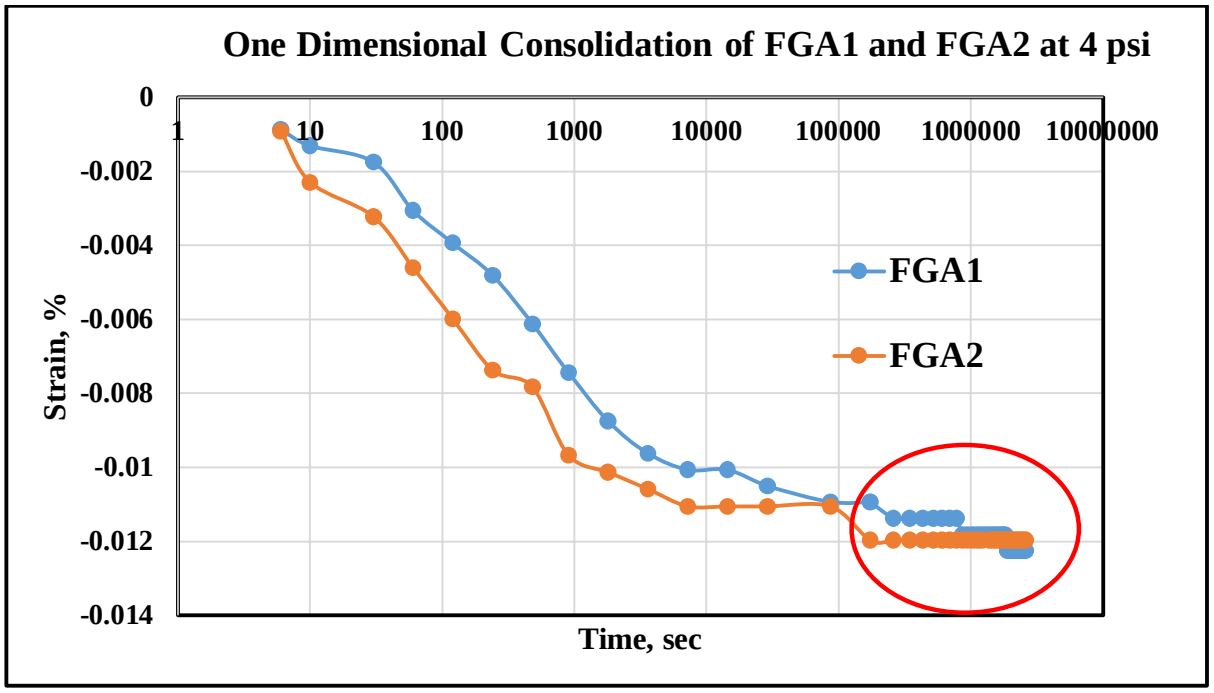

FIGURE 48. 30 days one-dimensional consolidation on FGA1 under a static load of 4 psi

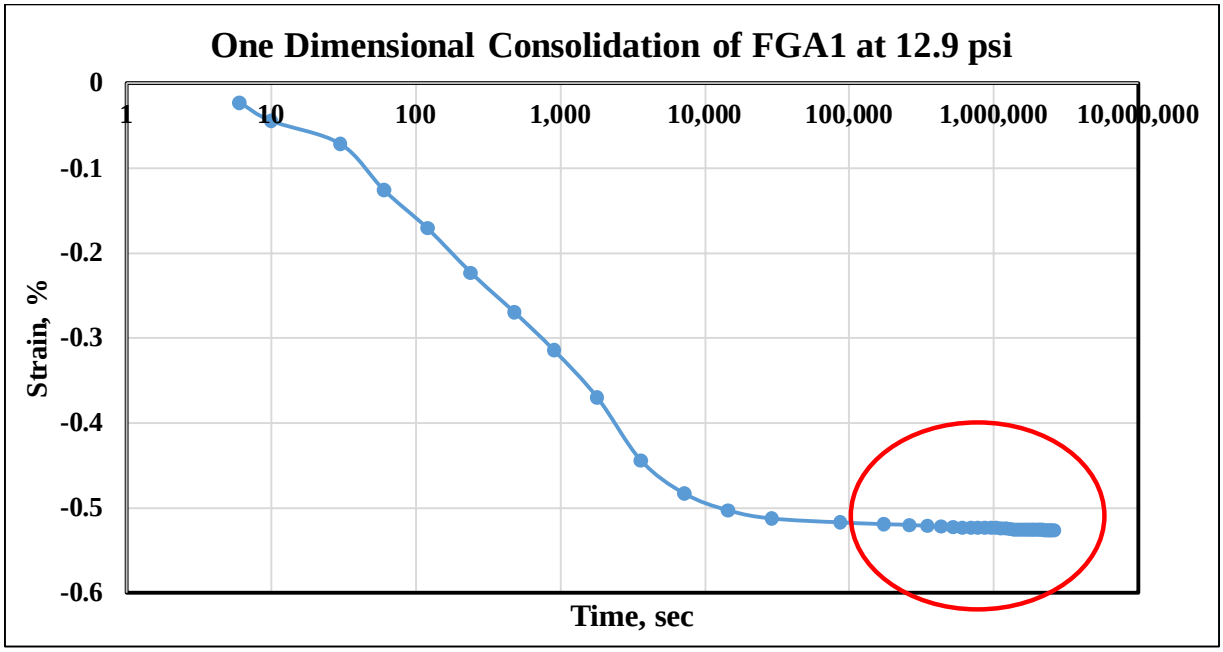

FIGURE 49. 30 days one-dimensional consolidation on FGA1 under a static load of 12.9 psi

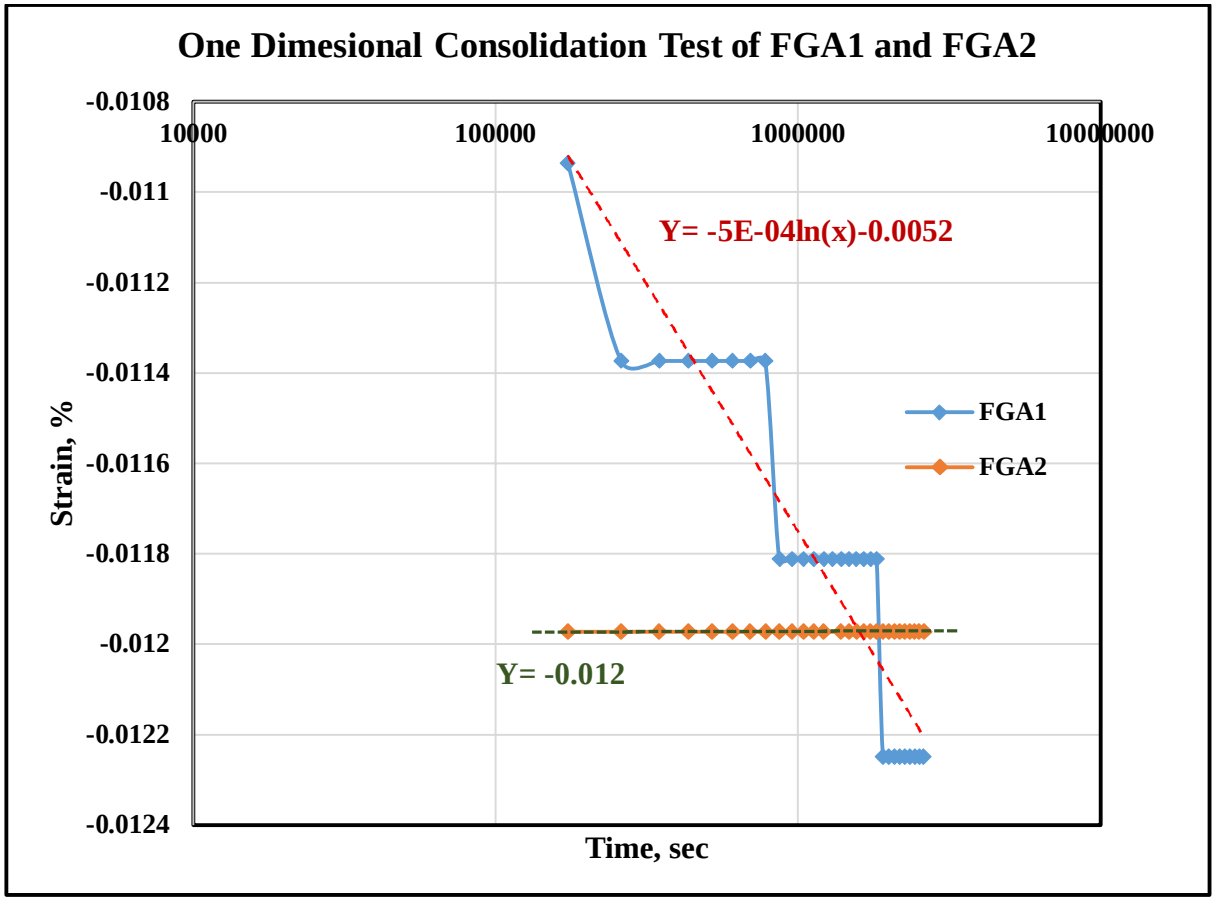

FIGURE 50. Regression for 50-year creep projection at 4psi

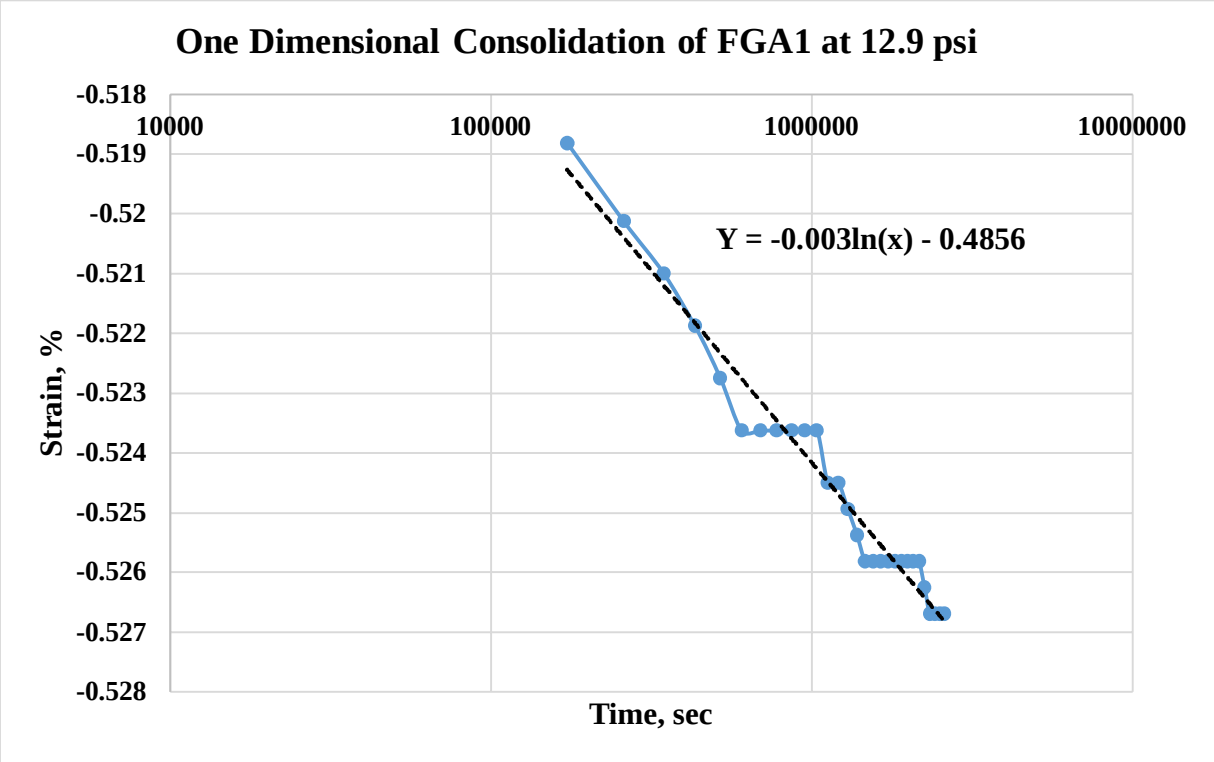

FIGURE 51. Regression for 50-year creep projection at 12.9 psi

4.5.3 Multiple Stress Incremental Levels

Although the average pressure in a typical embankment layer was determined to be 4 psi, materials at different depths of the embankment or under a structure footing may experience higher or lower stress levels. Therefore, the behavior of FGA1 and FGA2 was investigated under various load increments and then compared to the performance of sand and EMB1 under similar conditions.

To serve the purpose, FGA1, FGA2, EMB1, and sand were tested under controlled-stress loading conditions in accordance with AASHTO T216. EMB1 and sand were prepared at their OMC and compacted to 95% of their MDD. Incrementally applied loads were introduced, ranging from 1.8 psi to 29 psi, with a load increment ratio of one, to evaluate the materials' behavior under increasing stress levels.

Figure 52 shows the relationship between applied stress and cumulative strain for FGA1, FGA2, sand, and EMB1. The cumulative strain observed for FGA1 and FGA2 was comparable. When compared to EMB1, the strain in FGA1 and FGA2 was approximately 14 times lower, indicating significantly higher stiffness. Up to 14.5 psi, both FGA1 and FGA2 demonstrated a

performance level close to that of sand. However, beyond that, as the applied pressure increased to 29 psi, the sand exhibited higher stiffness than FGA1 and FGA2. Using the stiffness of sand as a benchmark, the maximum pressure on FGA should not exceed 14.5 psi (or 2,088 psf). This value is very close to a maximum pressure of 2,500 psf specified by PennDOT's special provision.

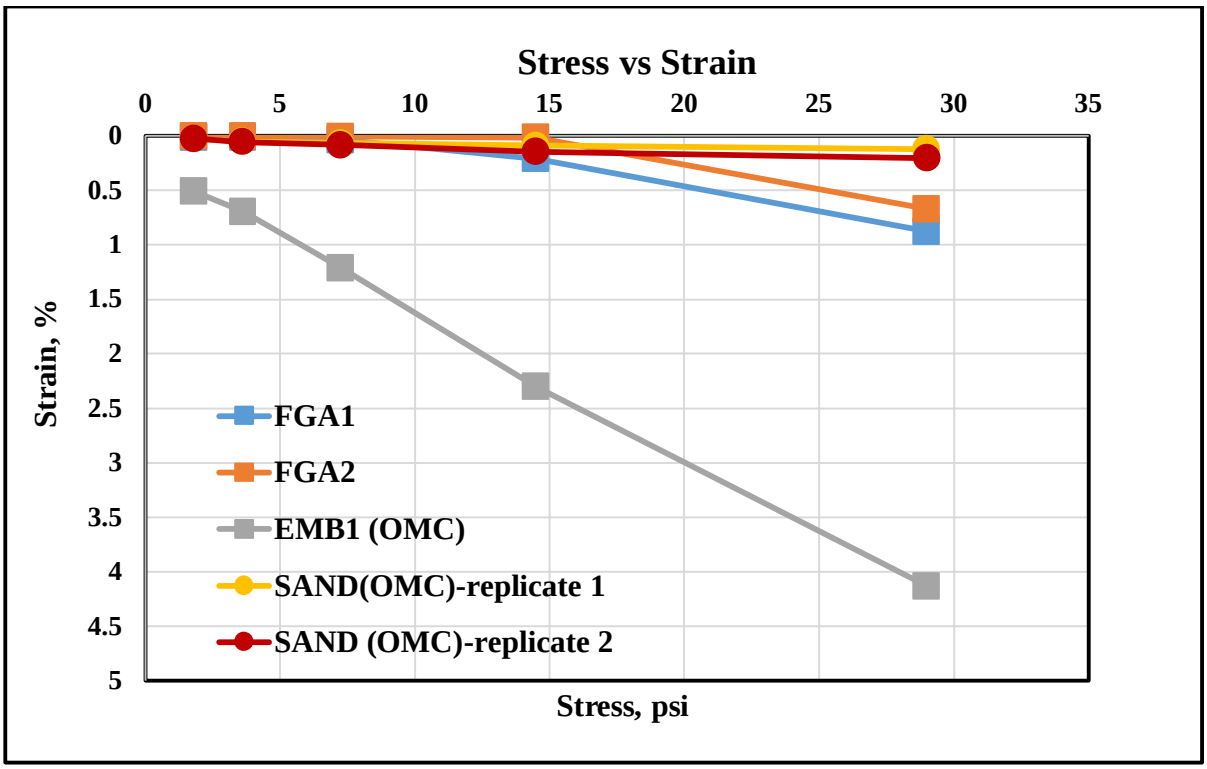

FIGURE 52. One dimensional consolidation of FGA1, FGA2, Sand and EMB1 under multiple incremental stresses

Table 15 presents the compression index (C_c) values of the tested materials under the same conditions, as a reference.

TABLE 15. Summary of Compression Index (*Cc*)

Material	*Cc*
FGA1	0.05
FGA2	0.04
EMB1	0.2
Sand	0.003

4.6 Direct Shear Test

Like many conventional soils, FGA exhibits nonlinear behavior under different stress conditions, and to capture that, power models, as illustrated in Figure 53, were also developed to represent the nonlinear relationship between shear strength and confining pressure.

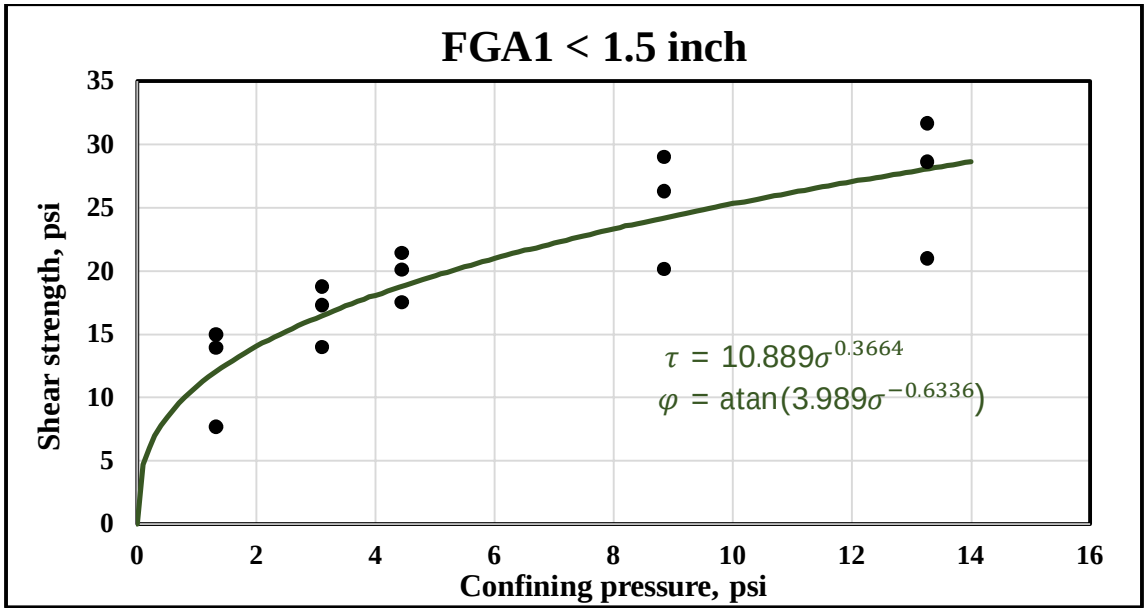

(a)

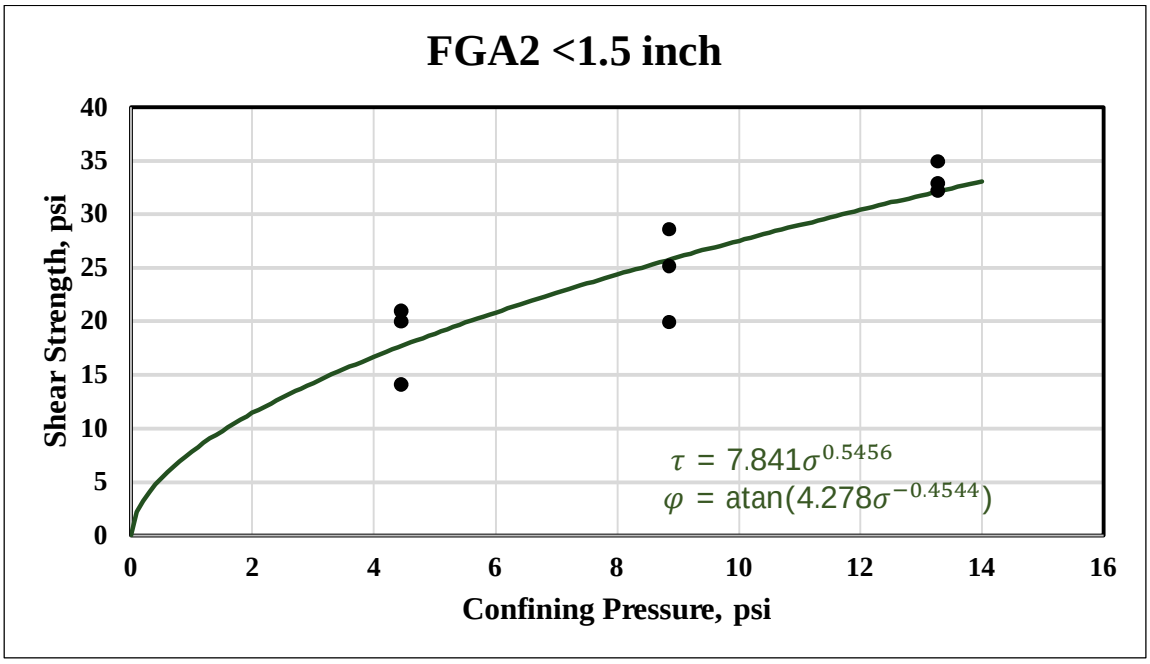

(b)

FIGURE 53. Power models of direct shear results for statically compacted: (a) FGA1 and (b) FGA2 <1.5 inch at 10% volume reduction

The power relationships between confining pressures and shear strengths for FGA1 and FGA2 are as follows in Equations 3 and 4:

$$\text{FGA1: } \tau = 10.889\sigma^{0.3664} \quad (3)$$

$$\text{FGA2: } \tau = 7.841\sigma^{0.5456} \quad (4)$$

Correspondingly, the slopes of the curves (i.e., the tangents of the friction angles) were determined by taking the first derivatives of Equations 3 and 4, respectively, to calculate the friction angles, as shown in Equations 5 and 6.

$$\text{FGA1: } \varphi = \text{atan}\,(3.989\sigma^{-0.6336}) \quad (5)$$

$$\text{FGA2: } \varphi = \text{atan}\,(4.278\sigma^{-0.4544}) \quad (6)$$

The results indicated that different friction angles for FGA should be used depending on the depth of the FGA layers and/or the applied pressure levels, for example, under a structural footing. FGA2 exhibits higher friction angles than FGA1, particularly at higher confining or normal stress levels. Example friction angles for FGA1 and FGA2 are provided in Table 16. It is noted that, for MSE wall design, the Illinois DOT specifies that the friction angle of MSE select fill shall not exceed 40° for design calculations.

TABLE 16. Friction Angles of FGA1 and FGA2 (passed through 1.5 inch)

Normal Stress Levels, psi	FGA1	FGA2
1	75.9°	76.8°
3	62.5°	68.9°
5	53.9°	64.1°
7	47.6°	60.4°
9	42.9°	57.6°
11	39.1°	55.2°
13	36.0°	53.1°

Figure 54 also illustrates the variation of friction angle with confining (normal) pressure for FGA1 and FGA2 using an alternative approach. The relationship between shear strength and confining pressure can be represented as bilinear, with a transition point at a confining pressure of 4.44 psi for FGA1. Additionally, the blue dashed line represents a hypothetical relationship for FGA1 below 1.33 psi of confining pressure, as FGA is not expected to exhibit true cohesion. A similar dashed line of the same color is shown for FGA2, as the results at low confining stress levels are not considered reliable due to significant dilation observed during shear tests. These

results suggest that different friction angles should be used in MSE wall select fill design, depending on the depth of each FGA layer. The friction angles and apparent (or pseudo) cohesion based on the bilinear relationships are provided in Table 17.

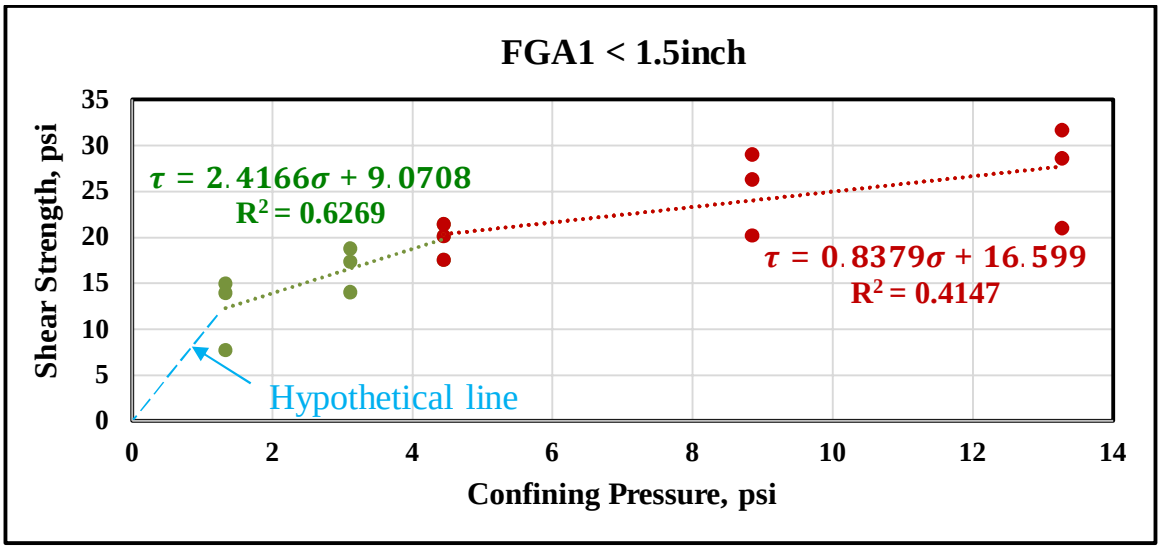

(a)

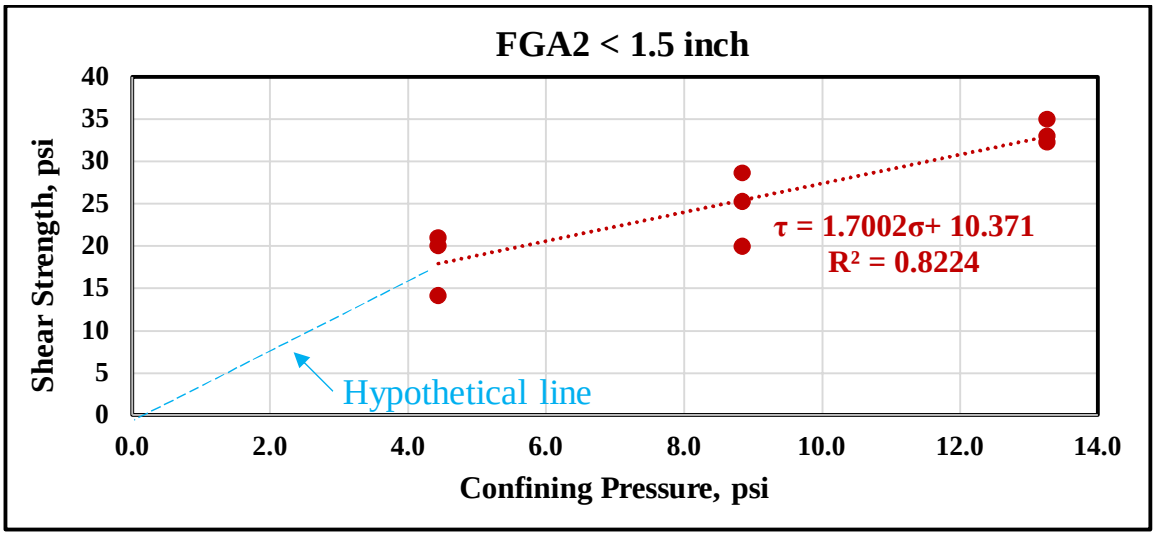

(b)

FIGURE 54. Bi-linear model of direct shear results for statically compacted: (a) FGA1 and (b) FGA2 <1.5 inch at 10% volume reduction

TABLE 17. Friction Angles of FGA1 and FGA2 (passed through 1.5 inch)

Type of material	Normal stress, psi	Apparent Cohesion, psi	Friction Angle, degrees
FGA1	1.33-4.44	9.07	67.5
	4.44-13.27	16.60	40.0
FGA2	<4.44	0	76.0
	4.44-13.27	10.37	59.5

For ease of implementation, a single linear envelope, as shown in Figure 55, was applied to FGA1 and FGA2, respectively. For FGA1, the friction angle and apparent cohesion were 50° and 12.7 psi, respectively, while for FGA2, they were 59.5° and 10.4 psi. However, these friction angles are still subject to a maximum of 40°, as specified by the Illinois DOT.

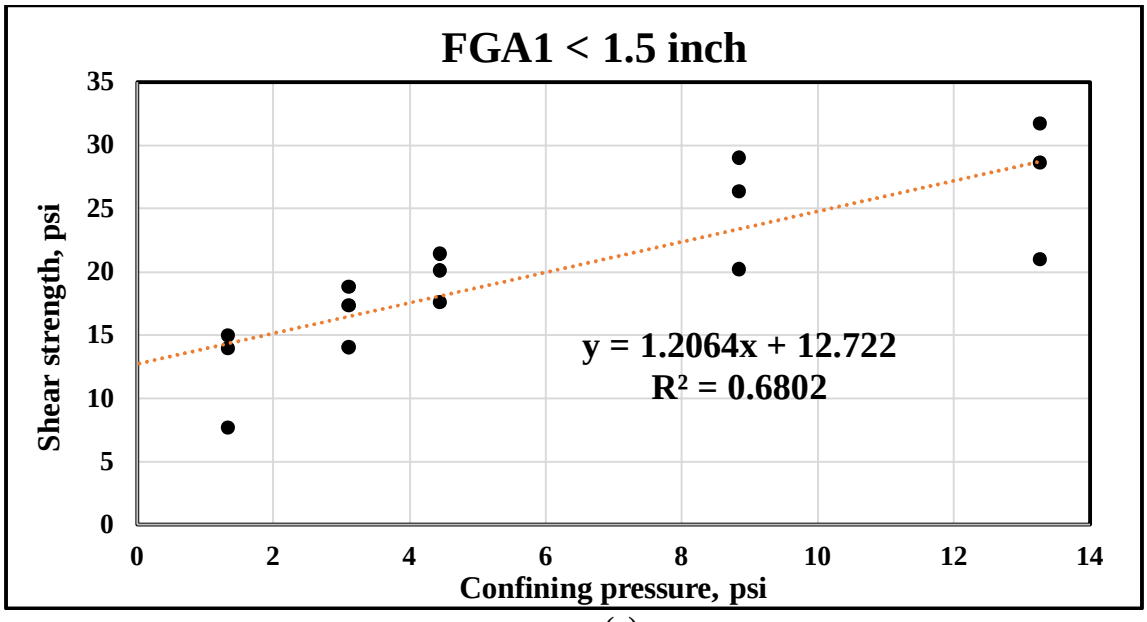

(a)

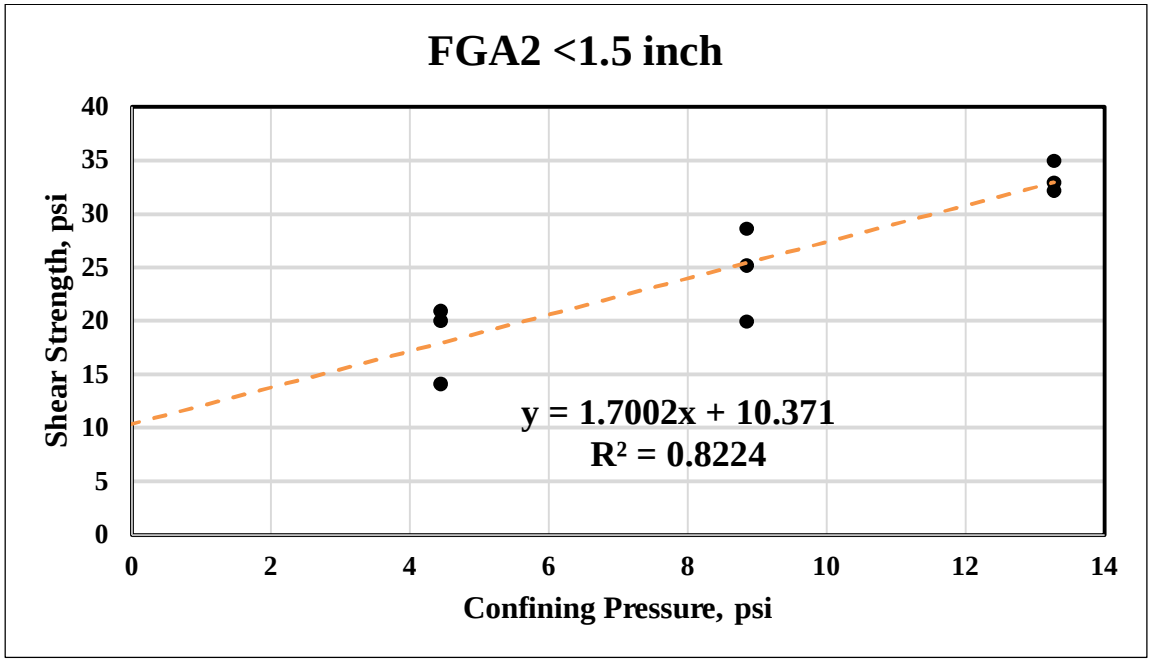

(b)

FIGURE 55. Linear strength envelope models of direct shear results for statically compacted: (a) FGA1 and (b) FGA2 <1.5 inch at 10% volume reduction

4.7 Dynamic Triaxial Test

To measure traffic-induced settlement under traffic load, dynamic triaxial tests were conducted on FGA1 and FGA2, as well as EMB1. Based on EverFE analysis results, the confining, seating, and cyclic stresses were set at 4.35 psi, 2.9 psi, and 2.9 psi, respectively, to simulate the stress state in an embankment immediately under the pavement structure. Each cycle consists of 0.1-second cyclic load and 0.9-second rest, in addition to the confining and seating loads. Long-term dynamic triaxial tests were also conducted for 7 days (or 0.56 million cycles), maintaining the aforementioned test conditions, to evaluate the degradation of FGA particles. FGA samples were compacted to 10% height reduction, based on static compaction. As shown in Figure 56, FGAs have comparable permanent strain compared to compacted clay EMB1 for short-term duration (less than 7,000 cycles). For long-term tests (0.56 million cycles), Figure 57 depicts the resilient modulus (applied cyclic stress over recoverable strain) of FGAs measured with overhead frame LVDT readings. FGA1 has an average resilient moduli of 19,000 psi and 17,000 psi for FGA2. No sign of degradation of modulus up to 0.56 million cycles was observed for either FGA1 or FGA2.

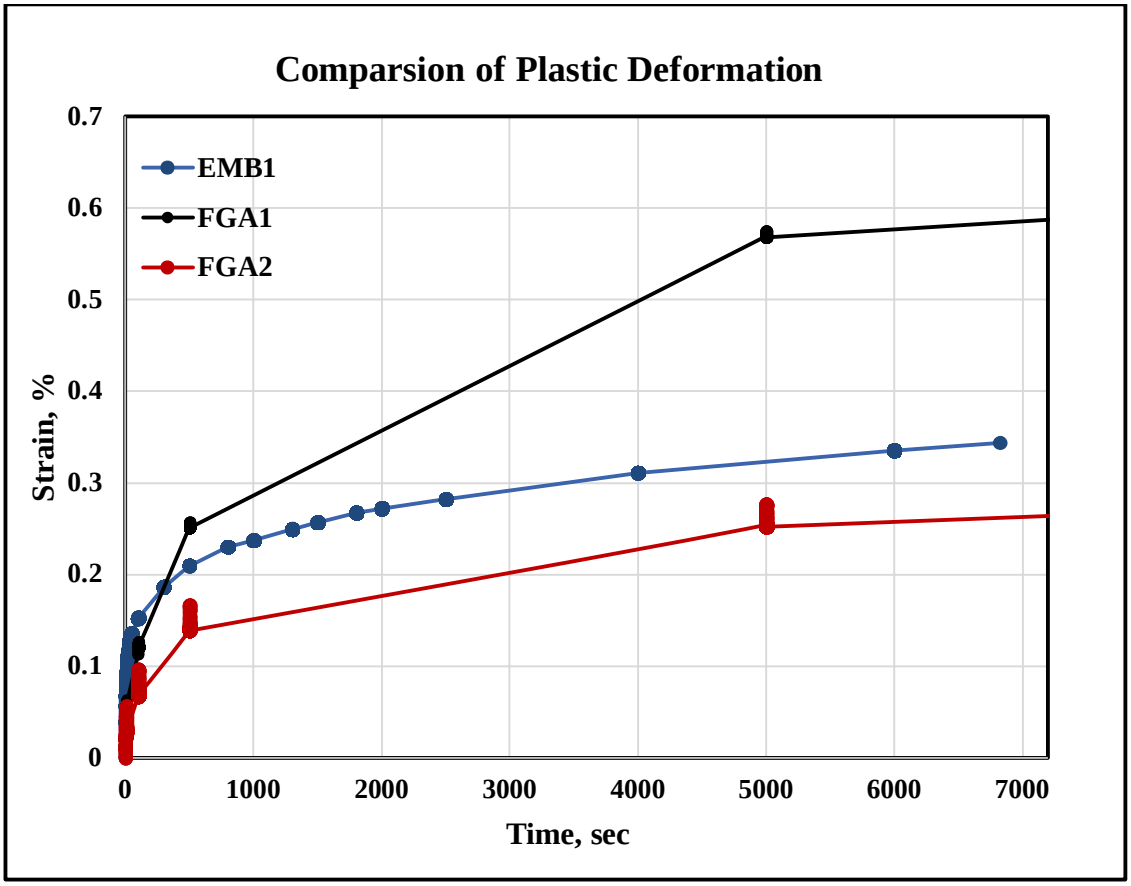

FIGURE 56. Comparison of permanent strain under dynamic loads: FGA1, FGA2, and EMB1

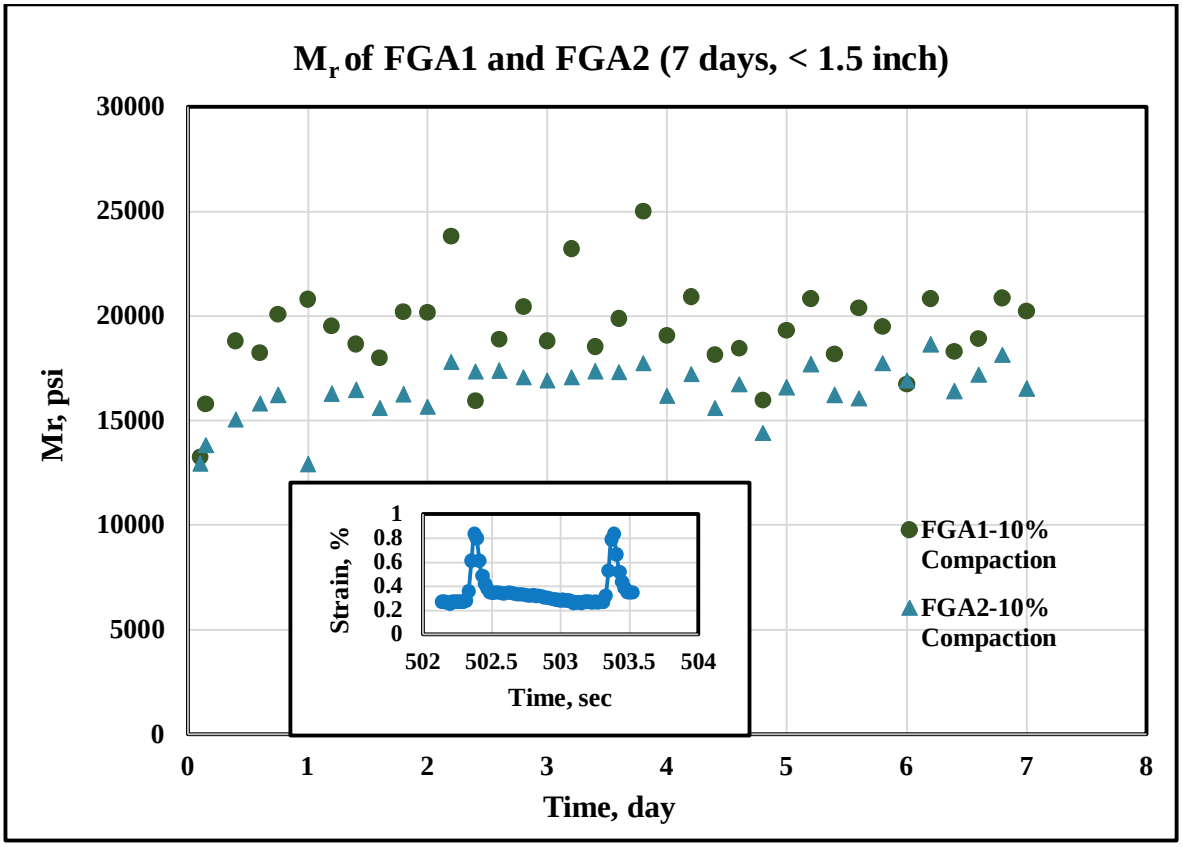

(b)

FIGURE 57. Dynamic triaxial tests results: resilient modulus evolution (embedded chart: individual cycles at 502-503 seconds)

4.8 Pilot Construction

A field compaction experiment was conducted on FGA1 using a tracked backhoe with a ground pressure of 900 psf. Density was measured with a nuclear density gauge, and surface elevation was recorded in tracked areas after each of the six passes. Figures 58, 59, and 60 showed the changes of thickness, percent thickness reduction, and density with the increase of passes, respectively. For compaction of open-graded base course, Illinois Tollway Test Procedure TTP 012 specifies the determination of rolling patterns based on (1) change of elevation less than ½" between three consecutive passes, or (2) change of density less than 1 pcf. The density from a nuclear density gauge based on direct transmission did not produce consistent measurements. The absolute density of FGA1 from the nuclear density gauge using the backscatter method was unreasonably high, around 50 pcf, compared to the expected density of 20 pcf or less. In addition, the density decreased with the increase of passes, which may be due to the breakdown of particles. The density decreased quickly during the initial passes and then stabilized after 3 passes, which

can be considered as a relative compaction index. Nonetheless, measuring the change in elevation with each successive pass seemed to be a quick and accurate method when compared to the nuclear density method. Sieve analysis was performed on samples taken from the left and right wheel paths at depths of 6 and 12 inches to evaluate changes in FGA1 gradation. As shown in Figure 61, all samples displayed comparable particle size distributions. In summary, the determination of a rolling pattern based on elevation measurements seemed to be a viable approach for assessing the compaction of FGA. TTP 012 specifies the determination of rolling patterns based on a change of elevation less than ½" for a 10-in lift between three consecutive passes. However, a change of elevation less than ¾" for three consecutive passes is recommended for a typical 2-ft lift, as shown in Figure 62.

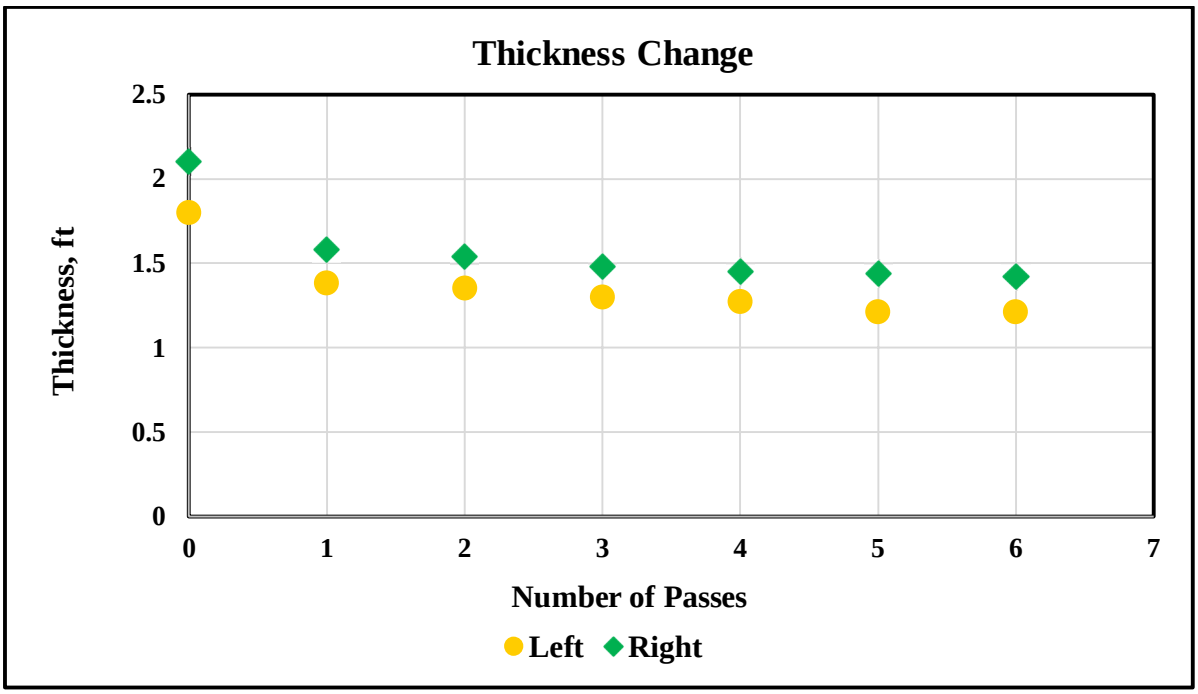

FIGURE 58. Change of FGA1 thickness

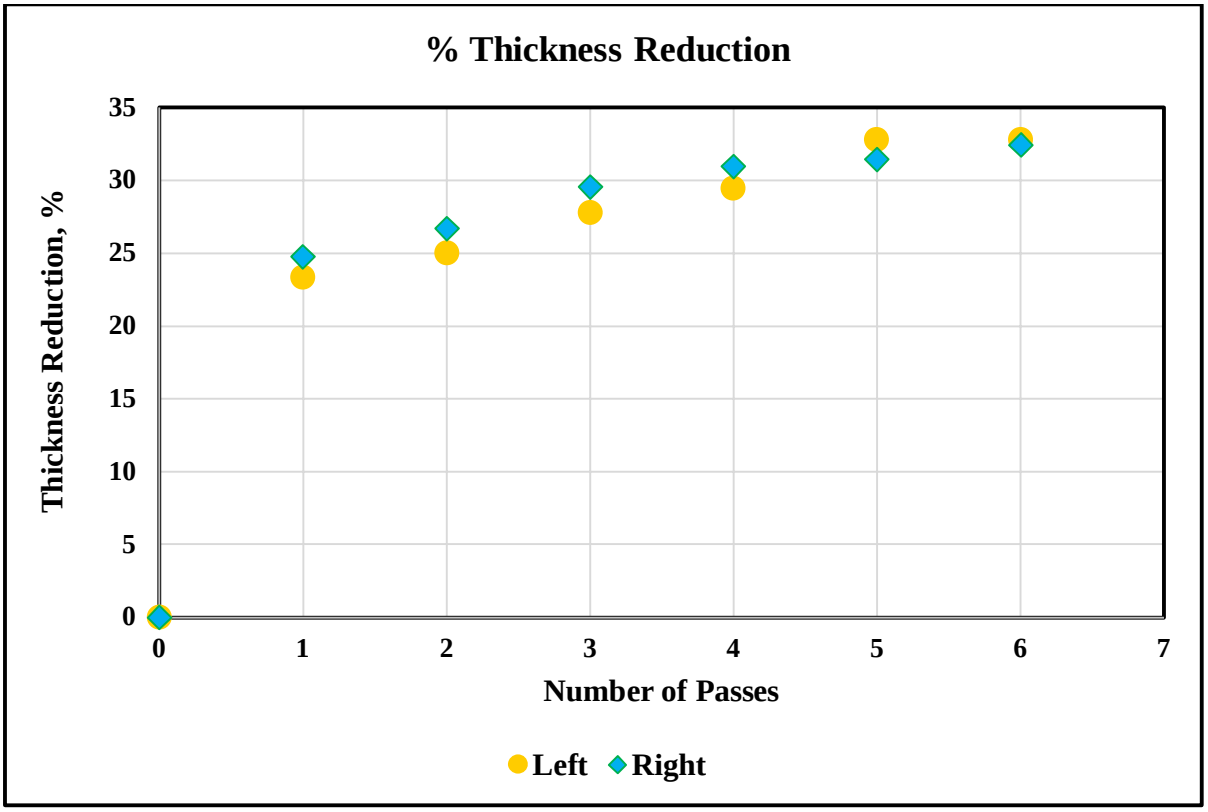

FIGURE 59. Percent thickness reduction

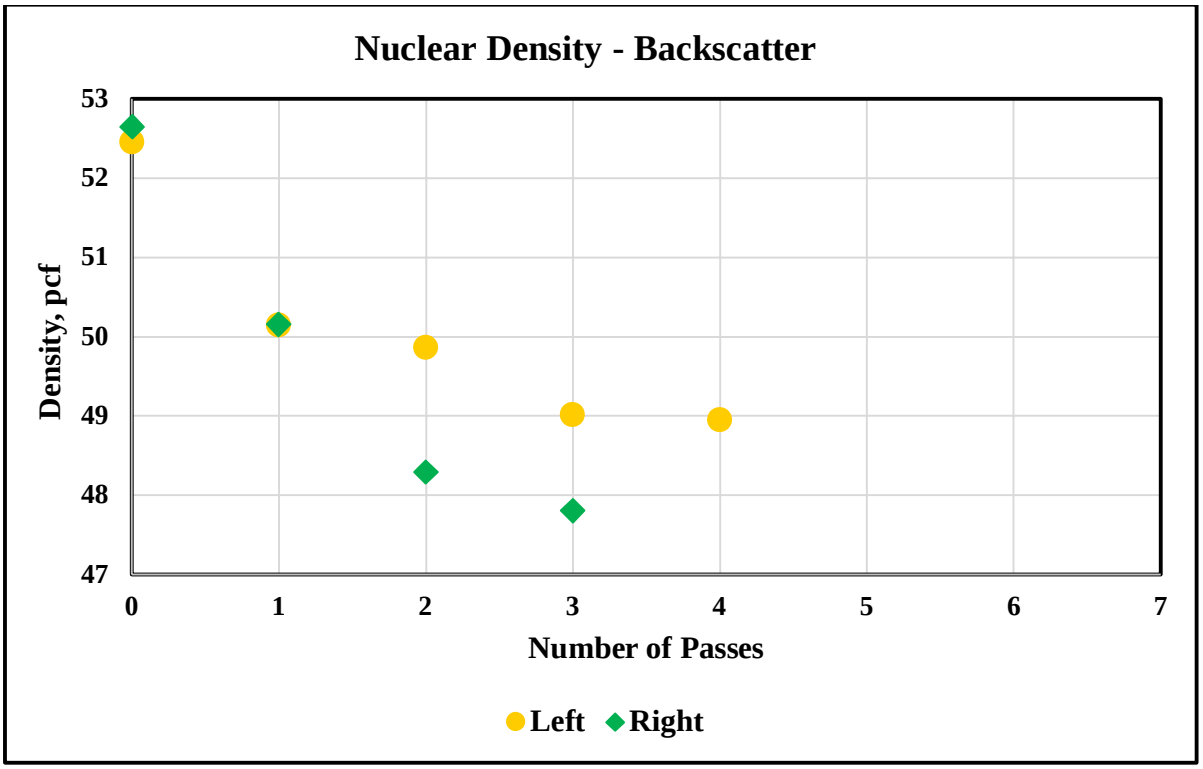

FIGURE 60. Change of density from nuclear density gauge

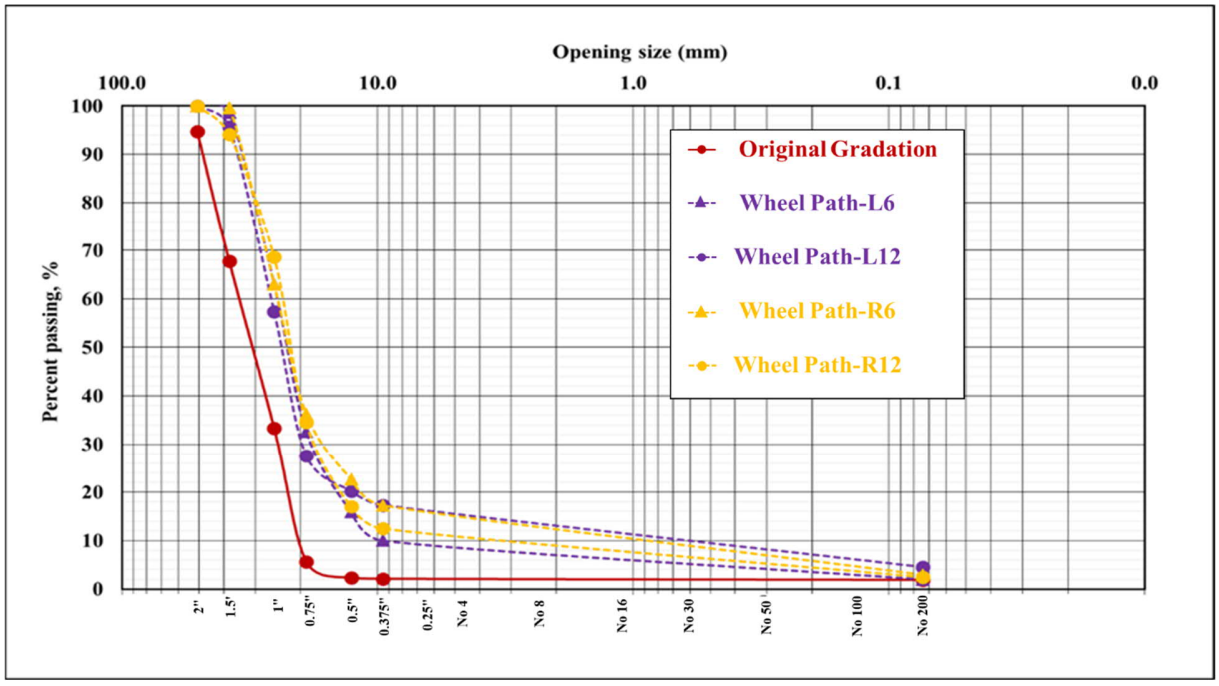

FIGURE 61. Gradation of FGA1 before and after compaction

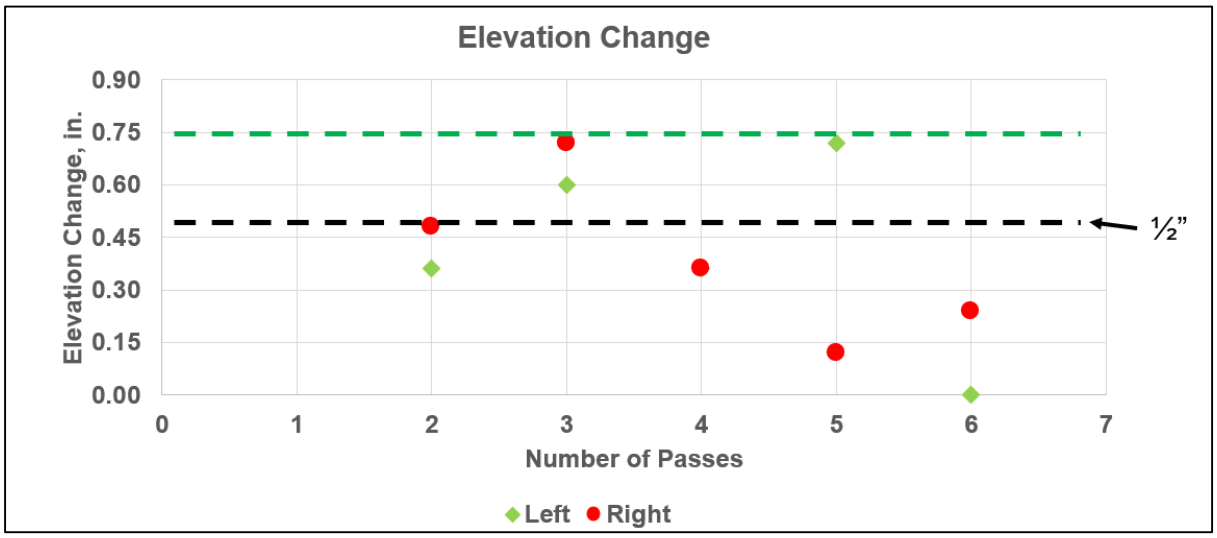

FIGURE 62. Incremental elevation change with each pass during compaction

4.9 Economical and Environmental Analysis

An economic analysis for FGA1 was conducted and compared with lightweight cellular concrete (LCC), as the Illinois Tollway uses LCC when site conditions require lightweight fill. Aero Aggregate provided information related to FGA, and Illinois Tollway supplied bidding costs and quantities for LCC. The costs of both FGA1 and LCC included material, transportation, and placement. Since the FGA plant may not be locally available, the shipping costs of FGA can be

significant and hence were considered. However, the placement of LCC can be more expensive than FGA, which is placed as a granular material. Consequently, it is essential to factor this into the entire cost.

Aero Aggregate indicated that the unit cost of FGA1 is not significantly affected by quantity, as follows:

- Material and bagging cost = \$92.5+\$7.5= **\$100** per **bulk** cubic yard (cy)
- Shipping costs (\$3/mile/load)
    - Shipping cost from Philadelphia to Chicago (800 miles) per load (88 cy) is 800 miles ×\$3/mile/load= **\$2,400/load**
    - Shipping cost from Philadelphia to Chicago per cy = \$2400/88cy= **\$27.3** per **bulk** cy
- Placement cost **(\$10/cy)**
- Total cost, including materials, transportation and placement, is (\$100 + \$27.3) ×1.25 (compaction factor) +\$10= **\$169.1/cy (in place)**

As shown in Figure 63, the cost of FGA1 (\$169.1/cy) is higher than the low-quantity LCC cost (\$150/cy). Shipping cost from Philadelphia to Chicago is as high as \$27.3/cy. A hypothetical scenario was created, assuming an FGA plant is available in the City of Chicago and the shipping distance from the plant to the construction site is only 10 miles. The cost of FGA1 reduces to \$135/cy (solid blue line in Figure 63).

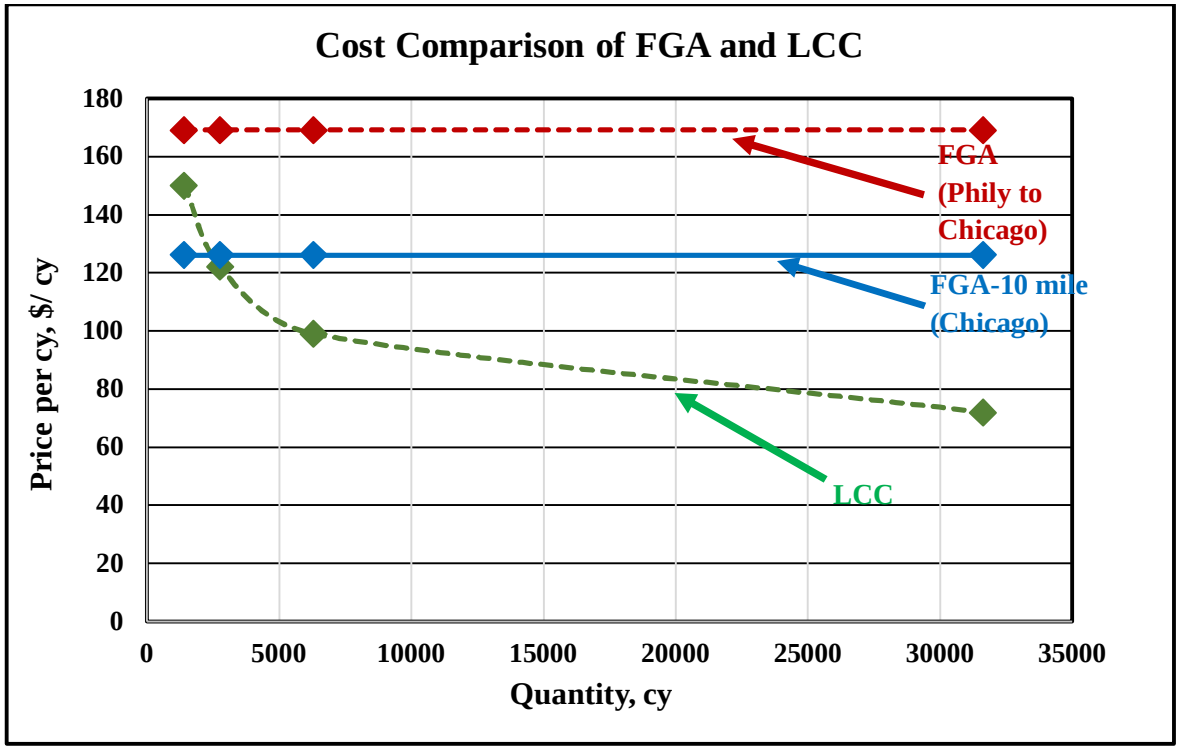

FIGURE 63. Cost comparison of FGA and LCC [Arrow and Annotations Added]

The environmental effects of FGA1 were compared to those of LCC, which is used by Illinois Tollway when lightweight materials are needed for geotechnical applications. The analysis was centered on the "cradle-to-gate" phase, which encompasses all procedures from the extraction of raw materials to the point at which the product is ready for use. Due to a lack of published data in the U.S., Environmental Product Declarations (EPDs) (EPD FOAMGLAS® Wallboard, 2019; EPD Glasopor AS, 2017; EPD Hasopor Foam Glass, 2017; EPD MISAPOR Foam Glass, 2015; EPD Norsk Glassgjenvinning AS, 2014; EPD T3+ Boards, 2019) from European manufacturers, who primarily use electric kilns, were employed in the analysis of FGA for the “cradle-to-gate” phase. These EPDs were developed based on standards such as ISO 14025, EN 15804, ISO 21930, etc. The environmental analysis of LCC was also based on relevant literature within the current body of research (Font et al., 2018; Font et al., 2020; Fouad et al., 2023; Ming Hui Fang et al., 2013; Pešta & Prošek, 2022; Reyes-Quijije et al., 2022; Zimele et al., 2019). For comparison, the data sources for the two materials were standardized based on unit volume (one cubic meter).

Figure 64 compares key environmental indicators for LCC and FGA. FGA showed a significantly lower environmental impact across all indicators, including Global Warming Potential (kg CO_2- eqv), Ozone Depletion Potential (ODP, kg CFC11- ekv), Potential for

Photochemical Oxydant Formation (POCP, kg C_2H_4-ekv), Acidification Potential (AP, kg SO_2-eqv), Eutrophication Potential (EP, $(PO_4)_3$-ekv), Abiotic Depletion of Elements (ADPM, kg Sb-eqv), and Abiotic Depletion Potential for Fossil Resources (ADPE, MJ), highlighting its lower carbon footprint and reduced resource depletion. Overall, the data suggests that FGA is a more environmentally sustainable option compared to LCC in terms of reducing greenhouse gas emissions and resource use. It is noted that the "cradle-to-gate" analysis does not cover environmental impacts from other phases of material usage, such as construction, service, end-of-life removal, and recycling activities. In addition, a North American EPD developed under ISO standards should be created for both FGA and LCC.

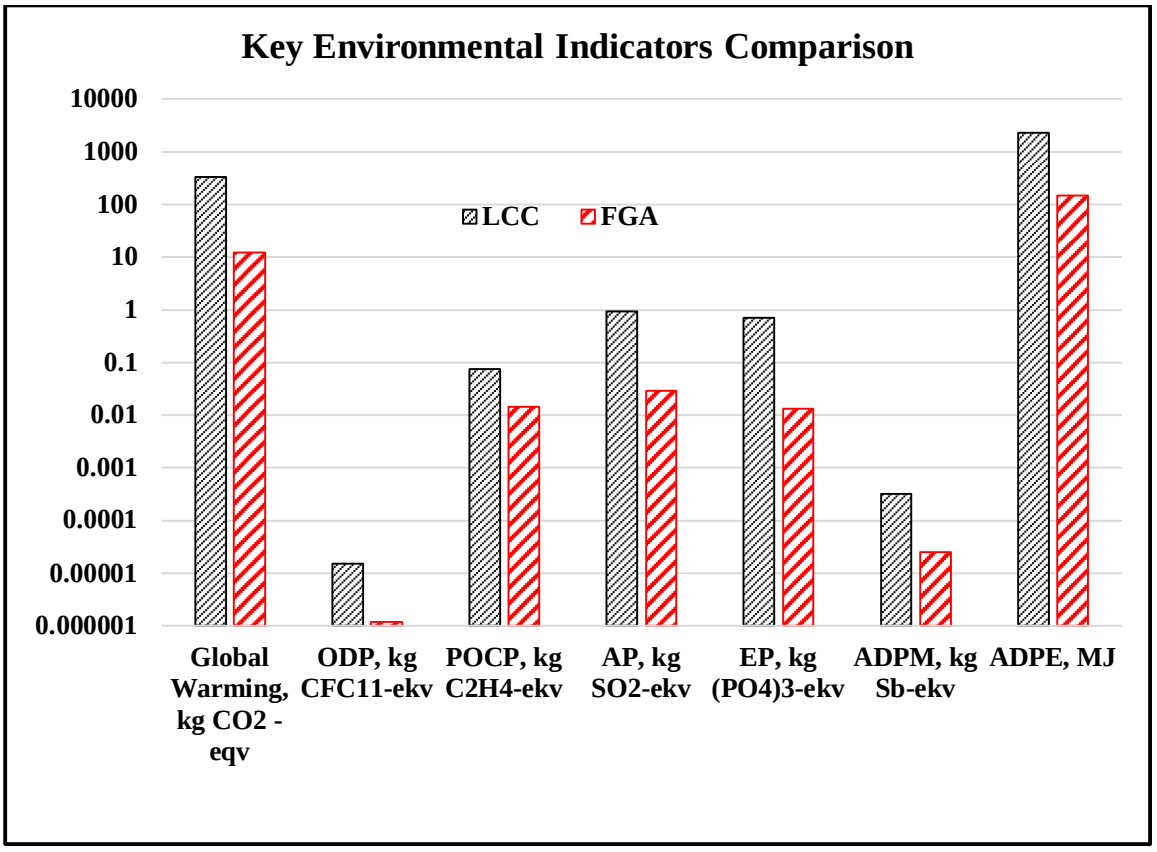

FIGURE 64. Comparison of the environmental analysis of FGA and LCC

CHAPTER 5: CONCLUSIONS AND RECOMMENDATIONS

In this study, the research team investigated the use of two sources of FGA—FGA1, produced by dry foaming, and FGA2, produced by wet foaming—as embankment material. Based on a literature review, survey results, laboratory experiments, pilot construction, and analyses, the following conclusions and recommendations can be made.

5.1 Conclusions

1. The dry loose bulk densities of the FGAs studied in this project are 12.6 pcf for FGA1 and 10.0 pcf for FGA2. The water absorption rates of FGAs depend on the duration of submersion, reaching 23.6% and 16.2% by weight after four weeks of soaking, respectively.
2. The organic, sulfate, and chloride contents of both FGA1 and FGA2 meet the Illinois Department of Transportation (IDOT) specifications. However, the pH levels exceeded IDOT's upper limit of 10.0 for steel reinforcement, and the resistivity values were below IDOT's minimum requirement of 3,000 ohm-centimeters.
3. Based on aerodynamic test results, FGAs require coverage with conventional materials to prevent erosion under high wind conditions.
4. Various laboratory compaction methods for FGAs were evaluated. Severe crushing of FGA particles was observed in some methods. Considering particle integrity and practicality, static compaction to achieve a 10% height reduction may be the most feasible approach.
5. In terms of 1-D compression, both FGA1 and FGA2 exhibited significantly less deformation compared to EMB1 (a glacial clay) and sand under a static load of 4 psi (a typical embankment pressure) over 24 hours.
6. Based on 30-day 1-D compression test results, a 50-year secondary settlement projection indicated minimal creep at both 4 psi and 12.9 psi.
7. FGAs exhibited high friction angles and a nonlinear relationship between normal stress and friction angle, indicating the need for depth- or stress-dependent selection of friction angles.
8. Under dynamic triaxial conditions, FGA materials showed plastic deformations comparable to or lower than compacted clay (EMB1). The resilient modulus of FGAs ranged from 15,000 to 19,000 psi. No degradation in the moduli of FGAs was observed up to 0.56 million load cycles.

9. Field pilot construction demonstrated that measuring elevation changes is an effective method for FGA compaction acceptance. It is recommended that compaction be accepted when elevation changes are less than ¾ inch between three consecutive passes for a typical 2-ft lift thickness.
10. Economic analysis indicates that the cost of FGAs can be significantly affected by shipping distance, and FGA prices are higher than those of low-quantity lightweight cellular concrete.
11. Based on the environmental impact assessment of FGAs published in Europe and lightweight cellular concrete (LCC) for the "cradle-to-gate" phase, FGAs are a more environmentally sustainable option than LCC in terms of reducing greenhouse gas emissions and resource use.

5.2 Recommendations for Further Study

Based on this study, the following considerations and topics are recommended for further study.

1) Currently, there is no widely accepted national specification for testing the pH and resistivity of FGA. It is recommended that Illinois Tollway monitor the development of such tests to ensure consistent and accurate assessments of these properties, especially for MSE wall select fill. PennDOT is currently conducting a research study on the electrochemical properties of lightweight materials.
2) It is recommended that the Illinois Tollway conduct pilot projects in which FGA is used as embankment material in place of lightweight cellular concrete (LCC). Such projects would provide valuable data on the construction process, performance, and long-term behavior of FGA in real-world conditions, aiding in the evaluation of its suitability as an alternative to LCC.

5.3 Proposed Draft Special Provision on Foamed Glass Aggregate (see next page)

5.4 Proposed Design Guidance on Foamed Glass Aggregate (Appendix A)

Draft Special Provision on Foamed Glass Aggregate (modified based on Pennsylvania DOT specification)

1. DESCRIPTION—This work is furnishing, transporting, placing, and compacting foamed glass aggregate (FGA) lightweight fill for the construction of embankments and for backfilling behind structures, except for mechanically stabilized earth walls.

2. MATERIAL—

(a) Foamed Glass Aggregate (FGA). Provide FGA conforming to the following requirements:

TABLE A
Foamed Glass Aggregate Physical Requirements[(1)]

Property	Test Method	Value
Dry Loose Bulk Density, as manufactured (pcf)	ASTM C29/C29M, Method C[(2)]	15 (max.)
Moist Loose Bulk Density, as delivered (pcf)	ASTM C29/C29M, Method C[(2)]	20 (max.)
Confined Compression Load Required to Obtain 10% Vertical Deformation (psi)	EN 1097-11:2013[(3)]	34.7 (5,000 psf)
Confined Compression Load Required to Obtain 20% Vertical Deformation (psi)	EN 1097-11:2013[(3)]	90.3 (13,000 psf)

(1) All values are minimum unless indicated otherwise.

(2) ASTM C29/C29M modified to perform tests in the field on as-received material particle size and density.

(3) EN 1097-11-2013 (European Committee for Standardization, 2013) modified for particle size and density for as-manufactured material.

TABLE B
Foamed Glass Aggregate Size and Grading Requirements, as Manufactured Based on Laboratory Sieve Tests, ASTM C136/C136M[(1)], Square Openings

Sieve Size	Percent Passing
4-inch	100
2 ½-inch	85-100
3/8-inch	0-15

(1) ASTM C136 modified for particle size and density of as-manufactured material.

- Provide FGA produced from at least 98% recycled glass.
- Provide material delivered in bulk.
- Provide the manufacturer's name and material physical properties certification showing conformance to the values as specified in Tables A and B.

(b) Geotextile. 1080.02

(c) Embankment Materials. Section 205

(d) Subbase. Section 311

(e) Topsoil. Section 211

3. CONSTRUCTION—

(a) Delivery, Storage, and Handling. Deliver, store, and handle materials according to the manufacturer's recommendations.

During all stages of manufacture, shipment, storage, and construction, minimize the amount of handling to prevent physical damage to the material. Store material in an area not prone to flooding. Minimize the amount of trafficking on FGA until geotextile and an adequate thickness of capping material is placed over the FGA. Do not use the FGA placement area as a haul road.

(b) Placement. Before placement of FGA at or below original ground, remove standing water in excess of 6-in deep prior to placement of the FGA. Do not place FGA on frozen ground.

Submit documentation for the equipment make, model, and corresponding ground pressure for compaction/tracked equipment to the Engineer for verification and acceptance. Allow 10 working days for review and approval of the compaction or tracked equipment to be used for compaction of FGA.

Before placement of FGA, place geotextile as indicated on the drawings. The geotextile shall be installed as specified in Section 210. Remove and replace the geotextile damaged during construction. Lap fabric over damaged areas and secure fabric lap with sewing, heat bonding, or by overlapping a minimum of 24 inches in all directions.

The FGA manufacturer's representative is to remain on-site for the duration of the placement of the FGA material to answer any questions regarding the placement of FGA as deemed necessary by the Engineer.

Place FGA as indicated on the drawings. Minimize the use of wheeled, tracked, or other equipment on the surface of the FGA for activities other than for placement and compaction of FGA. Rollers are not permitted directly on the FGA layer. Avoid compaction that crushes or changes the gradation of the FGA.

During placement of FGA, do not allow storm water to accumulate in the FGA installation area until a sufficient thickness of FGA, embankment material, or capping material is placed above the anticipated flood elevation to act as ballast. Alternatively, a temporary ballast material or system may be used if approved by the Engineer to secure the FGA in the event of flooding.

For compaction using tracked equipment, place the FGA in uncompacted lift thicknesses of 24 inches. For uncompacted lift thicknesses between 12 and 24 inches, perform compaction with a tracked excavator or dozer with ground pressures of between 625 psf and 1,025 psf. After placing the initial loose lift, compact the FGA by raising the blade or bucket and tracking over the layer.

The proper compaction pattern shall be determined using a growth curve with survey elevation data. The FGA shall be compacted to an acceptable number of passes until survey data shows that the compaction of the material is negligible (less than 3/4-inch) between three consecutive passes and acceptable to the Engineer. Use paint to mark the locations of measurements. A steel plate of 8" wide × 8" long × minimum 0.125" thick shall be placed under the elevation rod at the time of measurement. Avoid foot traffic on measurement locations by staying clear 1 ft from the measurement spot. The measurement spots shall be 15 ft or less apart in any direction, or acceptable to the Engineer.

The Contractor must verify the compaction pattern once per week, or every time a new piece of equipment is used, or at the Engineer's request. The compaction pattern development must be performed in the presence and to the satisfaction of the Engineer.

The specified number of passes determined by the verification will be the required number of passes used for each lift of the FGA material and that particular equipment for the project. If the Contractor wishes to change compaction equipment during the project, then a new compaction pattern must be developed.

For areas not accessible by tracked equipment (e.g., around structures, utilities, etc.), place FGA in maximum uncompacted lifts of 12 inches and compact the material with a plate compactor having a static weight of between 110-220 lbs. The FGA shall be compacted to an acceptable number of passes until survey data shows that the compaction of the material is negligible (less than ½-inch) between three consecutive passes and acceptable to the Engineer.

When FGA is utilized in the embankment and is not capped on top and sides with impermeable materials, permanent subsurface drainage facilities shall be provided to prevent water from collecting within the embankment as required by the Engineer. This may include shaping of the embankment material to allow water to drain to a perforated pipe, placement of perforated pipes with a maximum diameter of 6 in. (150 mm) in either the longitudinal or transverse direction, or other features. If transverse pipes are used, they shall be placed at sag vertical curves and no more than 500 ft (150 m) apart. If longitudinal pipes are used, they shall be placed on the low sides of the roadway crown. All pipes shall be sloped to provide drainage and be equipped with headwalls.

Before placement of capping material, place geotextile over the FGA as indicated on the drawings. Install the geotextile as specified in Section 282, except overlap fabric roll-ends and edges a minimum of 24 inches with adjacent material. Remove and replace the geotextile damaged during construction. Lap fabric over damaged areas and secure fabric lap with sewing, heat bonding, or by overlapping a minimum of 24 inches in all directions.

(c) Testing. Test each truckload of delivered FGA for moist loose bulk density (per ASTM C29/C29M Method C) to ensure it meets specifications as provided in Table A. Perform bulk density testing in the presence of the Engineer.

(d) Capping Material Placement. Place and compact capping material immediately after placement of the geotextile.

Use one of the following capping materials over or on the slope of FGA:

- Embankment material over FGA in a pavement structure and/on the slope of the FGA, placed as specified in Section 205.
- Subbase over the FGA, placed as specified in Section 311;
- Topsoil on the slope of the FGA, placed as specified in Section 211;

Place at least six (6) inches of compacted thickness of capping material over FGA in a pavement structure or 2 feet on the open slope of the FGA in all locations. Do not allow the geotextile to be damaged or disturbed by blading out the capping material. To preclude damage to the geotextile, do not use padfoot rollers for compacting the first six-inch capping material. Complete placement of capping material on top and/or on the slope of the FGA prior to using rollers to compact the fill materials over and/or on the slope. the FGA capping material. Repair any damage to the geotextile that occurs before or during fill placement.

Method of Measurement. FOAMED GLASS AGGREGATE will be measured in place, and the volume computed in cubic yards from cross sections taken before and after placement. The width and depth for measurements will be as shown on the plans or as directed by the Engineer.

Basis of Payment. This work will be paid at the Contract unit price per cubic yard for FOAMED GLASS AGGREGATE.

REFERENCES

AASHTO. (2017). *Guide Specifications for LRFD Seismic Bridge Design, 4th edition.* American Association of State Highway and Transportation Officials, Washington, DC.

AERO Aggregates. (2019). UL-FGA 25+ Years of Proven Performance. https://static1.squarespace.com/static/61576f778e4f9f0f36f99dc3/t/62fa580f0d23a76e27e70cdb/1660573711460/CaseTN525_NassauExpressway.pdf.

AERO Aggregates. (2023). Foamed Glass Aggregates Supplier Aero Aggregates Celebrates Reopening of I-95 Corridor. PR Newswire. https://www.prnewswire.com/news-releases/foamed-glass-aggregates-supplier-aero-aggregates-celebrates-reopening-of-i-95-corridor-301861229.html#:~:text=EDDYSTONE%2C%20Pa.%2C%20June%2023,95)%20in%20Philadelphia%2C%20which%20collapsed.

AERO Aggregates - TN220. (2022). Comparison of Manufacturing Methods and Corresponding Properties of Ultra-Lightweight Foamed Glass Aggregate.

AERO Aggregates – TN303. (2018). Foamed Glass Aggregate: A Lightweight Fill Alternative Finds The U.S. Market.

Arulrajah, A., Disfani, M. M., Maghoolpilehrood, F., Horpibulsuk, S., Udonchai, A., Imteaz, M., & Du, Y. J. (2015a). Engineering and Environmental Properties of Foamed Recycled Glass as a Lightweight Engineering Material. *Journal of Cleaner Production, 94*, 369–375. https://doi.org/10.1016/j.jclepro.2015.01.080

Arulrajah, A., Horpibulsuk, S., Maghoolpilehrood, F., Samingthong, W., Du, Y. J., & Shen, S. L. (2015b). Evaluation of Interface Shear Strength Properties of Geogrid Reinforced Foamed Recycled Glass Using a Large-Scale Direct Shear Testing Apparatus. *Advances in Materials Science and Engineering*, 2015. https://doi.org/10.1155/2015/235424

Auvinen, T., Pekkala, J., & Forsman, J. (2013). Covering the Highway E12 in the Centre of Hämeenlinna-Innovative Use of Foamed Glass as Light Weight Material of Approach Embankment. *The XXVIII International Baltic Road Conference.* https://www.foamit.fi/wp-content/uploads/2016/10/COVERING_THE_HIGHWAY_E12_IN_THE_CENTRE_OF_HAMEENLINNA_INNOVATIVE_USE_OF_FOAMED_GLASS_AS_LIGHTWEIGHT_MATERIAL_OF_APPROACH_EMBANKMENT.pdf

Barzegar, M., Wen, H., Akin, I. D., & Edil, T. (2023). Laboratory Assessment of Recycled Asphalt Pavement as Roadway Embankment Material. *Transportation Research Record, 2677*(7), 112–121. https://doi.org/10.1177/03611981221151025

Bergaya, F., Lagaly, G., & Vayer, M. (2013). Chapter 2.11 - Cation and Anion Exchange. *Developments in Clay Science, 5*, 333-359. https://doi.org/10.1016/B978-0-08-098259-5.00013-5

Bernardo, E., & Albertini, F. (2006). Glass Foams from Dismantled Cathode Ray Tubes. *Ceramics International*, *32*(6), 603–608. https://www.sciencedirect.com/science/article/pii/S0272884205001409?via%3Dihub

Betti, G., Pinori, U., & Marradi, A. (2014). The Use of Recycled Glass Foam Aggregates for Lightweight Embankment. *Sustainability, Eco-Efficiency and Conservation in Transportation Infrastructure Asset Management*, 245-254.

Camargo, F. F., Wen, H., Edil, T., & Son, Y. H. (2013). Comparative Assessment of Crushed Aggregates and Bound/Unbound Recycled Asphalt Pavement as Base Materials. *International Journal of Pavement Engineering, 14*(3), 223–230. https://doi.org/10.1080/10298436.2012.655737

Christopher, B. R., Schwartz, C. W., & Boudreau, R. L. (2006). *Geotechnical Aspects of Pavements: Reference Manual*. No. (NHI-05-037). US Department of Transportation, Federal Highway Administration. https://www.fhwa.dot.gov/engineering/geotech/pubs/05037/

Edil, T. B., Tinjum, J. M., & Benson, C. H. (2012). *Recycled Unbound Materials*. (No. MN/RC 2012-35). Minnesota Department of Transportation, Research Services Section. https://rmrc.wisc.edu/wp-content/uploads/2017/05/201235-1.pdf

EPD (Environmental Product Declaration) FOAMGLAS® Wallboard (WF). (2019). https://www.health.belgium.be/language_selection?destination=b-epd

EPD (Environmental Product Declaration) Glasopor AS. (2017). https://www.epd-norge.no

EPD (Environmental Product Declaration) Hasopor Foam Glass 10–60 mm. (2017). https://www.environdec.com/home

EPD (Environmental Product Declaration) MISAPOR Foam Glass 10/50. (2015). https://ibu-epd.com/

EPD (Environmental Product Declaration) Norsk Glassgjenvinning AS epd-norge logo. (2014). https://www.epd-norge.no

EPD (Environmental Product Declaration) T3+ Boards (FOAMGLAS®). (2019). https://ibu-epd.com/

European Committee for Standardization. (2013). *Tests for mechanical and physical properties of aggregates – Part 11: Determination of compressibility and confined compressive strength of lightweight aggregates (BS EN 1097-11:2013)*. British Standards Institution.

Font, A., Borrachero, M. V., Soriano, L., Monzó, J., Mellado, A., & Payá, J. (2018). New eco-cellular concretes: sustainable and energy-efficient materials. *Green Chemistry*, *20*(20), 4684–4694. https://doi.org/10.1039/c8gc02066c

Font, A., Soriano, L., Tashima, M. M., Monzó, J., Borrachero, M. V., & Payá, J. (2020). One-part eco-cellular concrete for the precast industry: Functional features and life cycle assessment. *Journal of Cleaner Production*, *269*, 122203. https://doi.org/10.1016/j.jclepro.2020.122203

Fouad, F., Ramadan, W., Schoch, T., & Kirby, J. (2023). Environmental performance of autoclaved aerated concrete in the USA. *Ce/Papers*, *6*(2), 5–14. https://doi.org/10.1002/cepa.2223

Frydenlund, T. E., & Aabøe, R. (2007). Foamglass – A New Vision in Road Construction. *Research Projects by SINTEF*.

Guo, H. W., Wang, X. F., Gong, Y. X., Liu, X. N., & Gao, D. N. (2010). Improved Mechanical Property of Foam Glass Composites Toughened by Glass Fiber. *Materials Letters*, *64*(24), 2725–2727. https://doi.org/10.1016/j.matlet.2010.09.012.

Guthrie, W. S., Jackson, K. D., & Knighton, J. T. (2015). *Laboratory Resilient Modulus Measurements of Aggregate Base Materials in Utah* (No. UT-16.12). Utah. Dept. of Transportation. Research Division. https://rosap.ntl.bts.gov/view/dot/37417

Hanson, J. L., Edil, T. B., and Yesiller, N., "Thermal Properties of High Water Content Materials," Geotechnics of High Water Content Materials, ASTM STP 1374, American Society for Testing and Materials, West Conshohocken, PA, 1999.

Horpibulsuk, S., Munsrakest, V., Udomchai, A., Chinkulkijniwat, A., & Arulrajah, A. (2014). Strength of Sustainable Non-Bearing Masonry Units Manufactured from Calcium Carbide Residue and Fly Ash. *Construction and Building Materials*, *71*, 210–215. https://doi.org/10.1016/j.conbuildmat.2014.08.033.

Illinois Department of Transportation. (2022). *Standard Specifications for Road and Bridge Construction*. Authority of the State of Illinois.

Kong, X. (2016). Prediction of Subgrade Settlement Based Fuzzy Self Adaptable Method of Artificial Intelligence. *Proceedings - 2016 9th International Symposium on Computational Intelligence and Design, ISCID 2016.* https://doi.org/10.1109/ISCID.2016.1041

König, J., Lopez-Gil, A., Cimavilla-Roman, P., Rodriguez-Perez, M. A., Petersen, R. R., Østergaard, M. B., Iversen, N., Yue, Y., & Spreitzer, M. (2020). Synthesis and Properties of Open- and Closed-Porous Foamed Glass with a Low Density. *Construction and Building Materials, 247*. https://doi.org/10.1016/j.conbuildmat.2020.118574

König, J., Nemanič, V., Žumer, M., Petersen, R. R., Østergaard, M. B., Yue, Y., & Suvorov, D. (2019). Evaluation of the Contributions to the Effective Thermal Conductivity of an Open-Porous-Type Foamed Glass. *Construction and Building Materials*, *214*, 337–343. https://doi.org/10.1016/j.conbuildmat.2019.04.109

Lee, K. W., Marcus, A. S., Mooney, K., Vajjhala, S., Kraus, E., & Park, K. (2003). *Development of Flexible Pavement Design Parameters for Use with the 1993 AASHTO Pavement Design Procedures*. Rhode Island Department of Transportation.

Lenart, S., & Kaynia, A. M. (2019). Dynamic Properties of Lightweight Foamed Glass and Their Effect on Railway Vibration. *Transportation Geotechnics, 21*. https://doi.org/10.1016/j.trgeo.2019.100276

Loux, T. A., Filshill, A., & Zhang, Z. (2019). Foamed Glass Aggregate Lightweight Fill Over Compressible Soils. *Geo St. John's 2019.* https://members.cgs.ca/conferences/GeoStJohns2019/papers/Geo2019Paper467.pdf.

Loux, T. A., & Filshill, A. (2021a). Foamed Glass Aggregate for Resilient Waterfront Construction. *Geo-Extreme 2021*, 435–444. https://doi.org/10.1061/9780784483688.043

Loux, T.A., and Filshill, A. (2021b). "Ultra-Lightweight Foamed Glass Aggregate as MSE Wall Backfill: Properties and Case Studies." *Geosynthetics 2021*, 570-582, Industrial Fabrics Association International, 22-25 February 2021, Virtual Event.

McGuire, M. P., Loux, T. A., & Vandenberge, D. R. (2021). Field-Scale Tests to Evaluate Foamed Glass Aggregate Compaction. *IFCEE 2021*, 157-168. https://ascelibrary.org/doi/abs/10.1061/9780784483435.015.

Méar, F., Yot, P., Cambon, M., & Ribes, M. (2006). The Characterization of Waste Cathode-Ray Tube Glass. *Waste Management, 26(*12), 1468–1476. https://doi.org/10.1016/j.wasman.2005.11.017

Méar, F., Yot, P., Viennois, R., & Ribes, M. (2007). Mechanical Behaviour and Thermal and Electrical Properties of Foam Glass. *Ceramics International, 33*(4), 543–550. https://doi.org/10.1016/j.ceramint.2005.11.002

Ming Hui Fang, Zhi Hong Wang, Fei Fei Shi, Bo Xue Sun, Ming Nan Zhao, Su Ping Cui, & Xian Ce Meng. (2013). Analysis on Life Cycle CO_2 Emission of Aerated Concrete Production in China. *Materials Science Forum, 743-744*, 509–515. https://doi.org/10.4028/www.scientific.net/msf.743-744.509

Mitchell, J. K., & Soga, K. (2005*). Fundamentals of Soil Behavior (Vol. 3)*. John Wiley & Sons New York.

Mucsi, G., Csőke, B., Kertész, M., & Hoffmann, L. (2013). Physical Characteristics and Technology of Glass Foam from Waste Cathode Ray Tube Glass. *Journal of Materials, 2013*, 1–11. https://doi.org/10.1155/2013/696428

Mustafa, W. S., Nagy, B., & Szendefy, J. (2022). Impact of Compaction Ratio and Loading Period on Compressional Behavior of Foam Glass Aggregates. *Construction and Building Materials, 343*. https://doi.org/10.1016/j.conbuildmat.2022.128111

Mustafa, W. S., & Szendefy, J. (2023a). Effect of Static Loading States on the Compressional Behavior of Foam Glass Aggregate. *Periodica Polytechnica Civil Engineering, 67*(4), 1203–1213. https://doi.org/10.3311/PPci.21973

Mustafa, W. S., Szendefy, J., & Nagy, B. (2023b). Thermal Performance of Foam Glass Aggregate at Different Compaction Ratios. *Buildings, 13*(7), 1844. https://doi.org/10.3390/buildings13071844

Mustafa, W. S., & Szendefy, J. (2023c). Uniaxial Dynamic Behavior of Foam Glass Aggregate under Oedometric (Fully Side Restrained) Condition at Different Compaction Ratios. *Construction and Building Materials, 396.* https://doi.org/10.1016/j.conbuildmat.2023.132327

Nicks, J. E., Ghaaowd, I. I., & Adams, M. T. (2024). Strength-Deformation Characteristics of Two Different Foamed Glass Aggregates under a Static Design Load. *Geotechnical Testing Journal, 47*(1). https://doi.org/10.1520/GTJ20220258

Oh H., Likos W. and Edil T. 2022. Qualitative Rating System for Drainability of Roadway Base Materials, *Transportation Research Record*, Vol. 2676(4) 683–696.

Østergaard, M. B., Petersen, R. R., König, J., Bockowski, M., & Yue, Y. (2019). Impact of Gas Composition on Thermal Conductivity of Glass Foams Prepared via High-Pressure Sintering. *Journal of Non-Crystalline Solids: X*, 1. https://doi.org/10.1016/j.nocx.2019.100014

Pešta, J., & Prošek, Z. (2022). Environmental perspectives of fine grounded concrete powder: LCA case study of light-weight concrete block. *Acta Polytechnica CTU Proceedings, 34*. https://doi.org/10.14311/app.2022.34.0069

Qamhia, I. I. A., Tutumluer, E., Nicks, J. E., Adams, M. T., & Khan, M. S. (2023). Lightweight and Alternative Backfills for Highway Applications: State-of-the-Art Practice in the U.S.A. *Transportation Research Record*. https://doi.org/10.1177/03611981231191519

Ramamurthy, T., Kanitkar, V. K., & Prakash, K. (1974). Behavior of Coarse-Grained Soils Under High Stresses. *Applied Mechanics, 4*(1). https://www.osti.gov/biblio/6636975

Recovery, recycled technology worldwide. (2018). Recovery, Glass Recycling – Current Market Trends. https://www.recovery-worldwide.com/en/artikel/glass-recycling-current-market-trends-3248774.html

Reyes-Quijije, M., Rocha-Tamayo, A., García-Troncoso, N., Baykara, H., & Cornejo, M. H. (2022). Preparation, Characterization, and Life Cycle Assessment of Aerated Concrete Blocks: A Case Study in Guayaquil City, Ecuador. *Applied Sciences, 12*(4), 1913. https://doi.org/10.3390/app12041913

Robert, D., Baez, E., & Setunge, S. (2021). A New Technology of Transforming Recycled Glass Waste to Construction Components. *Construction and Building Materials, 313*. https://doi.org/10.1016/j.conbuildmat.2021.125539

Sawangsuriya, A. (2012). Wave Propagation Methods for Determining Stiffness of Geomaterials. *Wave Processes in Classical and New Solids, 44*. http://dx.doi.org/10.5772/48562

Scarinci, G., Brusatin, G., & Bernardo, E. (2005). *Cellular Ceramics: Structure, Manufacturing, Properties and Applications*. Wiley Online Book Store. https://doi.org/10.1002/3527606696.ch2g

Skilling, T. (2014, October 14). *Ask Tom: What's city's highest wind speed?* Chicago Tribune. https://www.chicagotribune.com/2014/10/14/ask-tom-whats-citys-highest-wind-speed/

Skogstad, H. B., Geving, S., Hägglund, J., & AS, H. C. (2005). Hygrothermal Material Properties for Granulated Cellular Glass Used in Ground Constructions. *7th Symposium on Building Physics in the Nordic Countries*. https://citeseerx.ist.psu.edu/document?repid=rep1&type=pdf&doi=f149f9c86cdbf07fdb43b615edb3be97987e8388

Steurer, A. (2012). Behavior of Foam Glass Aggregate Under Static Loads. *Proceedings of the 22nd European Young Geotechnical Research*, 15-20. https://publik.tuwien.ac.at/files/PubDat_209468.pdf

Swan, R. H., Yeom, S., Sjoblom, K. J., Asce, M., Stark, T. D., Asce, F., & Filshill, A. (2016). Engineering Properties of Foamed Recycled Glass as a Lightweight Fill. *Geo-Chicago 2016*, 11-22. https://doi.org/10.1061/9780784480151.002.

Thakur, J. K., & Han, J. (2015). Recent Development of Recycled Asphalt Pavement (RAP) Bases Treated for Roadway Applications. *Transportation Infrastructure Geotechnology, 2*(2), 68–86. https://doi.org/10.1007/s40515-015-0018-7

Wen, H., Barzegar, M., Mivehchi, M., Edil, T., Akin, I., & Muhunthan, B. (2022). Utilization and limitations of using recycled asphalt pavement (RAP) as roadway embankment material. Report submitted to Illinois Tollway.

Zimele, Z., Sinka, M., Korjakins, A., Bajare, D., & Sahmenko, G. (2019). Life Cycle Assessment of Foam Concrete Production in Latvia. *Environmental and Climate Technologies, 23*(3), 70–84. https://doi.org/10.2478/rtuect-2019-0080

Zou, C., Wang, Y., Lin, J., & Chen, Y. (2016). Creep Behaviors and Constitutive Model for High Density Polyethylene Geogrid and Its Application to Reinforced Soil Retaining Wall on Soft Soil Foundation. *Construction and Building Materials, 114,* 736-771. https://doi.org/10.1016/j.conbuildmat.2016.03.194

APPENDIX A – Design Guide

Foamed Glass Aggregate Use and Design Guide (modified based on Pennsylvania DOT design guide)

1.0 INTRODUCTION

This document presents guidelines for the use of foamed glass aggregate (FGA) on Department projects. FGA is an alternative lightweight material that can be used to construct embankments and backfill behind structures. This document includes a discussion of the typical properties of FGA, applications where FGA may be beneficial, and FGA design and construction requirements and considerations. This document also includes details of a typical FGA embankment for use on Department projects.

Foamed Glass Aggregates are extremely lightweight, manufactured aggregates produced from recycled glass. The manufacturing process takes recycled glass powder and mixes it with a foaming agent, where it is then sent through a kiln and softened. During this process, bubbles are created within the softened glass due to the foaming agent creating foamed glass aggregates.

1.1 Typical Geotechnical Uses of Foamed Glass Aggregate

FGA is intended to be used as a lightweight fill for embankments, backfill behind retaining structures, or placed as fill over existing buried structures or utilities where the weight of conventional backfill can result in excessive settlement and/or structural damage.

1.2 Foamed Glass Aggregate Properties

The physical properties of FGA in lightweight fill applications are as follows,

1. Unit Weight: The unit weight a designer may consider will depend on the maximum, typical, minimum value, bulk vs. compacted state (and specified percent compaction), and moisture content. The bulk dry unit weight of FGA typically ranges from 10 to a maximum of 15 pcf. Moist bulk unit weights can vary between 15 and 18.75 pcf, corresponding to a moisture content ranging from 0% to 25% by weight. A moist, in-place unit weight of 23.5 pcf can be conservatively used for design, considering a 1.25 compaction factor.

2. Buoyant Unit Weight: It is noted that the bubbles in the glass foam are closed cell and therefore are not expected to absorb any significant amount of water.

   The Saturated Unit Weight is equal to the bulk density when all the voids between the particles are filled with water. The Buoyant Unit Weight is the saturated unit weight minus the unit weight of water. This definition is applicable when the material is submerged below standing water or below the groundwater table.

   The buoyant unit weight of FGA has been determined through testing to be -15 pcf. Applying a factor of safety of 1.5, the design buoyant unit weight of FGA is -22 pcf.

3. Shear Strength: Shear strength parameters are a function of the proposed normal stress. The friction angle and apparent cohesion are determined in accordance with ASTM D3080, modified for testing on nominally compacted dry material using the standard 2.5" diameter ring, with particles larger than 1/4" (6.35 mm) removed. The design friction angle shall be 40 degrees (the

maximum currently allowed by the Illinois DOT) or the measured friction angle at normal stress levels up to a minimum of 15 psi, whichever is smaller. Note that the apparent friction angle tends to decrease further at stress levels exceeding 3,000 psf. Any application involving design stresses in the FGA layer greater than 2,500 psf will require additional analysis and/or product testing (see Section 1.2.8).

4. Permeability: The grain size distribution for FGA (pre- and post-compaction) and the particle shape makes FGA comparable to gravel and crushed aggregate.
5. Resilient Modulus, M_r: The resilient modulus of FGA at a representative compacted unit weight should be tested per AASHTO T 307-99, Standard Method of Test for Determining the Resilient Modulus of Soils and Aggregate Materials. The average M_r results for samples with dry unit weights between 16.4 and 17.2 pcf (corresponding to approximately 20% vertical deformation) vary between 14,800 and 47,400 psi under a range of confining and cyclic deviator stresses. Conservatively, a minimum M_r value of 10,875 psi can be assumed for design. The design resilient modulus for a layer of FGA can be utilized for pavement subgrade conditions in a linear-elastic analysis of a pavement cross-section.
6. To avoid crushing the material, traffic wheel loads distributed through the pavement section should not exceed 2,000 psf (13.8 psi) by the time the load reaches the top of the FGA material.
7. Elastic Modulus, E: The elastic modulus for FGA may vary based on the overlying, adjacent, and underlying layers. Typically, the elastic modulus is between 7,250 and 10,000 psi, determined through 12-12-inch plate load test or lightweight deflectometer (LWD) testing on compacted FGA.
8. Creep: Creep testing on FGA up to a stress of 2,000 psf extrapolates that creep deformation (i.e., the deformation that will occur after one day) at 50 years will be less than 0.1%. For stresses up to 5,200 psf (2.6 tsf), testing extrapolates creep deformation to a range between 0.6% and 1.8% at 50 years. At higher stresses up to 10,400 psf (5.2 tsf), creep deformations are extrapolated to be over 6% at 50 years. Therefore, to limit the potential for creep deformation, a maximum static stress of 2,000 psf is allowed in the FGA layer. For applications where the static stress in the FGA layer is greater than 2,000 psf, including the design of structures bearing on the FGA layer, further analysis and/or product testing is required. At a minimum, any such analysis should consider the thickness of FGA, the bearing pressure of the structure on the FGA layer, the static stress within the layer, and the allowable settlement.

2.0 DESIGN REQUIREMENTS AND CONSIDERATIONS

Geotechnical analyses are required to design FGA for lightweight fill applications. At a minimum, settlement and global slope stability analyses must be performed. In some cases, additional analyses, including bearing resistance and sliding, must be performed. These analyses are discussed below, along with other design requirements and considerations for the use of FGA on Department projects.

2.1 Settlement Analyses (Creep/Static Load Conditions)

FGA can be used as an option to eliminate or reduce the estimated settlement from embankment construction to a tolerable level. A typical FGA embankment section is shown in Figure 2.1-1. Settlement analyses of underlying soil must be performed, not only to justify the need for the use of FGA in place of more standard or other lightweight fill materials (i.e., embankment material or, in rare cases, structural

backfill), but to also determine the required limits of the FGA within the embankment cross-section. Immediate, consolidation, and secondary consolidation settlement must be considered for underlying fine-grained soil layers. The settlement of underlying soils can be evaluated using the design unit weight for FGA and other overlying layers. A differential settlement analysis of the underlying soil layers should be evaluated for the FGA roadway section and adjacent sections. If differential settlement is a concern, the FGA layer may be sloped in a transition section.

For structures, settlement analyses should also consider the elastic and creep settlement of the FGA layer in addition to the settlement of the soil layers underlying the FGA layer. As indicated in 1.2.8, at this time, a method to determine the extent and duration of creep of settlement for structures bearing directly on FGA has not been established. Structures founded on FGA are not to induce static stress in the FGA layer of greater than 2,000 psf. For structures exceeding this threshold stress within the FGA, a detailed analysis addressing creep is to be submitted for approval.

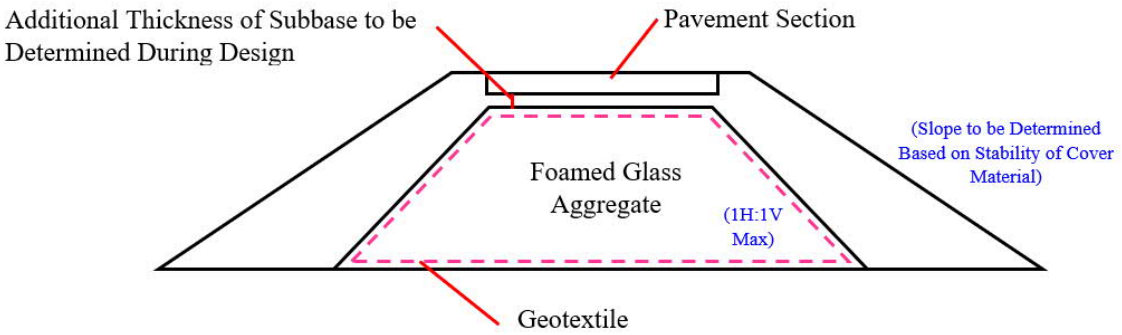

Figure 2.1-1 – Typical FGA Embankment Section

2.2 Global Slope Stability Analyses

Global slope stability analyses should be performed similar to analyses performed for conventional embankments constructed with earth materials. Since the in-situ foundation material will often be saturated, cohesive soil, both undrained and drained shear strength parameters must be used in the analyses. In general, a 45-degree friction angle for embankments or walls that are 50 feet or less in height is appropriate for FGA. For embankments greater than 50 feet or those with special loading conditions, such as under structures, a more detailed analysis of stress conditions will be necessary. Based on the results of this analysis, the FGA layer may be subdivided and assigned the appropriate friction angle based on the anticipated normal stress (Refer to Section 1.2.3).

2.3 Buoyancy

Closed-cell FGA is buoyant and susceptible to uplift when submerged in water because of its low unit weight. Consequently, when FGA is proposed on Department projects, FGA should be placed above the static groundwater level and above the anticipated high-water level (i.e., 500-year storm elevation) if used in the vicinity of a stream, river, etc. However, if it is necessary to place FGA below groundwater or the anticipated high-water level, an analysis must be performed to ensure all other options have been considered, that submersion of FGA is the best alternative, and that the proposed cover material provides enough ballast force to prevent movement of the FGA. Additionally, in the event the area is subject to flooding/ponding, the contractor should provide a staging plan or propose other measures to ensure that

all placed FGA is properly ballasted. Traffic loads and any other temporary or short-term loads should not be included when calculating the uplift resisting force. Use a minimum safety factor of 1.2 if the hydrostatic uplift force is a short-term condition; a safety factor of 1.5 is required if the uplift force is a long-term condition, such as when FGA is submerged beneath the static/long-term groundwater level or on cyclical basis in tidal areas, or similar regularly fluctuating groundwater levels. The design value to be used for the buoyant unit weight is provided in Section 1.2.

Follow the Bridge Manual and AASHTO load factors for FGA used in conjunction with structures.

2.4 FGA Dynamic/Live Load Conditions

The anticipated dynamic loads in flexible pavement systems should be properly considered in the pavement design, where FGA is an underlying layer. While FGA does not replace subbase in a flexible pavement system, the design resilient modulus for a layer of FGA can be utilized for pavement subgrade conditions in a linear-elastic analysis of a pavement cross-section.

During construction, vehicles and other construction equipment may have limited travel over the FGA layer after a minimum of 6 inches of compacted capping material is placed. If a haul road is to be located over the FGA layer, an evaluation of the capping material thickness under the haul road must be completed and submitted to the Department for approval.

2.5 Bearing Resistance

The bearing capacity/resistance analysis method similar to that for spread footings on soil presented in the Bridge Manual should be used if a bearing resistance analysis is necessary (especially where treatment for settlement involves soft foundation materials). In general, the placement of signs, lights, and other structures with significant bearing pressures should be avoided within the FGA layer. The typical detail for a lighting foundation is shown in Figure 2.5-1 and is supported on crushed stone or natural material. However, the concrete footing shown in Figure 2.5-1 should be moved so that the induced pressure distribution only acts within conventional backfill material, or the dissimilar bearing materials shall be accounted for in the design. If structures are proposed on the FGA layer that induce stress in the FGA layer more than 2,000 psf, a proper settlement analysis using creep data should be completed.

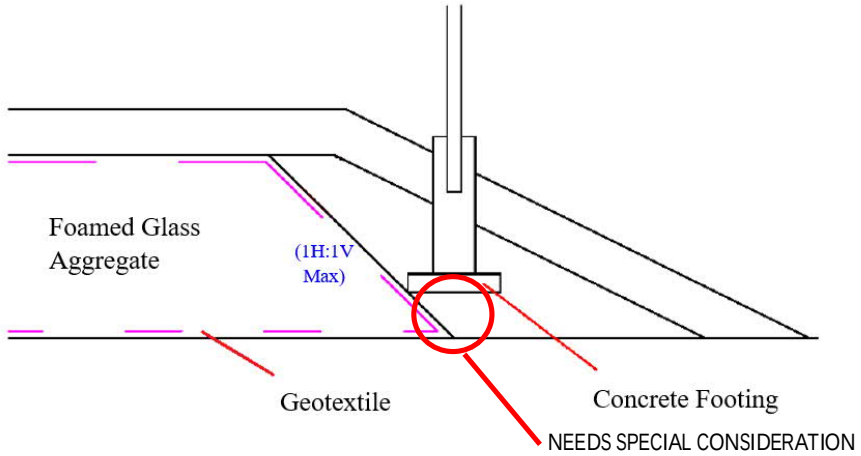

Figure 2.5-1 – Typical Detail of Lighting Foundation where FGA is used.

Roadway embankments typically contain drainage pipes and inlet boxes, and often also have underground utilities, utility poles, light poles, signs, guard rail posts, and other appurtenances. These can be incorporated into an FGA embankment, but careful consideration should be given during design. When possible, locate these appurtenances outside the limits of the FGA or in the embankment cover material above the FGA.

2.6 Lateral Load/Earth Pressure Considerations

Lateral earth pressure from soil or aggregate backfills placed behind FGA must be considered during design. For example, if FGA is used to backfill behind an abutment or retaining wall and embankment material is used to construct the remainder of the embankment cross-section, lateral earth pressure from the embankment material may be applied to the FGA, which in turn will transfer the lateral load to the wall or abutment. To avoid developing lateral earth pressure, the embankment material behind the FGA must be placed at a slope that is independently stable, such as 2H:1V (i.e., sufficiently beyond the active earth pressure wedge such that no lateral loads can be transferred to the wall) or the lateral loads from the fill placed behind the FGA must be accounted for in the design.

2.7 Cover Requirements

Permissible Capping Material(s) and Placement: Embankment material, installed in accordance with Section 205; Subbase, installed in accordance with Section 311; Topsoil on the slope of FGA, installed in accordance with Section 211;

Thickness: The minimum compacted lift thickness of capping material in non-live load situations shall be six (6) inches over FGA in a pavement structure or two feet on an open slope of FGA. For live load conditions, see Section 2.4.

The Engineer will determine the total thickness of overlying material (including capping material and the pavement structure) under the roadway profile based upon project-specific conditions (e.g., ADT, pavement material properties, pavement layer thicknesses, subgrade soil properties, etc.).

2.9 Removal and Reuse of FGA Material

FGA may be removed and reused. FGA will always be separated from other materials with a geotextile, which will enable easy separation from other soils during excavation. If FGA is reused in design, it is suggested that the design unit weight be increased by 25% to account for the crushing of material during handling. Alternatively, field tests may be conducted to verify the in-situ density of the repositioned FGA.

2.10 Pipe Backfill Envelope

If FGA is proposed for use within a pipe backfill envelope, submit a detailed design, in accordance with AASHTO and Bridge Manual as applicable (loading and load factors) to the Department for review and approval. The design is to demonstrate that the proposed pipe installation using FGA in the pipe backfill envelope meets structural and service requirements.

3.0 CONSTRUCTION REQUIREMENTS AND CONSIDERATIONS

Construction requirements for the use of FGA to construct embankments are provided in the Standard Special Provision on Foamed Glass Aggregates. The requirements below must be accounted for during the design of FGA embankments.

3.1 Subgrade Preparation, Placement, and Drainage

In general, the subgrade must be prepared in accordance with Section 205. FGA may be placed over poor subgrade soils. Removal of ponded water is required. Placement of a geotextile (Article 1080.02 of Illinois DOT's Standard Specification) is required both above and below the FGA. FGA should be placed in accordance with the contract drawings and as directed by the Representative.

FGA is a highly permeable layer (similarly to other open graded gravel soils) and will provide water storage (exhibit a "bathtub effect") if the adjacent soil is less permeable and no other drainage is provided. Provide sufficient drainage for FGA using grading or a pipe collector system. Follow Illinois DOT's Standard Specification (Section 205.04) to install pipe underdrain.

3.2 Capping/Cover Requirements:

A minimum of 6 inches of compacted capping material is required on top of FGA, or 2 feet of compacted capping material on an open slope of FGA. FGA may be placed directly under a porous granular embankment (PGE) without capping materials. However, drainage has to be provided at the bottom of FGA (see Section 3.1) if no capping material is placed between FGA and PGE. See Section 2.7 for Cover types and installation requirements.

The capping material must be placed within 2 weeks after placement of the geotextile to help prevent degradation of the geotextile.